THE ASTROPHYSICAL JOURNAL

An International Review of Spectroscopy and Astronomical Physics

FOUNDED IN 1895 BY GEORGE E. HALE AND JAMES E. KEELER

EDITORS

EDWIN B. FROST†
Yerkes Observatory of the University of Chicago

FREDERICK H. SEARES
Mount Wilson Observatory of the Carnegie Institution of Washington

HENRY G. GALE
Ryerson Physical Laboratory of the University of Chicago

OTTO STRUVE
Yerkes Observatory of the University of Chicago

COLLABORATORS

WALTER S. ADAMS, *Mount Wilson Observatory;* JOSEPH S. AMES, *Johns Hopkins University;* WILLIAM W. CAMPBELL, *Lick Observatory;* HENRY CREW, *Northwestern University;* CHARLES FABRY, *Université de Paris;* ALFRED FOWLER, *Imperial College, London;* EDWIN HUBBLE, *Mount Wilson Observatory;* HEINRICH KAYSER, *Universität Bonn;* ROBERT A. MILLIKAN, *Institute of Technology, Pasadena;* HUGH F. NEWALL, *Cambridge University;* FRIEDRICH PASCHEN, *Reichsanstalt, Charlottenburg;* HENRY N. RUSSELL, *Princeton University;* FRANK SCHLESINGER, *Yale Observatory;* SIR ARTHUR SCHUSTER, *Twyford;* HARLOW SHAPLEY, *Harvard College Observatory*

† Deceased May 14, 1935.

VOLUME 81

JANUARY–JUNE 1935

THE UNIVERSITY OF CHICAGO PRESS
CHICAGO, ILLINOIS

THE CAMBRIDGE UNIVERSITY PRESS, LONDON
THE MARUZEN COMPANY LIMITED, TOKYO
THE COMMERCIAL PRESS, LIMITED, SHANGHAI

PUBLISHED JANUARY, MARCH, APRIL, MAY,
JUNE, 1935

COMPOSED AND PRINTED BY THE UNIVERSITY OF CHICAGO PRESS
CHICAGO, ILLINOIS, U.S.A.

CONTENTS

NUMBER I

PAGE

THE SPECTRUM AND COMPOSITION OF THE GASEOUS NEBULAE. I. S. Bowen 1

LUNAR RADIATION AS RELATED TO PHASE. Edison Pettit 17

REMARKS ON LUNAR RAY CRATERS. S. G. Hacker and J. Q. Stewart . 37

THE SIGNIFICANCE OF RIGHT-ASCENSION ERRORS IN TRIGONOMETRIC PARALLAXES. T. E. Sterne 45

THE SPECTRUM OF P CYGNI. Otto Struve 66

NUMBER II

SIR ARTHUR SCHUSTER. George E. Hale 97

THE CLASSIFICATION OF STELLAR SPECTRA. H. N. Russell, Cecilia H. Payne Gaposchkin, and D. H. Menzel 107

SYSTEMATIC DISPLACEMENTS OF LINES IN THE SPECTRA OF CERTAIN BRIGHT STARS. Walter S. Adams and Elizabeth MacCormack . . 119

ON THE RADIAL-VELOCITY VARIATION OF THE CEPHEID VARIABLE FF AQUILAE. Roscoe F. Sanford 132

ON THE RADIAL VELOCITY-CURVES FOR THE CEPHEID VARIABLE Y OPHIUCHI. Roscoe F. Sanford 140

RADIAL VELOCITIES OF RR LYRAE IN 1928, 1929, AND 1930. ROSCOE F. Sanford 149

TRIGONOMETRIC PARALLAXES DETERMINED WITH THE 60- AND 100-INCH MOUNT WILSON REFLECTORS. Adriaan van Maanen 152

LENS SYSTEMS FOR CORRECTING COMA OF MIRRORS. Frank E. Ross . 156

NOTE

THE PHOTO-ELECTRIC COLOR OF β LYRAE. C. T. Elvey 173

NUMBER III

THE DEGREE OF VARIABILITY OF CALCIUM CONTENT IN STELLAR ATMOSPHERES. Ernest Öpik 177

THE SPECTROSCOPIC ABSOLUTE MAGNITUDES AND PARALLAXES OF 4179 STARS. Walter S. Adams, Alfred H. Joy, Milton L. Humason, and Ada Margaret Brayton 187

PHOTO-ELECTRIC OBSERVATIONS OF ζ AURIGAE. C. M. Huffer . . . 292

A DETERMINATION OF THE UPPER LIMIT OF INTERNAL MOTIONS IN THE PRAESEPE CLUSTER. P. van de Kamp 297

NUMBER IV

PAGE

On the Apsidal Motion in α Virginis. W. J. Luyten and E. Ebbighausen 305
The Spectrum of R Aquarii, 1919–1934. Paul W. Merrill 312
Angular Rotations of Spiral Nebulae. Edwin Hubble 334
Internal Motions in Spiral Nebulae. Adriaan van Maanen . . . 336
Chromospheric Emission in the Wings of H and K. A. D. Thackeray 338
On the Spectrum of γ Cassiopeiae. J. F. Heard 341
The Velocity-Curve of 27 Canis Majoris. Otto Struve 345
A Peculiar Spectroscopic Phenomenon in the Algol System. W. W. Morgan 348
Notes
Partial List of c Stars of Classes B and A. Paul W. Merrill . . 351
An Unusual Pair of Nebulae: NGC 5216 and 5218. Philip C. Keenan 355
Tables for the Computation of the Orbit Radii of Eclipsing Binaries. G. R. Miczaika 356
Reviews

NUMBER V

The Spectrum Analysis of the Hot Carbon Star, R Coronae Borealis. Louis Berman 369
ζ Aurigae: The Structure of a Stellar Atmosphere. William H. Christie and O. C. Wilson 426
Photographic Magnitudes of ζ Aurigae during the 1934 Eclipse. P. Th. Oosterhoff 461
The Emission Line λ 4511 in Late-Type Variables. A. D. Thackeray 467
Note on Dispersing and Condensing Tendencies in a Viscous, Compressible Gas. Gustaf Strömberg 474
The Spectrographic Orbit of W Ursae Minoris. Alfred H. Joy and O. L. Dustheimer 479
Notes
On the Color Temperature of Nova Herculis. R. M. Petrie . . 482
Spurious Correction of Radial Velocities in the *Cape Annals*. Joseph Lunt 484
Note on the Foregoing Paper by Dr. Lunt. H. Spencer Jones . 487

JAN 21 1935

VOLUME 81 NUMBER 1

THE ASTROPHYSICAL JOURNAL

AN INTERNATIONAL REVIEW OF SPECTROSCOPY AND ASTRONOMICAL PHYSICS

Founded in 1895 by GEORGE E. HALE *and* JAMES E. KEELER

Edited by

EDWIN B. FROST
Yerkes Observatory of the University of Chicago

FREDERICK H. SEARES
Mount Wilson Observatory of the Carnegie Institution of Washington

HENRY G. GALE
Ryerson Physical Laboratory of the University of Chicago

OTTO STRUVE
Yerkes Observatory of the University of Chicago

JANUARY 1935

THE SPECTRUM AND COMPOSITION OF THE GASEOUS NEBULAE - *I. S. Bowen* 1

LUNAR RADIATION AS RELATED TO PHASE - - - - - - - - *Edison Pettit* 17

REMARKS ON LUNAR RAY CRATERS - - - - - *S. G. Hacker and J. Q. Stewart* 37

THE SIGNIFICANCE OF RIGHT-ASCENSION ERRORS IN TRIGONOMETRIC PARALLAXES - T. E. Sterne 48

THE SPECTRUM OF P CYGNI - - - - - - - - - - - - - - - Otto Struve 66

THE UNIVERSITY OF CHICAGO PRESS
CHICAGO, ILLINOIS, U.S.A.

January 1935 Vol. 81, No. 1

THE ASTROPHYSICAL JOURNAL

AN INTERNATIONAL REVIEW OF SPECTROSCOPY AND ASTRONOMICAL PHYSICS

Founded in 1895 by GEORGE E. HALE *and* JAMES E. KEELER

Edited by

EDWIN B. FROST
Yerkes Observatory of the University of Chicago

FREDERICK H. SEARES
Mount Wilson Observatory of the Carnegie Institution of Washington

HENRY G. GALE
Ryerson Physical Laboratory of the University of Chicago

OTTO STRUVE
Yerkes Observatory of the University of Chicago

WITH THE COLLABORATION OF

WALTER S. ADAMS, Mount Wilson Observatory
JOSEPH S. AMES, Johns Hopkins University
WILLIAM W. CAMPBELL, Lick Observatory
HENRY CREW, Northwestern University
CHARLES FABRY, Université de Paris
ALFRED FOWLER, Imperial College, London
EDWIN HUBBLE, Mount Wilson Observatory
HEINRICH KAYSER, Universität Bonn
ROBERT A. MILLIKAN, Institute of Technology, Pasadena
HUGH F. NEWALL, Cambridge University
FRIEDRICH PASCHEN, Reichsanstalt, Charlottenburg
HENRY N. RUSSELL, Princeton University
FRANK SCHLESINGER, Yale Observatory
HARLOW SHAPLEY, Harvard College Observatory

The Astrophysical Journal is published by the University of Chicago at the University of Chicago Press, 5750 Ellis Avenue, Chicago, Illinois, during each month except February and August. ¶ The subscription price is $6.00 a year; the price of single copies is 75 cents. Orders for service of less than a half-year will be charged at the single-copy rate. ¶ Postage is prepaid by the publishers on all orders from the United States, Mexico, Cuba, Porto Rico, Panama Canal Zone, Republic of Panama, Dominican Republic, Canary Islands, El Salvador, Argentina, Bolivia, Brazil, Colombia, Chile, Costa Rica, Ecuador, Guatemala, Honduras, Nicaragua, Peru, Hayti, Uruguay, Paraguay, Hawaiian Islands, Philippine Islands, Guam, Samoan Islands, Balearic Islands, Spain, and Venezuela. ¶ Postage is charged extra as follows: for Canada and Newfoundland, 30 cents on annual subscriptions (total $6.30); on single copies, 3 cents (total 78 cents): for all other countries in the Postal Union, 80 cents on annual subscriptions (total $6.80), on single copies, 8 cents (total 83 cents). ¶ Patrons are requested to make all remittances payable to The University of Chicago Press, in postal or express money orders or bank drafts.

The following are authorized agents:

For the British Empire, except North America, India, and Australasia: The Cambridge University Press, Fetter Lane, London, E.C. 4. Prices of yearly subscriptions and of single copies may be had on application.

For Japan: The Maruzen Company, Ltd., Tokyo.

For China: The Commercial Press, Ltd., 211 Honan Road, Shanghai. Yearly subscriptions, $6.00; single copies, 75 cents, or their equivalents in Chinese money. Postage extra, on yearly subscriptions 80 cents, on single copies 8 cents.

Claims for missing numbers should be made within the month following the regular month of publication. The publishers expect to supply missing numbers free only when losses have been sustained in transit, and when the reserve stock will permit.

Business correspondence should be addressed to The University of Chicago Press, Chicago, Illinois.

Communications for the editors and manuscripts should be addressed to: Otto Struve, Editor of THE ASTROPHYSICAL JOURNAL, Yerkes Observatory, Williams Bay, Wisconsin.

The cable address is "Observatory, Williamsbay, Wisconsin."

The articles in this journal are indexed in the *International Index to Periodicals*, New York, N.Y.

Applications for permission to quote from this journal should be addressed to The University of Chicago Press, and will be freely granted.

Entered as second-class matter, January 17, 1895, at the Post-Office, Chicago, Ill., under the act of March 3, 1879.
Acceptance for mailing at special rate of postage provided for in Section 1103, Act of October 3, 1917, authorized on July 13, 1918.

PRINTED IN THE U.S.A.

THE ASTROPHYSICAL JOURNAL

AN INTERNATIONAL REVIEW OF SPECTROSCOPY AND ASTRONOMICAL PHYSICS

VOLUME 81 JANUARY 1935 NUMBER 1

THE SPECTRUM AND COMPOSITION OF THE GASEOUS NEBULAE

By I. S. BOWEN

ABSTRACT

I. The primary source of nebular luminosity is the emission of radiation on the return of electrons after ionization by extreme ultra-violet starlight. Additional luminosity is produced by the following secondary mechanisms:

1. *Ionization by secondary radiation.*—Additional atoms are ionized by extreme ultra-violet quanta emitted by the primary mechanism.

2. *Excitation by secondary radiation.*—Line absorption of secondary quanta may excite an atom of the same kind as the primary emitting atom, or any other atom that has absorption lines which coincide with lines of the emitting atom. This mechanism, made possible by certain chance coincidences between lines of *He* II, *O* III, and *N* III, explains the presence with a high intensity of a selected group of *O* III and *N* III lines while all other lines of these elements are missing.

3. *Excitation by secondary electrons ejected by the primary mechanism.*—This is practically the sole source of excitation of the forbidden lines.

II. A study of nebular line intensities in the light of the foregoing processes indicates that *H* is the most abundant element and *He* is the second. *N*, *O*, *Ne*, *S*—and possibly *C* and *A*—are present but are very much rarer. The lines of these heavier elements are strong, not because the elements are very abundant but because they are able to make use of large sources of energy that are not available to the predominent *H* and *He*. Lines of *F*, *Na*, *Si*, *P*, *Cl*, *K*, and *Ca* are missing.

I. MECHANISM OF EXCITATION

It is now generally recognized that the emission spectrum of the diffuse and planetary nebulae is produced by energy received from an adjacent star. The idea that the luminosity of the nebulae is excited by adjacent stars is one of some antiquity, appearing first to have been suggested by Sir William Herschel[1] in his discussion of the so-called "nebulous stars" discovered by himself. On the basis of

[1] *Abridged Phil. Trans.*, **17**, 25, 1791.

information available to him, he was, however, disposed to favor a conception of the relationship of star to nebula that was unfavorable to this idea. As a consequence, this viewpoint received little attention for a century or more. Its revival in recent years has resulted from the accumulation of observational data and from developments in the theory of radiation. The favorable consideration it is now accorded as a working hypothesis is especially due to Hubble's comprehensive discussion of observational data provided largely by V. M. Slipher, W. H. Wright, H. D. Curtis, and himself.[2]

The primary mechanism causing this line emission is the ionization of the atoms of the nebula by the absorption of stellar radiation of a wave-length shorter, i.e., of a frequency greater, than that corresponding to the ionization potential. Thus, an *H* atom can be ionized by all wave-lengths less than 912 A, *He* I by those less than 504 A, and *He* II by those less than 228 A, etc. The observed spectra of these atoms are then emitted on the return of the ejected electron. This mechanism was first suggested by D. H. Menzel[3] and by H. Zanstra,[4] the latter of whom has discussed quantitatively the relative intensities of the star and of the nebula excited by it on the basis of this mechanism.

In addition to this primary process, however, there is in operation a series of secondary mechanisms which materially change not only the total intensity of the nebular radiation but the type of spectrum emitted as well. In order to simplify the discussion of these secondary processes they will be considered in terms of the train of events which may follow the ionization by the primary mechanism of one type of atom, namely, *He* II. At some time after ionization the He^{++} ion picks up an electron, usually in some outer orbit, from which the electron returns to its normal state by a series of transitions. The first transitions are normally between outer orbits and give rise to the observed *He* II nebular lines. In every case, however, the last transition made ends in the normal state and corresponds to the emission of one of the series of extreme ultra-violet lines at 304, 256, 243 A, etc., depending on whether the final jump was made from the

[2] *Ap. J.*, **56**, 162, 400, 1922.

[3] *Pub. A.S.P.*, **38**, 295, 1926.

[4] *Ap. J.*, **65**, 50, 1927; *Zs. f. Ap.*, **2**, 1, 1931.

2p, 3p, or 4p orbit. One or more of the following secondary processes may then take place:

1. *Ionization by secondary radiation.*[5]—Since these extreme ultra-violet lines of *He* II are below the critical wave-length necessary to ionize both *H* and *He* I, they may ionize one of these atoms and thereby cause the emission of its observed spectrum. Indeed, if *He* I is ionized first, the radiations given off by it may in turn ionize an *H* atom.

2. *Excitation by secondary radiation.*—As the extreme ultra-violet lines of *He* II listed above are transitions to the normal state of the atom, they are very strongly absorbed by other *He* II atoms. When this type of absorption occurs, the *He* II atom is, of course, excited to the same upper state that the original emitting atom was in before the ultra-violet quantum was given off. In general, this *He* II atom thus excited can now re-emit the quantum absorbed, or if the excited state is above the 2p state, it may emit first a line of long wave-length, then another of the extreme ultra-violet lines. As pointed out by Zanstra,[6] a series of absorptions and re-emissions of this type soon results in the transformation of all of these extreme ultra-violet quanta into quanta of 304 A, plus some of the *He* II lines of longer wave-length which can immediately escape from the nebula, since they are not absorbed by the normal *He* II atom. Since many of these lines of longer wave-length fall in the observable range, this mechanism adds to the intensity of the observed *He* II lines.

As was recently pointed out,[7] a few of the *O* III and *N* III lines can be excited by these extreme ultra-violet *He* II lines by this same mechanism, which depends, in this case, on certain chance coincidences between the wave-lengths of *He* II, *O* III, and *N* III lines, as illustrated in the simplified Grotrian diagrams of Figure 1. From these diagrams it is at once evident that because of the near coincidence of the $s^2p^{2\,3}P_2 - s^2p3d^3P_2$ line of *O* III at 303.799 A with the 303.780 A resonance line of *He* II, the *O* III atom can be excited to the $s^2p3d^3P_2$ state by the absorption of this very intense *He* II line. From this level the electron can either return directly to the $s^2p^{2\,3}P$ states, thus re-emitting the line at 304 A, or it can jump first to a

[5] I. S. Bowen, *Ap. J.*, **67**, 14, 1928.

[6] *Ibid.*, **65**, 56, 1927.

[7] I. S. Bowen, *Pub. A.S.P.*, **46**, 146, 1934.

term of the s^2p3p configuration, next to a term of the s^2p3s configuration, and then to the normal state. Obviously, since the quantum is not lost when the 304 A line is re-emitted, the eventual result of several absorptions and re-emissions of this line is nearly always the production of two of the observed long wave-length *O* III lines followed by a quantum of 374 A.

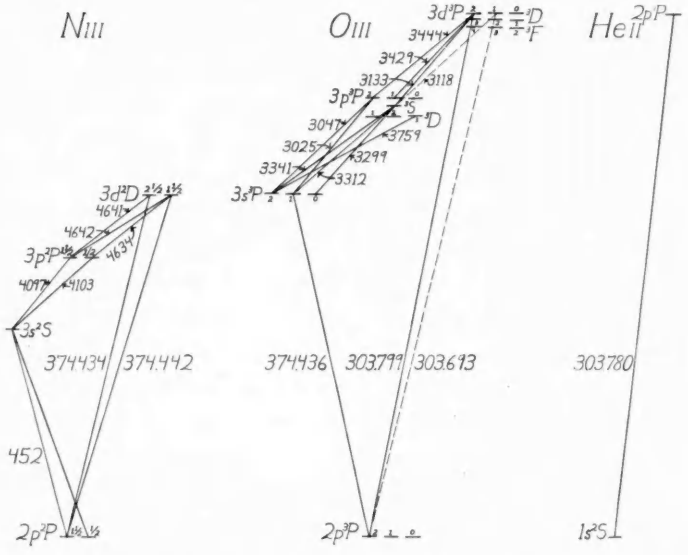

FIG. 1.—Terms of *N* III, *O* III, and *He* II taking part in secondary mechanism No. 2

A similar near coincidence between one of these 374 A lines of *O* III and the $s^2p^2P_{1\frac{1}{2}} - s^2 3d^2D_{2\frac{1}{2}}$ line of *N* III enables the observed *N* III lines to be excited by this same process.

In general, the absorption coefficient of an atom for radiation coinciding with one of its own natural frequencies emitted on the return of an electron to its normal state (secondary mechanism No. 2) is very much greater than the absorption coefficient for radiation having a wave-length below its ionization limit (primary mechanism or secondary mechanism No. 1). This fact enables the secondary mechanism (No. 2) to play a very important rôle in determining the excitation and therefore the appearance of the nebular spectra.

In the first place, the dimensions of the nebula are of the order of magnitude of the mean free path of a quantum before the primary

absorption with ionization occurs. Consequently this much higher absorption coefficient of the abundant *H* II atoms for their own 304, 256 A, etc., radiations prevents these radiations from escaping directly from the nebulae. Instead, these quanta must first be absorbed and re-emitted many times, and if they eventually escape at all, it is only after a slow outward diffusion to the boundary of the nebula. This, therefore, gives the other secondary processes a much larger chance to make use of the 304 A quanta before they escape from the nebula.

In the second place, it enables the majority of the 304 A quanta to excite the *O* III lines and they in turn the *N* III lines before these quanta are absorbed by the abundant *H* and *He* I atoms by means of the ionization process. Because of this, the intensities of the *O* III and *N* III lines are proportional to the rate of formation of the 304 A quanta, but are, through wide limits, independent of the abundance of *O* III and *N* III even though these atoms are much rarer than those of *H* and *He*.

That the observed *O* III and *N* III permitted nebular lines are almost entirely excited by this mechanism is shown in Table I, which gives all of the *O* III and *N* III permitted nebular lines that W. H. Wright[8] has observed in his very extensive studies. For comparison the stronger *O* III[9] and *N* III[10] lines that appear in laboratory sources are also listed. In *O* III it is seen that all possible transitions, in the observable range, from the $3d^2P_2$ state, and all transitions from the three states (s^2p3p^3S, $^3P_2{}^3D_3$) to which an electron in the $s^2p3d^3P_2$ is most likely to jump, are definitely present. On the other hand, all other *O* III lines, with one very faint exception, are completely missing, in spite of the fact that in the laboratory all of the other lines listed are much stronger than some that are observed in the nebulae. The one very faint exception at 3118 A ($s^2p3p^3S - s^2p3d^3P_1$) is doubtless also excited by the same mechanism, since a relative velocity of 90 km/sec., which may rarely occur, is enough to cause the excitation of the $s^2p3d^3P_1$ state by changing the wave-length of the *He* line

[8] *Pub. Lick Obs.*, **13**, 193, 1918; *Lick Obs. Bull.*, **17**, 1, 1934; *Pub. A.S.P.*, **46**, 142 and 280, 1934.

[9] A. Fowler, *Proc. R. Soc.*, A, **117**, 317, 1928.

[10] L. J. Freeman, *ibid.*, **121**, 318, 1928.

(304.780 A) to the wave-length (304.693 A) of the $s^2p^2{}^3P_2 - s^2p3d^3P_1$ line of *O* III.

Similarly, with *N* III the lines that may be excited by this secondary mechanism are present in the nebulae while all others are missing. Owing to the fivefold greater absorption coefficient of the 374.434 A ($s^2p^2P_{1\frac{1}{2}} - s^23d^2D_{2\frac{1}{2}}$) line than that of the 374.442 A ($s^2p^2P_{1\frac{1}{2}} - s^23d^2D_{1\frac{1}{2}}$) line, an unusually large number of atoms are excited to the $s^23d^2D_{2\frac{1}{2}}$ state, with the result that the 4641 A line and the 4642 A line, which are not resolved in the nebular spectrum, should be about seven times as strong as 4634 A. Wright[11] has noted just such a discrepancy between the laboratory and the nebular intensities. In case of high relative velocities between the *O* III and *N* III, this discrepancy in intensity between 4641 and 4634 A may be reduced by the absorption of the $2p^2P_{\frac{1}{2}} - 3d^2D_{1\frac{1}{2}}$ line of *N* III at 374.204 A, which differs by only 0.039 A, equivalent to a velocity of 32 km/sec., from another component of the 374 A *O* III multiplet.

TABLE I

PERMITTED LINES OF *O* III AND *N* III

Classification	λ Lab.	Int. Lab.	λ Nebulae	Classification	λ Lab.	Int. Lab.	λ Nebulae
	O III				*O* III—*Continued*		
$3s^3P_1 - 3p^3P_2$	3023.45	5	3025	$3s^3P_2 - 3p^3D_3$	3759.87	9	3759
$3s^3P_2 - 3p^3P_2$	3047.13	8	3047	$3s^3P_1 - 3p^3D_1$	3774.00	6	.....
$3s^3P_2 - 3p^3P_1$	3059.30	6	.....	$3s^3P_2 - 3p^3D_2$	3791.26	6	.....
$3p^3S - 3d^3P_1$	3121.71	5	3118	$3s^1P - 3p^1S$	3961.59	8	.....
$3p^3S - 3d^3P_2$	3132.86	6	3133.0	$3s^1P - 3p^1D$	5592.37	6	.....
$3p^3D_2 - 3d^3F_3$	3260.98	8	.....				
$3p^3D_3 - 3d^3F_4$	3265.46	10	.....		*N* III		
$3s^3P_0 - 3p^3S$	3299.36	3	3299				
$3s^3P_1 - 3p^3S$	3312.30	5	3312.1				
$3s^3P_2 - 3p^3S$	3340.74	6	3340.9	$3s^2S - 3p^2P_{1\frac{1}{2}}$	4097.31	10	4097.3
$3p^3P_1 - 3d^3P_2$	3428.67	3	3428.5	$3s^2S - 3p^2P_{\frac{1}{2}}$	4103.37	9	*Hδ*
$3p^3P_2 - 3d^3P_2$	3444.10	5	3444.1	$4f^2F - 5g^2G$	4379.09	10	.....
$3p^3P_1 - 3d^3D_2$	3707.24	6	.....	$3p^2P_{\frac{1}{2}} - 3d^2D_{1\frac{1}{2}}$	4634.16	8	4634.1
$3p^3P_2 - 3d^3D_3$	3715.08	6	.....	$3p^2P_{1\frac{1}{2}} - 3d^2D_{2\frac{1}{2}}$	4640.64	10	4640.9
$3s^3P_1 - 3p^3D_2$	3754.67	7	.....				

Further support for this mechanism of excitation of the *O* III and

[11] *Pub. A.S.P.*, **67**, 149, 1934.

N III lines is given by the fact that the sizes of the monochromatic images of the nebulae given by these lines are very nearly equal to those obtained with the *He* II lines but differ widely from the image sizes of the *O* III forbidden lines. Likewise, the variation in the intensities of these lines in going from nebulae to nebulae parallels that of the *He* II lines much more closely than it does that of the forbidden lines of *O* III.

This mechanism may also play quite a rôle in determining the appearance of the spectra of novae, although due to the much wider lines present there a larger number of lines of *O* III and *N* III may be excited by it, thus making the evidence for the mechanism less striking. If this is the case, the concentration of the 452 A *N* III line, emitted at the end of the series of processes, may become very great in these somewhat denser objects. It may be this high radiation density of the resonance lines of *N* III that causes the nitrogen to appear to "blow up" at certain stages of the development of the novae, as indicated by the very sudden and marked widening of the nitrogen lines.[12]

It is possible that the abnormally high intensity of the 4686 A ($3S,P,D-4S,P,D,F$) line of *He* II in the nebulae may partially, at least, be due to the fact that the high intensity of 304 A keeps an appreciable number of atoms in the $2s^2S$ state, which is probably metastable. From this state it may be raised to the $4p^2P$ state by absorption of the still more intense 1216 A resonance line of *H*. A relative velocity of 120 km/sec. between the *H* and the *He* II atoms is required, but in view of the lightness of both atoms this may not be too rare an occurrence.

3. *Excitation by secondary electrons.*[13]—Since in general the quantum of energy absorbed by the atom in the primary process has more than enough energy to ionize the atom, the electron is ejected with a considerable velocity. Thus, as will be discussed in the next section, the only atoms abundant enough to play any large rôle in the primary process are *H*, *He* I, and *He* II, whose ionization potentials are 13.5, 24.5, and 54.1 electron volts, respectively. Since the primary radiation from the star is continuously distributed in wave-

[12] W. H. Wright, *Pub. Lick Obs.*, **14**, 84, 1921.

[13] I. S. Bowen, *Ap. J.*, **67**, 13, 1928.

length, it is evident that the electrons will come off with energies up to at least the differences between these, i.e., 10–30 electron volts. The same is true of the electrons ejected from *H* and *He* I by the secondary radiations 304, 374, 452, and 585 A. The electrons with these energies may then excite other atoms by impact.

This mechanism is particularly effective in exciting the forbidden lines, since these represent transitions from metastable states whose excitation potentials are very low. Thus the nebular pair at 4959 and 5007 A has an excitation potential of only 2.50 electron volts, while those of other forbidden lines range from 1.83 to 5.33 electron volts. In comparison with these, the lowest excitation potentials of the very abundant *H*, *He* I, and *He* II atoms are 10.2, 19.7, and 40.6 electron volts, respectively. Consequently the very large source of energy in the form of electrons having energies of 10 or less electron volts is only available for the excitation of the forbidden lines. The intensity of these lines is therefore independent, over a wide range, of the abundance of the elements involved in comparison with the predominant *H* and *He*.

This mechanism is practically the sole source of excitation of the forbidden lines since, as will be shown in the next section, the permitted lines of the elements concerned are almost entirely missing. These permitted lines should be emitted first if the electron arrived in the metastable state by returning after ionization by the primary mechanism.

II. CHEMICAL COMPOSITION

From the foregoing discussion of the mechanisms of excitation of the nebular lines it is evident that the strength of the forbidden lines or of the permitted *O* III and *N* III lines excited by line absorption is not necessarily an indication of the high relative abundance of the elements emitting them. In order to make even a rough estimate of the relative abundance of various elements it is therefore necessary to make comparisons among permitted lines excited by the primary mechanism or among forbidden lines.

Table II gives all of the permitted nebular lines, found in Wright's[14] lists, that are excited chiefly by the primary mechanism. The intensities listed are Wright's values obtained with the quartz

[14] See n. 8, also *Pub. A.S.P.*, **32**, 63, 1920.

spectrograph in the region below 3850 A, and with the glass spectrograph above this wave-length. If we neglect the 4686 A line of *He* II, which may be abnormally strong owing to the secondary mechanism discussed above, we see that hydrogen is the predominant element in the nebulae. While considerably weaker than those of *H*, the *He* I and *He* II lines are also definitely and consistently present. Besides those of *H* and *He*, however, only four lines that might be identified as permitted lines are found. Two of them, 3935 and 4416 A, were marked by Wright as only suspected, since they were very faint and were observed in only one nebula each. In the case of 3935 A, provisionally identified as *Ca* II, the nebula is an abnormal one (BD 30°3639) and evidence discussed later indicates that *Ca* is not present in the more normal nebulae. The other two lines, 4267 and 4650 A, were also very weak and were found in but four and two nebulae, respectively. Since in each of the four cases but one or two lines are attributed to a given ion, the identifications are all very doubtful.

It is therefore evident that all elements except *H* and *He* are very rare in the nebulae. Consequently the only reason that certain lines of the heavier elements, such as the forbidden lines or the fluorescent lines of *O* III and *N* III, are strong is that they can be excited by large sources of energy that are not available to the predominant *H* and *He*.

It is also evident that the permitted lines of the heavier elements are either missing or so weak and uncertain that they cannot satisfactorily be used to estimate the relative abundance of these atoms. This forces one to make use of the intensities of the forbidden lines which, while they are not comparable with permitted lines, may be compared among themselves to estimate roughly the relative abundance of those heavier elements that are capable of emitting forbidden lines in the observable range. That the forbidden lines are much more sensitive for the detection of the rare elements is at once obvious. Thus none of the *O* III permitted lines that are excited by the primary mechanism is strong enough to appear, while its forbidden lines at 4959 and 5007 A are by far the strongest lines in the whole spectrum of many nebulae.

Table III lists the predicted positions of all forbidden lines that

TABLE II

PERMITTED LINES EXCITED BY PRIMARY MECHANISM

Classification	λ Nebulae	Intensity	
		NGC 7027	NGC 6572
	H I		
$2^2S,P-16^2S,P,D$	3704 *He* I	.....	.....
2 −15	3712	.....	.....
2 −14	3722	.....	.....
2 −13	3734	.....	.....
2 −12	3750	3	5
2 −11	3771	4	8
2 −10	3798	5	10
2 − 9	3835.5	8	14
2 − 8	3888.96 *He* I	10	15
2 − 7	3970.08	30	40
2 − 6	4101.74	70	60
2 − 5	4340.46	80	70
2 − 4	4861.32	80	60
2 − 3	6562.79	100	60
	He I		
$2s^3S-4p^3P$	3188	.....	.....
$2p^3P-7d^3D$	3704 *H* I	.....	.....
$2p^3P-6d^3D$	3820	1	.....
$2s^3S-3p^3P$	3888.96 *H* I	10	15
$2s^1S-4p^1P$	3964.8	.....	2
$2p^1P-7d^1D$	4009	.....	1
$2p^3P-5d^3D$	4026.2 *He* II	1	10
$2p^3P-5s^3S$	4120.6	.....	1
$2p^1P-6d^1D$	4144.0	.....	1
$2p^1P-5d^1D$	4388.0	.....	2
$2p^3P-4d^3D$	4471.54	8	20
$2p^3P-4s^3S$	4712.6	8	5
$2p^1P-4d^1D$	4922.2	.....	2
$2s^1S-3p^1P$	5017	1	2
$2p^3P-3d^3D$	5875.7	8	20
$2p^1P-3d^1D$	6677	1	1
$2p^3P-3s^3S$	7065	2	.....
	He II		
$3^2S,P,D-5^2S,P,D,F$	3203.1	.....	.....
$4^2S,P,D,F-13^2S,P,D,F,G$	4026.2 *He* I	1	10
4 −11	4200	1	.....
4 − 9	4541.4	2	.....
$3^2S,P,D-4^2S,P,D,F$	4685.76	90	.....
$4^2S,P,D,F-7^2S,P,D,F,G$	5411.3	4	.....

TABLE II—*Continued*

Classification	λ Nebulae	Intensity	
		NGC 7027	NGC 6572
	C II		
$3d^2D-4f^2F$	4267.1	.....	2
	C III		
$3s^3S-3p^3P$	4649.2 *O* II	1	2
	O II		
$3s^2P-3p^2D$	4416	.....	1
$3s^4P_{2\frac{1}{2}}-3p^4D_{3\frac{1}{2}}$	4649.2 *C* III	1	2
	Ca II		
$4s^2S-4p^2P_{1\frac{1}{2}}$	3935	.....	.....

any of the elements up to *Ca* are likely to emit in the observable range between 2900 and 10,000 A. The uncertainty indicated in the fourth column is the maximum tolerance that is allowable in the predicted positions. In general, uncertainties below 10 A are due to the large errors in wave-number units that are inherent in the extreme ultra-violet measurements on which these predictions depend. Larger uncertainties than this occur only in cases where direct measurements are not available and the predicted wave-lengths depend on interpolations or extrapolations from nearby atoms of the same structure. On account of a much lower excitation potential, transitions from the ^1D or ^2D states will, in any given atom, be much stronger than transitions from the ^1S or ^2P states.

The nebular wave-lengths and intensities are again taken from Wright's list, except that three values in the extreme red are obtained from P. W. Merrill.[15] The references in the first and third columns indicate the spectroscopic data used in making the predic-

[15] *Pub. A.S.P.*, **40**, 254, 1928.

TABLE III

FORBIDDEN LINES

ATOM	CLASSIFICATION	PREDICTED λ	TOLERANCE	Δν	λ NEBULAE	INTENSITY	
						NGC 7027	NGC 6572
C I*	$^3P_1-{}^1S$	4621.4	1				
	$^1D-{}^1S$	8727.4	3				
	$^3P_1-{}^1D$	9822.9	3				
	$^3P_2-{}^1D$	9849.5	3				
N I†	$^4S-{}^2P$	3466.4	.5				
	$^4S-{}^2D_{1\frac{1}{2}}$	5198.5	1				
	$^4S-{}^2D_{2\frac{1}{2}}$	5200.7	1				
N II*	$^3P_1-{}^1S$	3063.0	.5				
	$^1D-{}^1S$	5755.0	1		5754.8‖	4	2
	$^3P_1-{}^1D$	6548.4	1		6548.1¶	10	10
	$^3P_2-{}^1D$	6583.9	1		6583.6¶	30	30
O I	$^3P_1-{}^1S$	2972.31	.05				
	$^1D-{}^1S$	5577.341‡	.02		5577.350**		
	$^3P_2-{}^1D$	6300.23§	.2		6302††	3	5
	$^3P_1-{}^1D$	6363.88§	.2		6364††	1	2
O II*	$^4S-{}^2D_{1\frac{1}{2}}$	3726.2	1		3726.16¶	15	8
	$^4S-{}^2D_{2\frac{1}{2}}$	3729.1	1		3728.91¶	7	4
	$^2D_{2\frac{1}{2}}-{}^2P_{1\frac{1}{2}}$	7318.6	2				
	$^2D_{2\frac{1}{2}}-{}^2P_{1\frac{1}{2}}$	7319.4	2		7319.9¶‡‡	3	3
	$^2D_{1\frac{1}{2}}-{}^2P_{1\frac{1}{2}}$	7329.9	2				
	$^2D_{1\frac{1}{2}}-{}^2P_{1\frac{1}{2}}$	7330.7	2		7330.4¶‡‡	2	2
O III*	$^1D-{}^1S$	4363.2	1		4363.21¶	20	80
	$^3P_1-{}^1D$	4959.5	2		4958.91¶	80	200
	$^3P_2-{}^1D$	5007.6	2		5006.84¶	250	800
F II	$^1D-{}^1S$	4158.9§§	4				
	$^3P_2-{}^1D$	4774‖‖	50	343§§			
	$^3P_1-{}^1D$	4853‖‖	50				
F III§§	$^4S-{}^2D_{1\frac{1}{2}}$	2931.2	3				
	$^4S-{}^2D_{2\frac{1}{2}}$	2933.8	3				
	$^2D_{2\frac{1}{2}}-{}^2P$	5721.9	6				
	$^2D_{1\frac{1}{2}}-{}^2P$	5732.0	6				
F IV	$^1D-{}^1S$	3530.2§§	3				
	$^3P_1-{}^1D$	3997.1¶¶	3				
	$^3P_2-{}^1D$	4059.9¶¶	3				
Ne III	$^1D-{}^1S$	3342.8***	2		3342		
	$^3P_2-{}^1D$	3752‖‖	200	643***	3868.74†††	50	70
	$^3P_1-{}^1D$	3845‖‖	200		3967.51†††	50	70

* B. Edlén, *Nova Acta Reg. Soc. Sci. Upsaliensis*, **9,** No. 6, 1934.

† E. Ekefors, *Zs. f. Phys.*, **63,** 437, 1930 (corrected to air).

‡ J. C. McLennan and J. H. McLeod, *Proc. R. Soc.*, A, **115,** 515 (direct observation).

§ J. J. Hopfield, *Phys. Rev.*, **37,** 160, 1931 (direct observation).

‖ F. Becker and W. Grotrian, *Ergebnisse der Exakten Naturwissenschaften*, **7,** 65, 1928.

¶ I. S. Bowen, *Ap. J.*, **67,** 1, 1928.

** Auroral green line. Wave-length measured by H. D. Babcock, *ibid.*, **57,** 209, 1923. Identification by J. C. McLennan, J. H. McLeod, and R. Ruedy, *Phil. Mag.*, **6,** 558, 1928.

†† I. S. Bowen, *Phys. Rev.*, **36,** 600, 1930; F. Paschen, *Naturwissenschaften*, **18,** 752, 1930.

‡‡ Measurements by Merrill, *Pub. A.S.P.*, **40,** 254, 1928.

§§ I. S. Bowen, *Phys. Rev.*, **45,** 82, 1934.

‖ ‖ Extrapolated or interpolated values. In the case of *F* II and *Na* IV, these are calculated with the aid of term values for *Ne* III obtained by assuming the identifications of 3869 and 3967 A are correct.

¶¶ B. Edlén and P. Swings, *C.R.*, **198,** 1842, 1934.

*** J. C. Boyce, *Phys. Rev.*, **46,** 378, 1934.

††† J. C. Boyce, D. H. Menzel, and C. H. Payne, *Proc. Nat. Acad.*, **19,** 581, 1933.

TABLE III—*Continued*

Atom	Classification	Predicted λ	Tolerance	Δν	λ Nebulae	Intensity	
						NGC 7027	NGC 6572
Ne IV***	$^2D_{2\frac{1}{2}}-{}^2P_{1\frac{1}{2}}$	4713.0	4				
	$^2D_{2\frac{1}{2}}-{}^2P_{\frac{1}{2}}$	4715.2	4				
	$^2D_{1\frac{1}{2}}-{}^2P_{1\frac{1}{2}}$	4718.6	4				
	$^2D_{1\frac{1}{2}}-{}^2P_{\frac{1}{2}}$	4720.8	4		4725.5?†††		4
Ne V|| ||	$^1D-{}^1S$	2972	20				
	$^3P_1-{}^1D$	3344	20	696|| ||	3345.8‡‡‡		8
	$^3P_2-{}^1D$	3424	20		3425.8‡‡‡		20
Na IV|| ||	$^3P_2-{}^1D$	3245	30	1106§§§			
	$^3P_1-{}^1D$	3366	30				
Na V§§§	$^2D_{2\frac{1}{2}}-{}^2P_{1\frac{1}{2}}$	4011.2	3				
	$^2D_{1\frac{1}{2}}-{}^2P_{1\frac{1}{2}}$	4015.3	3				
	$^2D_{2\frac{1}{2}}-{}^2P_{\frac{1}{2}}$	4017.5	3				
	$^2D_{1\frac{1}{2}}-{}^2P_{\frac{1}{2}}$	4021.6	3				
Mg VI§§§	$^2D_{2\frac{1}{2}}-{}^2P_{1\frac{1}{2}}$	3485.5	3				
	$^2D_{1\frac{1}{2}}-{}^2P_{1\frac{1}{2}}$	3488.1	3				
	$^2D_{2\frac{1}{2}}-{}^2P_{\frac{1}{2}}$	3500.4	3				
	$^2D_{1\frac{1}{2}}-{}^2P_{\frac{1}{2}}$	3503.0	3				
Al VII§§§	$^2D_{1\frac{1}{2}}-{}^2P_{1\frac{1}{2}}$	3068.8	3				
	$^2D_{2\frac{1}{2}}-{}^2P_{1\frac{1}{2}}$	3074.0	3				
	$^2D_{1\frac{1}{2}}-{}^2P_{\frac{1}{2}}$	3093.4	3				
	$^2D_{2\frac{1}{2}}-{}^2P_{\frac{1}{2}}$	3098.7	3				
Si I|| || ||	$^3P_1-{}^1S$	6526.88	.1				
P I¶¶¶	$^4S-{}^2P_{1\frac{1}{2}}$	5331.1	3				
	$^4S-{}^2P_{\frac{1}{2}}$	5338.3	3				
	$^4S-{}^2D_{2\frac{1}{2}}$	8783.9	8				
	$^4S-{}^2D_{1\frac{1}{2}}$	8795.9	8				
P II|| ||	$^3P_1-{}^1S$	4539	300				
	$^1D-{}^1S$	7574	500				
S I****	$^3P_1-{}^1S$	4589.0	1				
	$^1D-{}^1S$	7724.4	3				
S II††††	$^4S-{}^2P_{1\frac{1}{2}}$	4068.5	2		4068.62§§§§	20	6
	$^4S-{}^2P_{\frac{1}{2}}$	4076.5	2		4076.22§§§§	2	3
	$^4S-{}^2D_{2\frac{1}{2}}$	6717.3	4		6716		
	$^4S-{}^2D_{1\frac{1}{2}}$	6731.5	4		6730§§§§	1	1
S III‡‡‡‡	$^3P_1-{}^1S$	3662	200				
	$^1D-{}^1S$	6141	300				
	$^3P_1-{}^1D$	9070	300	535			
	$^3P_2-{}^1D$	9533	300				

‡‡‡ P. Swings and B. Edlén, *C.R.*, **198,** 1748, 1934; I. S. Bowen, *Pub. A.S.P.*, **46,** 145, 1934.

§§§ J. Soderquist, *Nova Acta Reg. Soc. Sci. Upsaliensis*, **9,** No. 7, 1934.

|| || || A. Fowler, *Proc. R. Soc.*, A, **123,** 422, 1929.

¶¶¶ C. C. Kiess, *J. of Research, Bur. of Stand.*, **8,** 393, 1932.

**** J. E. Ruedy, *Phys. Rev.*, **44,** 757, 1933. Ruedy's identification of $s^2p^{11}S-s^2p^3(^2P)4s^2P$ has been changed to the line at 1782.25 A to make the relationships of terms of the s^2p^4 configuration agree better with other atoms of similar structure.

†††† M. Gilles, *Ann. d. Phys.*, **15,** 267, 1931.

‡‡‡‡ I. S. Bowen, *Phys. Rev.*, **46,** 377, 1934.

§§§§ I. S. Bowen, *Nature*, **123,** 450, 1929.

TABLE III—*Continued*

Atom	Classification	Predicted λ	Tolerance	Δν	λ Nebulae	Intensity NGC 7027	Intensity NGC 6572
Cl II|| ||.....	$^3P_1-{}^1S$	3703	200	.....	.....	.....	.....
	$^1D-{}^1S$	6209	400	.....	.....	.....	.....
	$^3P_2-{}^1D$	8589	200	692	.....	.....	.....
	$^3P_1-{}^1D$	9132	200	.....	.....	.....	.....
Cl III|| || || ||	$^4S-{}^2P_{1\frac{1}{2}}$	3342.7	2	.....	.....	.....	.....
	$^4S-{}^2P_{\frac{1}{2}}$	3353.4	2	.....	.....	.....	.....
	$^4S-{}^2D_{2\frac{1}{2}}$	5517.2	4	.....	.....	.....	.....
	$^4S-{}^2D_{1\frac{1}{2}}$	5537.7	4	.....	.....	.....	.....
	$^2D_{1\frac{1}{2}}-{}^2P_{1\frac{1}{2}}$	8433.6	8	.....	.....	.....	.....
	$^2D_{2\frac{1}{2}}-{}^2P_{1\frac{1}{2}}$	8481.6	8	.....	.....	.....	.....
	$^2D_{1\frac{1}{2}}-{}^2P_{\frac{1}{2}}$	8501.8	8	.....	.....	.....	.....
	$^2D_{2\frac{1}{2}}-{}^2P_{\frac{1}{2}}$	8550.5	8	.....	.....	.....	.....
Cl IV‡‡‡‡...	$^3P_1-{}^1S$	3118.3	2	.....	.....	.....	.....
	$^1D-{}^1S$	5322.2	4	.....	.....	.....	.....
	$^3P_1-{}^1D$	7530.9	8	.....	.....	.....	.....
	$^3P_2-{}^1D$	8046.1	8	.....	.....	.....	.....
A III|| ||.....	$^3P_1-{}^1S$	3124	200	.....	.....	.....	.....
	$^1D-{}^1S$	5234	500	.....	.....	.....	.....
	$^3P_2-{}^1D$	7141	100	1112.5¶¶¶¶	7135.6?*****‡‡	5	5
	$^3P_1-{}^1D$	7757	100	.....	.....	.....	.....
A IV.....	$^4S-{}^2D_{2\frac{1}{2}}$	4709|| ||	50	130¶¶¶¶	4711.4?††††††	.....	.....
	$^4S-{}^2D_{1\frac{1}{2}}$	4738|| ||	50	.....	4740.2?††††††	20	5
	$^2D_{1\frac{1}{2}}-{}^2P_{1\frac{1}{2}}$	7171.1¶¶¶¶	4	.....	.....	.....	.....
	$^2D_{2\frac{1}{2}}-{}^2P_{1\frac{1}{2}}$	7238.6¶¶¶¶	4	.....	.....	.....	.....
	$^2D_{1\frac{1}{2}}-{}^2P_{\frac{1}{2}}$	7263.3¶¶¶¶	4	.....	.....	.....	.....
	$^2D_{2\frac{1}{2}}-{}^2P_{\frac{1}{2}}$	7332.6¶¶¶¶	4	.....	.....	.....	.....
A V|| ||.....	$^1D-{}^1S$	4738	200	.....	.....	.....	.....
	$^3P_1-{}^1D$	6432	200	1267¶¶¶¶	6313?	2	.....
	$^3P_2-{}^1D$	7003	200	.....	.....	.....	.....
K IV.....	$^1D-{}^1S$	4524|| ||	200	.....	.....	.....	.....
	$^3P_2-{}^1D$	6101.1*****	6	.....	.....	.....	.....
	$^3P_1-{}^1D$	6794.8*****	6	.....	.....	.....	.....
K V.....	$^4S-{}^2D_{2\frac{1}{2}}$	4112|| ||	100	237*****	.....	.....	.....
	$^4S-{}^2D_{1\frac{1}{2}}$	4153|| ||	100	.....	.....	.....	.....
	$^2D_{1\frac{1}{2}}-{}^2P_{1\frac{1}{2}}$	6223.4*****	5	.....	.....	.....	.....
	$^2D_{2\frac{1}{2}}-{}^2P_{1\frac{1}{2}}$	6316.6*****	5	.....	.....	.....	.....
	$^2D_{1\frac{1}{2}}-{}^2P_{\frac{1}{2}}$	6349.5*****	5	.....	.....	.....	.....
	$^2D_{2\frac{1}{2}}-{}^2P_{\frac{1}{2}}$	6446.5*****	5	.....	.....	.....	.....
Ca V*****..	$^1D-{}^1S$	3996.3	5	.....	.....	.....	.....
	$^3P_2-{}^1D$	5308.9	5	.....	.....	.....	.....
	$^3P_1-{}^1D$	6085.9	5	.....	.....	.....	.....
Ca VI.....	$^4S-{}^2D_{2\frac{1}{2}}$	3646|| ||	200	417*****	.....	.....	.....
	$^4S-{}^2D_{1\frac{1}{2}}$	3703|| ||	200	.....	.....	.....	.....
	$^2D_{1\frac{1}{2}}-{}^2P_{1\frac{1}{2}}$	5460.0*****	5	.....	.....	.....	.....
	$^2D_{2\frac{1}{2}}-{}^2P_{1\frac{1}{2}}$	5587.2*****	5	.....	.....	.....	.....
	$^2D_{1\frac{1}{2}}-{}^2P_{\frac{1}{2}}$	5631.0*****	5	.....	.....	.....	.....
	$^2D_{2\frac{1}{2}}-{}^2P_{\frac{1}{2}}$	5766.4*****	5	.....	.....	.....	.....

\|\| \|\| \|\| \|\| Bowen, *Phys. Rev.*, **45,** 401, 1934.

¶¶¶¶ J. C. Boyce (unpublished).

***** I. S. Bowen, *Phys. Rev.* **46,** 791, 1934.

††††† P. Swings and B. Edlén, *C.R.*, **198,** 2071, 1934; J. C. Boyce, C. Payne-Gaposchkin, and D. H. Menzel, *Pub. A.S.P.*, **46,** 213, 1934.

Note added in proof: Lines 3342 and 6716 have just been observed by R. H. Stoy, *Pub. A.S.P.*, **46,** 297, 1934.

tions. The notations on the observed wave-lengths refer to the article in which the identifications were originally made.

From the table it is evident that *N*, *O*, *Ne*, and *S* are definitely present and that *O* is considerably more abundant than the others. Argon may be present, although there are serious inconsistencies in the nebular behavior of the *A* IV pair. Consequently, further observations in the extreme red are needed to determine whether the other component of the *A* III and *A* V pairs are definitely present or absent. The evidence is not conclusive in the case of *C* I, since the only line, 4621 A, in the observed range has, according to E. A. Codon's[16] calculations, less than 1/200 of the intensity of the $^1D-{}^1S$ line. It should therefore not be strong enough to be observed with any reasonable concentration of *C*. Likewise, the only *Mg* and *Al* lines in this range are weak transitions from the ^2P levels of stages of ionization so high that their production would be doubtful even though these elements were present. On the other hand, the lines of *F*, *Na*, *Si*, *P*, *Cl*, *K*, and *Ca* appear to be rather definitely missing and the abundance of these elements must therefore be small.

Unfortunately, the spectra of the astronomically common metals between *Ca* and *Cu* have not been analyzed to an extent that a systematic study of their forbidden lines is possible. However, for the first two stages of ionization of these elements the excitation potentials of the permitted lines are not much greater than those of the forbidden lines. Consequently, if these elements are present in these lower stages of ionization we should expect the permitted lines to be observed as well as the forbidden lines. The failure to observe these lines therefore seems to eliminate the possibility of any very large concentration of these heavier atoms, at least in low stages of ionization. Indeed, less than a dozen nebular lines remain unidentified, and all of these are of such low intensity that they are barely observable in from one to four of the brightest nebulae. Consequently one can, in general, assign an abundance lower than that of *N*, *Ne*, or *S* to all unidentified elements which have, in the observed range, either permitted or forbidden lines of low excitation potential, even though the position of these lines cannot be fixed at the present time.

[16] *Ap. J.*, **79**, 217, 1934.

From this qualitative survey one may conclude, therefore, that like most astronomical bodies the nebulae are made up largely of hydrogen. Helium is the next most abundant element. In the third place, but very much rarer than these, one finds *O*, or possibly *C* if its 4267 and 4650 A lines are correctly identified. Still rarer, but definitely present, are *N*, *Ne*, *S*, and possibly *A*. In comparison with the sun[17] there seems to be a tendency to favor the non-metals. Thus if, as is true in the sun, *Na*, *K*, and *Ca* were about equally common with *N* and ten times as abundant as *S*, we should doubtless find their lines in the nebular spectrum.

Unfortunately, our present knowledge of such factors as ultraviolet absorption coefficients, internal nebular velocities, nebular densities, velocity distribution of nebular electrons, etc., is so meager that a quantitative discussion of the abundance of the elements as a function of the intensities of nebular lines is not feasible.

In conclusion the writer wishes to express his indebtedness to Professor W. H. Wright and to Dr. J. C. Boyce for the use of unpublished data, and for various suggestions concerning observational material on which this article is based.

California Institute of Technology
October 1934

[17] Russell, *ibid.*, **70**, 11, 1929.

LUNAR RADIATION AS RELATED TO PHASE

By EDISON PETTIT*

ABSTRACT

Methods of observing.—An image of the moon, 0.87 mm maximum diameter, was formed by a concave mirror of 6.4 cm aperture and 8.8 cm focal length alternately upon the two receivers of a vacuum thermocouple. The planetary heat was separated from the light by a microscope cover-glass. The apparatus was calibrated by a standard lamp at 71.3 m distance. An air-mass meter was devised to read sec Z directly.

Reduction of the measurements.—The measurements were reduced to the zenith with the atmospheric extinction observed for the night or, when only one or two observations were made, by using the mean extinctions, 0.11 mag. for reflected light and 0.15 mag. for planetary heat. Small corrections were applied for the planetary heat transmitted, and light reflected, by the microscope cover-glass screen, and the measurements were then reduced to mean distance of sun and moon. The mean curves were corrected to no atmosphere for comparison with the theoretical formula.

Radiometric magnitude.—The radiometric magnitude of planetary heat per square second of arc for temperatures between 140° and 500° K is given by the empirical equation

$$m'_r+\Delta m'_r=\frac{1545}{T}-2.6\,.$$

The radiometric magnitude of the planetary heat from the full moon under normal conditions is -14.8, and that of the reflected light, -13.4.

Comparison with other data.—The measurements of planetary heat made by the Earl of Rosse are 10–20 per cent lower than the present values for most phases of the moon, and lower still for reflected light, although the uncertainty of the corrections which should be applied makes the comparison difficult. No great amount of asymmetry such as has been reported by others was observed in the phase-intensity curve. The theoretical curve is everywhere higher than the observed curve.

Transmission of ozone for planetary heat.—The transmission of an equivalent of 2 cm of ozone measured for the differential radiation between boiling water and liquid air was 0.92, which indicates that atmospheric ozone absorbs 4 per cent of the planetary heat from the moon.

It is well known that the radiation from the moon consists of two parts—reflected sunlight and radiant heat emitted by its warmed surface—the latter called planetary heat. A study of the radiation from the subsolar point and other particular areas on the moon was given in a previous paper.[1] It is now proposed to study the radiation from the moon as a whole.

More than sixty-five years ago this problem was studied by the

* *Contributions from the Mount Wilson Observatory, Carnegie Institution of Washington*, No. 504.

[1] Pettit and Nicholson, *Mt. W. Contr.*, No. 392; *Ap. J.*, **71**, 102, 1930.

Earl of Rosse,[2] using a 3-foot speculum reflector and two large thermopiles at atmospheric pressure upon which the lunar image was alternately focused by two secondary concaves. The light was separated from the planetary heat by means of a plate of glass the thickness of which is not stated. Our increased knowledge of the transmission coefficients of the atmosphere and the instruments, and of the proper methods of reducing the measurements, made it desirable to repeat this work with a more sensitive arrangement and under better atmospheric conditions.

The reflected light from the moon has been studied visually by several observers, and by J. Stebbins and F. C. Brown[3] with a selenium cell. The latter observers used an instrument which was sensitive throughout the visible spectrum but which, for the most of their observations, showed some preference for the region around λ 0.7 μ. Their measures were made by exposing the cell, contained in a blackened box, directly to moonlight and determining the distance at which an amyl acetate lamp gave the same deflection. More recently, G. Rougier has made measurements of moonlight with a photo-electric cell and amplifier.[4]

No such simple method can be used to measure the lunar radiation with a thermocouple, but the same result may be obtained by using an optical system which forms an image of the entire moon upon a vacuum thermocouple receiver without the secondary mirrors used by Lord Rosse. With the aid of a microscope cover-glass[1] the reflected light may be separated from the planetary heat with a minimum of loss, thus giving two sets of data, viz., the march with phase angle of the whole reflected solar radiation and of the planetary heat. Since we thus do with a smaller instrument what was done on the planet Mercury with the 100-inch telescope,[5] the results should be comparable.

[2] *Proc. R. Soc. Lon.*, **27**, 436, 1869; **29**, 9, 1870; *Phil. Trans. R. Soc. Lon.*, **163**, 587, 1873.

[3] *Ap. J.*, **26**, 326, 1907.

[4] *Ann. de l'Observatoire de Strasbourg*, **2**, 205, 1933. This paper gives a considerable history of the measurements of moonlight. See also *L'Astronomie*, **48**, 220 and 281, 1934.

[5] Pettit and Nicholson, *Pubs. A.S.P.*, **35**, 194, 1923; *Pop. Astr.*, **31**, 657, 1923, and **33**, 299, 1925.

THE APPARATUS

Figure 1 shows a diagram of the apparatus used in the investigation. A thermocouple, *T*, consisting of two junctions with receivers 1 mm square, separated 2.5 mm, is placed at the focus of a 6.4-cm parabolic mirror, *A*, of 8.8 cm focal length. Since the maximum

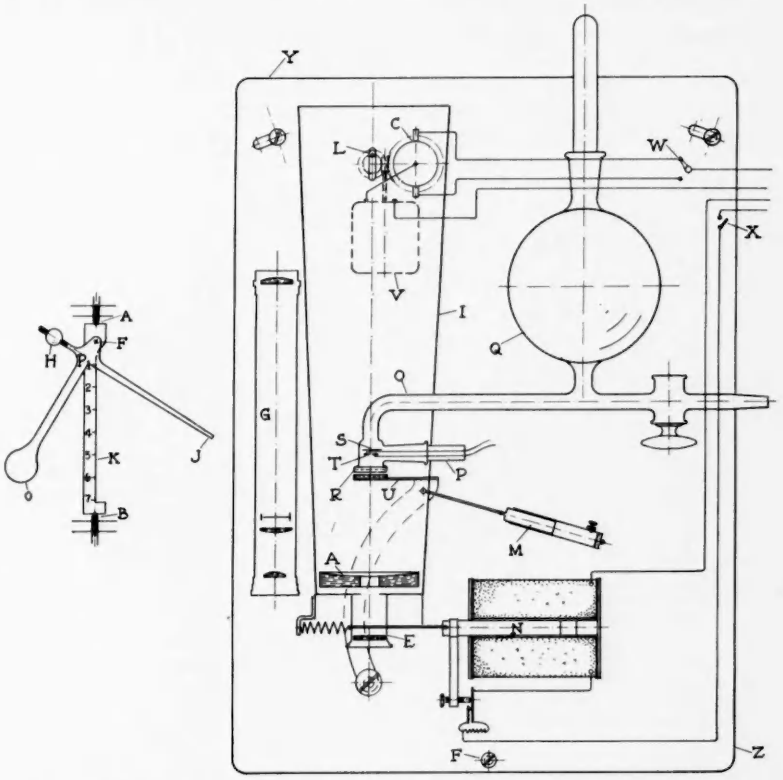

FIG. 1.—Diagram of thermoelectric lunar radiometer. The air-mass meter is shown at the left.

diameter of the image of the moon formed by this mirror is 0.87 mm, the receiver measures all the lunar radiation thus reflected. The thermocouple, *T*, is mounted in a small evacuated cell, 2 cm in diameter, connected with a large-capacity sphere, *Q*, and a calcium-filled tube used to assist in maintaining the vacuum. A rock-salt window, *R*, admits the radiation; and a white celluloid screen, *S*, cemented just behind the thermocouple, *T*, in the cell, assists in

finding the lunar image. The plug, P, containing the lead wires of the thermocouple, and the tube, O, are in the same plane, and therefore cast a common shadow on the mirror, A. A microscope coverglass, $\frac{1}{8}$ mm thick, is mounted on the arm, U, actuated by a plunger magnet, N, in such a way that it may be placed in front of the thermocouple or removed by operating the switch, X. The arm, U, is also in the plane of O and P and therefore in the common shadow. The mirror, A, has a hole, 13 mm diameter, in its center. By means of a single-lens eyepiece, E, the lunar image, 0.87 mm diameter, may be set on the thermocouple receivers. The instrument is mounted on a square aluminum plate, YZ, attached to a second plate by a fulcrum, F, about which it may rotate in its own plane. A small angular displacement of this plate about F is given by the motor-operated crank, L, working in a slot in the plate. The motor, V, also operates the commutator, C, which permits the crank to make only half a revolution, after which the motor circuit is broken through a relay. Reversing the switch, W, causes the crank to make another half-revolution. Hence, by operating the switch, W, the image of the moon may be moved from one junction of the thermocouple to the other. A guiding telescope, G, with one thread in right ascension and two in declination, serves to set the lunar image on the thermocouple receivers in daytime sky when working at crescent phases.

THE AIR-MASS METER

A device, K, which may be called an "air-mass meter," is also a part of the apparatus. It consists of a plummet, O, with a right-angle arm, J, balanced by the mass, H, and fixed by the fulcrum, F, to the spindle, AB, which may rotate about its length. The graduated edge of the spindle is the axis. The lower edge of the pointer, PJ, at all times lies in the plane of the horizon and in that of the vertical circle passing through the object. FP is 1 cm, and the scale edge is graduated in centimeters and millimeters. Since AB is set parallel to the optical axis of the reflector, A, and guiding telescope, G, the intersection of PJ with the scale AB gives the value of sec Z, or the air-mass. Although the readings cannot be made closer than about 0.05 air-mass, they are useful in checking the reduction for air-mass on a large number of observations.

PLATE I

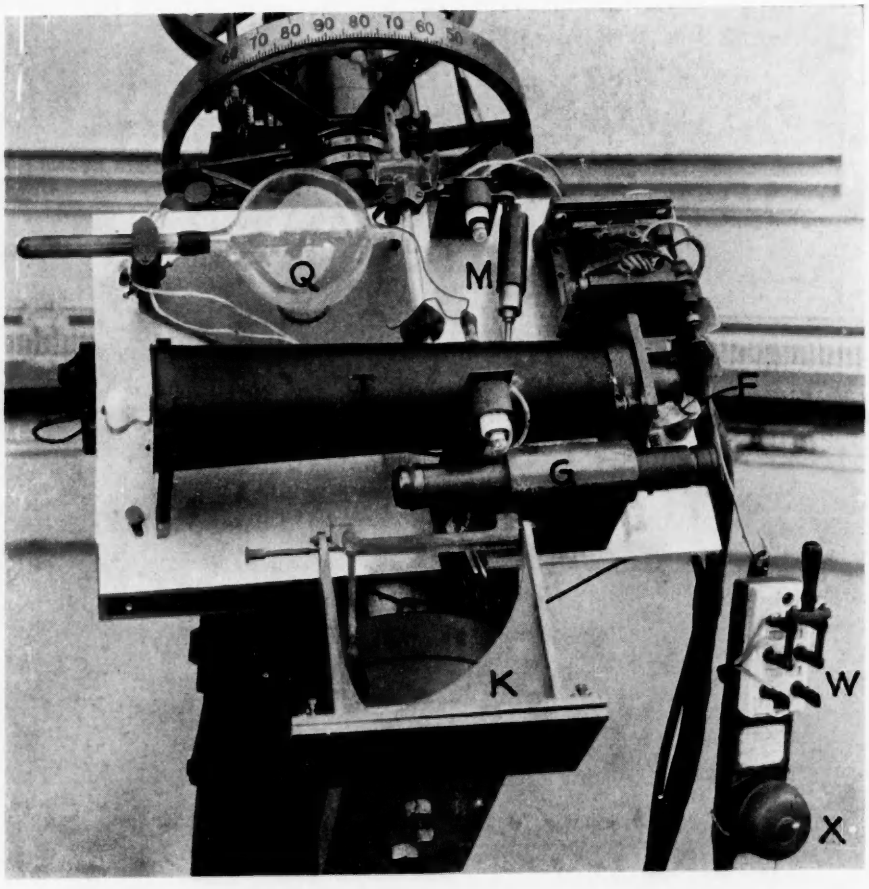

THERMOELECTRIC LUNAR RADIOMETER

UNIV. OF MICH.

The apparatus is mounted on the declination axis of the 6-inch telescope, replacing most of the counterweights (Pl. I). The telescope tube, *I*, is cut longitudinally and splayed in the plane of its rotation about the fulcrum *F*, to prevent vignetting and scattering of light from its walls. Suitable illumination is provided for the thermocouple junctions and for the scale of the air-mass meter. The thermocouple is connected with a D'Arsonval galvanometer whose deflections are read visually. When the knife switch, *W*, is reversed (only one side of the switch is used), the motor operates the crank and the image of the moon moves from one junction of the thermocouple to the other, thus making the deflection. The snap switch, *X*, controls the microscope cover-glass, moving it into or out of the beam for the separation of planetary heat from the reflected sunlight. The pneumatic check, *M*, prevents jar, which might destroy the thermocouple or cover-glass when the magnet, *N*, acts.

The apparatus was designed and constructed nearly ten years ago for use with a coelostat; but the coelostat appeared to introduce false deflections which could not easily be allowed for, particularly in daylight sky or when sunlight fell upon it. In the autumn of 1933 it was attached to the 6-inch telescope mounting in order that it might be pointed directly at the moon and thus avoid these disturbances.

OBSERVATIONS

The observations consisted of (1) a set of deflections on the moon, five free and five with the cover-glass in place; (2) a set of five deflections on a test lamp with the cover-glass in the beam. The test lamp was placed on the 60-foot tower telescope at a distance of 71.32 m. The tower itself, however, gave a considerable deflection, owing to its self-radiation, which was included in the free deflection on the test lamp. The deflection with the cover-glass was not affected by this long-wave radiation, and ordinarily only this deflection was used, since the principal purpose of the comparisons was to test the constancy of the sensitivity of the apparatus from night to night.

On part of the nights only one or two sets of deflections were made, when the moon was near meridian; but on many nights several were made at various air-masses to determine the atmospheric extinction.

On such occasions the air-mass meter was especially helpful, since the observations could be made for uniform intervals of air-mass, which greatly improves the plots from which the extinction is determined.

REDUCTION OF THE OBSERVATIONS

It has been pointed out[1] that when we consider the radiation from a planet, the following relations hold:

$$F=B+R\,, \tag{1}$$

$$Cg=BTr+Rtr\,, \tag{2}$$

$$B=\frac{Ftr-Cg}{tr-Tr}\,, \tag{3}$$

$$R=\frac{Cg-FTr}{tr-Tr}=\frac{Cg-BTr}{tr}\,, \tag{4}$$

where F is the free deflection (the deflection without the cover-glass in the beam); Cg the deflection with the cover-glass; B and R the parts of F due to planetary heat and reflected sunlight, respectively; Tr and tr the transmissions of the cover-glass for the planetary heat and the reflected light. It has also been shown that for moonlight the value of tr is very nearly 0.90.

The value of Tr as a function of the temperature of the planet has been tabulated,[6] but may be computed from the empirical formula

$$Tr=4\times 10^{-5}(T-264^\circ)^{3/2}, \qquad 264^\circ<T<700^\circ\,. \tag{5}$$

For $T<264^\circ$, $Tr=0$. Below 700° K this equation gives the tabular value of Tr to the second decimal, which is sufficient for most purposes. We may estimate the maximum value of Tr, which occurs at full moon, from the following argument. The distribution of radiation over the full moon[1] is represented by

$$E=a\cos^{3/2}\theta\,,$$

where θ is the angular distance of a point on the moon from the subsolar point. Integrating this equation over the disk, we find that the

[6] Pettit and Nicholson, *Mt. W. Contr.*, No. 392; *Ap. J.*, **71**, 102, Table I, 1930.

average energy is three-fourths the maximum value at the subsolar point. Since the temperature at the subsolar point is 374° K, the temperature corresponding to the average over the surface, by the fourth-power law, is 348° K, if we may regard the mixture of black-body energy emission as being itself a black-body emission. From equation (5) we see that Tr therefore has a maximum value of 0.031 and is zero when $T < 264°$. As a first approximation we may consider Tr equal to zero, whereupon equations (3) and (4) become

$$B_0 = F - 1.11\ Cg\,, \tag{6}$$

$$R_0 = 1.11\ Cg\,. \tag{7}$$

The observations were all reduced with equations (6) and (7) and the mean curves corrected whenever Tr became a sensible quantity.

It might be thought at first sight that equations (1) and (3) could be used to obtain R explicitly. This would necessitate a complete reduction and discussion of all the data for B before the work could proceed, which would not be economical of the computer's time; and, since the values of R_0 have already been formed in the preliminary determination of B_0 and B, their discussion can be carried on parallel with that of B_0. The same explanation applies to the combination of equations (1) and (4). It was decided therefore to treat the two variables alike and to correct the mean curves for Tr in the final solution.

ATMOSPHERIC EXTINCTION

On a number of nights the reflected light and planetary heat were observed with the moon at various zenith distances. Plots of log R_0 and log B_0 against sec Z (air-mass) are shown in Figure 2 for January 30. Although some curvature is noticeable, especially for the planetary heat, the plots are essentially straight lines. The logarithm of the transmission or extinction for unit air-mass can be obtained from these plots. For twenty-two nights on which suitable runs were made, the average transmissions for R_0 and B_0 were 0.90 and 0.87, respectively, and the equivalent extinctions 0.11 and 0.15 mag., respectively.

A plot of the individual determinations against phase angle, while

showing some fairly definite connection, is discordant because positive and negative phase angles do not agree in the general run, as might be expected since the equivalent temperatures of similar phases are substantially the same. The agreement is much better for reflected light than for planetary heat, however.

The atmospheric absorption and the extinction as used here are distinct entities. The atmospheric absorption of planetary heat is

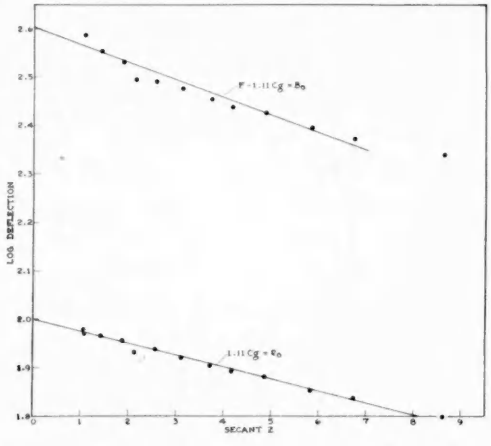

FIG. 2.—Plots to determine the atmospheric extinction. Planetary heat B_0 and reflected light R_0 separated by the cover-glass.

nearly complete except in the 8–14 μ transmission band, while the effect of change in air-mass which measures extinction is principally confined to the wings of this band and is therefore much reduced. While the extinction amounts to only about 0.15 mag., the atmospheric absorption exceeds 1 mag.

Since in the case of reflected light from the moon we have a combination of scattering and absorption phenomena, the absorption and extinction are more nearly comparable, the absorption being about 0.4 mag. and the extinction 0.11 mag.

On account of this relationship between absorption and extinction, the observations plotted in Figure 3 are those extrapolated to the zenith (unit air-mass) either by the observed extinctions for the night or by the mean value if only one or two observations were made. The upper curve (the heavy full line) in Figure 5 has been ob-

tained from the plot of B in Figure 3 by applying the absorption coefficients of the atmosphere.

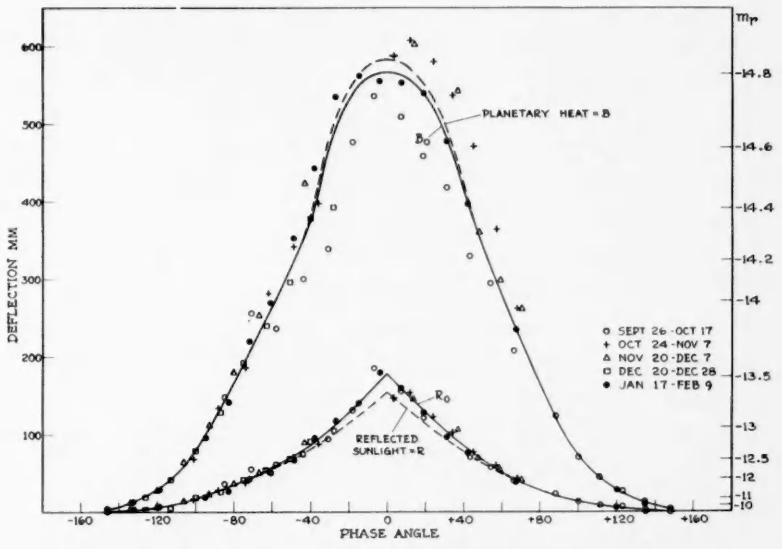
DEFLECTION MM
PHASE ANGLE
PLANETARY HEAT = B
REFLECTED SUNLIGHT = R
SEPT 26 - OCT 17
OCT 24 - NOV 7
NOV 20 - DEC 7
DEC 20 - DEC 28
JAN 17 - FEB 9

FIG. 3.—The full-line curves represent the reflected light R_0 and the planetary heat B_0 separated by the cover-glass of the thermoelectric lunar radiometer and are for the zenith on Mount Wilson. The dotted lines are R_0 and B_0, corrected for the lunar planetary heat transmitted by the cover-glass.

GEOMETRICAL CORRECTIONS

The data from the ephemeris give the position of the moon relative to the center of the earth. The value of sec Z for the position of the observer may be found by the formula

$$\sec Z = \sec\left(Z_0 + \sin^{-1}\frac{\sin Z_0}{\sqrt{3601 - 120\cos Z_0}}\right), \qquad (8)$$

where the last term is the parallax for the mean distance of the moon (60 terrestrial radii). For the purpose of computing the air-mass the empirical formulae

$$\log(\Delta \sec Z_0) = 1.7 \log(\sec Z_0 - 1) - 1.37, \qquad \sec Z_0 < 8, \qquad (9)$$
$$\sec Z = \sec Z_0 + \Delta \sec Z_0,$$

are more convenient. The value of Δ sec Z_0 is 0.1 air-mass for sec Z_0 = 2.6, 0.2 for sec Z_0 = 3.5, and becomes 1.0 air-mass at sec Z_0 = 7.3.

The correction to sec Z_0 given by equation (9) applies to the center of the moon regarded as a disk. An additional, but much smaller, correction should be applied when the phase angle is large, since the actual center of gravity of the emitted lunar radiation is off center. If both rising and setting moon are observed to obtain the atmospheric extinction, this correction will be nullified; and in the present work its value does not exceed 0°.2, which might make a difference of 0.19 in the air-mass at sec Z_0 = 7.3, where Δ sec Z_0 becomes 1.0 air-mass. This correction has been neglected. Had sec Z_0 been linear in equation (9), it could have been neglected, as only the zenith values of R_0 and B_0 are used.

Since the entire image of the moon falls on the receiver, a correction must be made for the size of the image, which varies with diurnal parallax. To reduce the observed deflection to what it would be if observed at the center of the earth, we apply the correcting factor

$$C = 1.0003 - \frac{1}{30 \sec Z_0}, \qquad (10)$$

which assumes the moon to be at a mean distance of 60 terrestrial radii. C varies between 1.0003 when the moon is on the rational horizon and 0.967 when in the zenith.

A third correction must be applied to reduce all observations to mean lunar and solar distances. This factor was applied in the customary manner to the final values of B_0 and R_0 reduced to the zenith.

PHASE ANGLE

The phase angle is given by

$$\cos i = \cos [180° - (M - S - E)] \cos \beta ,$$

where β is the latitude of the moon, E its elongation from the earth as seen from the sun, and M and S the longitudes of the moon and sun, respectively. The effect of β can usually be neglected except near full phase, and E cannot exceed 9′. Since the plots of B_0 and R_0

are made on co-ordinate paper divided into 2° units, the simpler formula

$$i = 180° - (M - S) \tag{11}$$

was used for most cases. The error in (11) does not exceed 1° when $+13° < i < -13°$.

During a series of measurements for atmospheric extinction, which may cover several hours, the phase angle changes. Since the plots are extrapolated to the zenith and the phase angle is computed for the moon at meridian transit, this change in i has no effect on the result.

PLANETARY HEAT AND REFLECTED LIGHT

The values of B_0 and R_0 plotted in Figure 3, which were obtained from the galvanometer deflections for each night, have been reduced to a standard test-lamp deflection of 59.7 mm. They are zenith values, reduced to the center of the earth, and correspond to the mean distances of the sun and moon. The heavy full lines represent the average values of these plots. We must now correct these curves for the planetary heat transmitted by the cover-glass, and in so doing obtain the curves of B and R.

Substituting 0.9 for tr in equations (3) and (4), we find the following simple relations

$$B = \frac{B_0}{1 - 1.11\, BTr}, \tag{12}$$

$$R = R_0 - 1.11\, BTr. \tag{13}$$

Since the temperature of the moon corresponding to average radiation from its surface is 348° at phase angle 0°, we may obtain a first approximation for Tr by assuming that the plot of B_0 in Figure 3 closely represents B and, applying the fourth-power law, obtain the temperature for each phase angle, and thus Tr from equation (5). It is found that Tr varies from 0.031 for $i = 0$ to zero for $i = \pm 72°$. The broken lines in Figure 3 are the curves for B and R obtained in this manner from equations (12) and (13). They deviate so little from B_0 and R_0 that a second approximation is unnecessary.

It will be noted that the corrected curves for both planetary heat

and reflected light are a maximum at full moon and sensibly symmetrical about phase angle $i = 0°$. At quarter phase the planetary heat has fallen to 17 per cent of the full-moon value, while the reflected light is 15 per cent. The two corrected curves have been transferred to Figure 4 as heavy continuous lines. The light-line curves in this figure show the results obtained by Lord Rosse. The

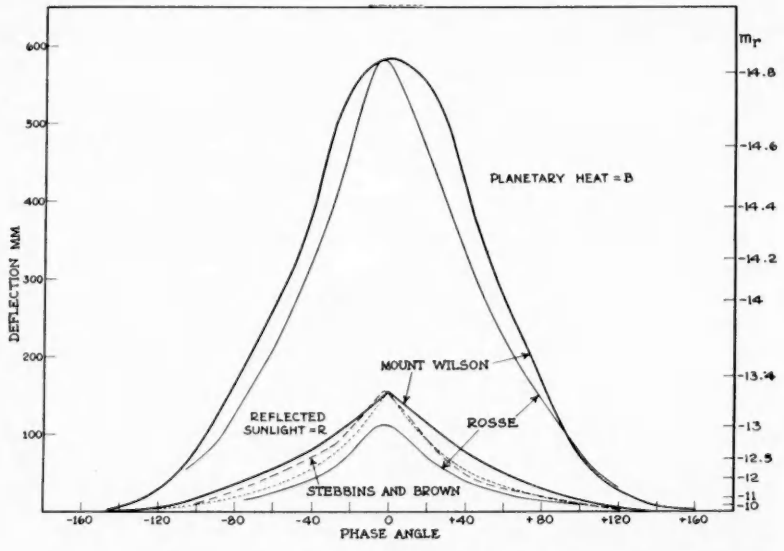

FIG. 4.—Heavy full-line curves, *R* and *B*, observed at Mount Wilson; light full-line curves, observations by Lord Rosse. The broken line is *R*, observed by Stebbins and Brown with the selenium cell; the dotted line, *R*, by Rougier with the photo-electric cell and amplifier.

broken line in the plot of reflected light is the curve obtained by Stebbins and Brown,[3] and the dotted line, that of Rougier. The asymmetry found by some observers does not show to any great extent in the curves obtained with the thermocouple on Mount Wilson, which in this respect agree with Rougier's recent work. The ordinates of Lord Rosse's curve of reflected light have been multiplied by 1.11 to correct for reflection from the glass plate. Further corrections should be made for absorption in the glass, the thickness of which is unknown, for the reflecting power of the mirrors used (speculum), and for the greater atmospheric absorption at Birr

Castle. If these corrections were known, the curve would probably agree much better with that observed on Mount Wilson.

Before discussing the appearance of these curves outside the atmosphere, it will be convenient to replace the scale of galvanometer deflections by one of radiometric magnitude. It has already been shown[1] that the radiometric magnitude of planetary heat per square second of arc, $m'_r+\Delta m'_r$, is given by

$$m'_r+\Delta m'_r=26.12-10\log T+\Delta m_r-2.5\log(1-1.11\,Tr)\,, \qquad (14)$$

where $\Delta m'_r$ is a correction which makes the temperature of a point on the moon determined with this equation equal to that obtained from the amount of the absorbed solar radiation which can be accounted for. It is supposed that the existence of this correction is due largely to inaccurately known atmospheric absorption Δm_r.

The values of m'_r and $\Delta m'_r$ as a function of T have been given in tabular form, but they may be represented by the simple equation

$$m'_r+\Delta m'_r=\frac{1545}{T}-2.6\,, \qquad 140^\circ<T<500^\circ \qquad (15)$$

within 5° of the tabular values of T. Between 400° and 800° K the formula

$$m'_r+\Delta m'_r=\frac{1864}{T}-3.3\,, \qquad 400^\circ<T<800^\circ \qquad (16)$$

represents the higher temperatures very well, there being no sensible error up to 700° K. Formula (14), or the empirical formulae (15) and (16), give the radiometric magnitude of the planetary heat per square second of arc at the zenith on Mount Wilson as a function of absolute temperature. Further, the radiometric magnitude corresponding to a 1 mm deflection may be determined by the use of a comparison standard. The radiation from a condensed filament Peerless Mazda lamp emitted at right angles to the filament was compared with that from a Hefner lamp in the laboratory at a distance of 2 m, with the result

$$\frac{\text{95 watt Peerless Mazda}}{\text{Hefner lamp}}=5.78\,.$$

Since the Hefner lamp radiates 156×10^{-5} cal cm^{-2} min^{-1} at 1 m distance, the Mazda lamp radiates 9.02×10^{-3} cal cm^{-2} min^{-1}, which is 83 per cent of the power input. Such a lamp working at 95 watts was set up beside the usual test lamp on the 60-foot tower telescope. After deducting the false deflection due to the tower, the value of A in the equation $F=ACg$ was found to be 1.13. A test of the 95-watt lamp in the laboratory at a distance of only 56 cm, where no false deflection was observable, gave $A=1.12$. It thus appears that the procedure of subtracting the false deflection on the tower to obtain the free deflection on the light is correct, and that for the lamp at normal voltage we may obtain the free deflection from the equation

$$F=1.12\,Cg\,.$$

It was also found that the deflection for the free radiation from the 95-watt lamp was equal to the radiation transmitted by the cover-glass from the test lamp multiplied by 1.165. Since all the observations in Figure 3 have been reduced to a common test-lamp sensitivity of 59.7 mm cover-glass deflection, the equivalent 95-watt lamp deflection for a distance of 7132 cm is 69.6 mm. The value E in energy units for a 1-mm deflection is

$$E'=\frac{9.02\times10^{-3}}{R^2d}=2.547\times10^{-8}\text{ cal cm}^{-2}\text{ min}^{-1}\,, \qquad (17)$$

where R is the distance of the lamp in meters and d the deflection corresponding to 95 watts. The relationship between energy and radiometric magnitude is

$$E'=17.3\times10^{-12}\times2.512^{-m_r}\text{ cal cm}^{-2}\text{ min}^{-1}\,; \qquad (18)$$

hence the radiometric magnitude of lunar radiation for any deflection in Figure 3 is given by

$$m_r=-26.905-2.5\log E'\,. \qquad (19)$$

The scale of radiometric magnitude for the whole moon used for Figure 3 was obtained from equations (18) and (19).

The propriety of using the inverse-square law in equation (17), when the test lamp is at so great a distance, may be questioned. Calculation shows that for a distance of 71.32 m the infra-red absorption bands of CO_2 would introduce a possible correction of 10 per cent.

To test this matter, deflections on a lamp at this distance were compared with deflections on the same lamp at 2 m with the light

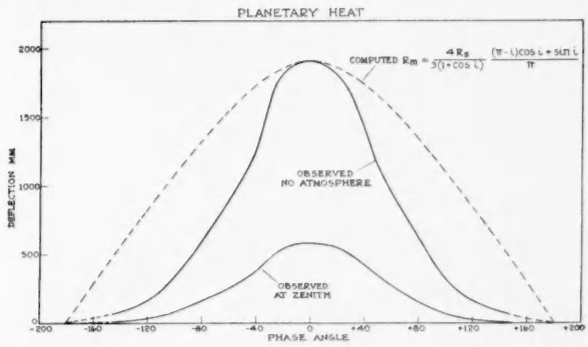

FIG. 5.—Planetary heat from the moon. Below, at the zenith on Mount Wilson; above, the full line is the observed curve for no atmosphere; the broken line, the theoretical curve.

cut down by a sector to 1 per cent. The sector was 16 inches in diameter and the opening was ruled on a circle dividing engine, then measured on the same instrument after cutting. In the zone employed, the actual sector factor was found to be 0.0098. On one occasion a larger sector of factor 0.0500 was used. Tests made on three clear nights in Pasadena showed nearly 10 per cent on one occasion, 5 per cent on another, and a null result on the third. The value obtained on Mount Wilson was 3 per cent. Altogether, it may be questioned whether this correction is real, and, if so, whether it is variable. It has not been used in the following computations.

The lunar energy outside the atmosphere as shown in Figure 5 may be obtained by subtracting Δm_r from the radiometric magnitude of lunar planetary heat per square second of arc $(m_r' + \Delta m_r')$. This may be obtained from Figures 3 and 4 by adding the area of the moon in square seconds expressed in magnitude, 16.09. The

relation between these variables has already been given,[6] but, for convenience, is reproduced in Table I.

The effect of Δm_r, the correction for atmospheric absorption, is to increase considerably the energy at crescent phases compared with that at full phase.

It can easily be shown that if the moon were a smooth non-conducting sphere acting like a black body, receiving and emitting

TABLE I

$m'_r+\Delta m'_r$	Δm_r	$m'_r+\Delta m'_r$	Δm_r
12 mag.	6.35 mag.	4 mag.	1.74 mag.
10	5.08	3	1.45
8	3.81	2	1.30
7	3.20	1	1.28
6	2.66	0	1.30
5	2.16	−1	1.25

energy proportional to the cross-section of the beam for every element of its surface, the phase-radiation relation for planetary heat would be given by

$$R_m=\frac{4\,R_s}{3(1+\cos i)}\,\frac{(\pi-i)\cos i+\sin i}{\pi}, \qquad (20)$$

where R_m is the mean intensity of the planetary heat over the apparent surface projected on the celestial sphere, R_s the intensity at the subsolar point, and i the phase angle. Tables of the second factor of this function have been given by Müller.[7] The locus of points computed by this equation shown in Figure 5 is directly comparable with the observed curve for no atmosphere.

The ratio of the planetary heat observed outside the atmosphere to that computed from equation (20) is unity when $i=0$, falls to 0.5 when $i=\pm 75°$, to 0.2 when $i=\pm 160°$, and probably decreases up to $i=180°$. This large deviation of the observed from the computed intensity of planetary heat is possibly due, in part at least, to the occulting effect of the mountains on the very rough surface of the moon and, in part, to its transparency.

[7] *Photometrie der Gestirne*, Anhang, Table I, 1897.

RADIOMETRIC MAGNITUDE OF MOONLIGHT AND PLANETARY HEAT

The radiometric magnitude of moonlight and of planetary heat may be read directly from Figure 3, or may be computed from the deflections. For full moon the deflections on reflected light and planetary heat, after correcting R_0 and B_0 for transmitted planetary heat by equations (12) and (13), are 154 and 584 mm, respectively. Multiplying by E' in equation (17), we obtain for the intensity of radiation

$$E'_R = 39.2 \times 10^{-7} \text{ cal cm}^{-2} \text{ min}^{-1},$$

$$E'_B = 149 \times 10^{-7} \text{ cal cm}^{-2} \text{ min}^{-1}.$$

Applying equation (19), we find the radiometric magnitude of moonlight at full moon, M_{rR}, and of planetary heat, M_{rB}, to be

$$M_{rR} = -13.4, \qquad M_{rB} = -14.8.$$

The sum of E'_R and E'_B gives for the radiometric magnitude of the whole radiation for the full moon

$$M_{r0} = -15.0.$$

In a previous paper[1] it was shown that integrating the drift-curves across the full moon observed at the 100-inch telescope gave the value $M_{rR} = -13.3$ mag. Since the corresponding mean phase angle was 12°, a correction of -0.19 mag. (Fig. 3) should be applied, making $M_{rR} = -13.49$ mag. The radiometric magnitude of the whole radiation of the full moon, according to these earlier data, would therefore be -14.9. Considering the approximate nature of the integration of the curves and that the data applied to a specific case only, we may regard the agreement as fair.

The visual magnitude of the full moon is usually[8] taken to be -12.55. If the heat index of moonlight can be determined, a value of the visual magnitude can be found from the present measures.

[8] Russell, Dugan, and Stewart, *Astronomy*, Vol. 1, Table IV, 1926.

The relationship of heat index to color index or to water-cell absorption may be used for this purpose.

It has been shown in a previous paper[9] that the color index of the moon on the Mount Wilson scale is 0.92 mag., corresponding to spectral class dKo, for which the observed heat index is 0.55 mag. The color index obtained from E. S. King's photographic magnitude and the above visual magnitude is 1.18 mag., corresponding to dK6, approximately. This result gives $HI = 1.2$ mag., a value almost certainly too high.

The water-cell absorption of moonlight may be obtained from the drift-curves[1] of lunar radiation made with the 100-inch telescope. If we correct the curve made with the cover-glass by equation (13), multiplied by 1.11, we find for the curves shown[10] that $WC = 0.61$ mag., which corresponds to $HI = 0.73$ mag. in the table of observed coefficients for dwarf stars.[11]

On February 22, 1923, a mountain just off the terminator on the dark side of the moon whose crest was illuminated by the sun was observed at the 100-inch telescope with the thermocouple[12] having a microscope cover-glass window. Since this mountain must have been at a very low temperature, no sensible part of the deflections can be attributed to planetary heat. The observation gave $WC = 0.63$ mag., corresponding to $HI = 0.77$ mag. on the dwarf branch.

Since the color index is not a sensitive means of finding the heat index, the values obtained with it should perhaps receive but nominal weight. The true heat index is probably in the neighborhood of 0.75 mag. For this value we have for the visual magnitude of the moon

$$M_v = HI + M_{rR} = -12.63 ,$$

in fair agreement with -12.55, the value usually given. Since there is at present little reason to suppose that HI is a function of phase angle, the curve for M_v should have the same form as that for M_{rR}.

[9] *Pub. A.S.P.*, **38**, 242, 1926.

[10] Pettit and Nicholson, *Mt. W. Contr.*, No. 392; *Ap. J.*, **71**, 102, Fig. 3, 1930.

[11] *Mt. W. Contr.*, No. 369; *Ap. J.*, **68**, 279, Table V, 1928.

[12] S. B. Nicholson assisting.

TRANSMISSION OF LOW TEMPERATURE RADIATION THROUGH OZONE

An absorption band of ozone occurs at 10 μ in the middle of the 8–14 μ transmission band of water vapor through which planetary heat is measured. The thickness of atmospheric ozone is approximately 0.3 cm at N.T.P. and varies some 50 per cent. One may ask what effect this variation may have on the measured planetary heat from the moon.

Since the temperature of the moon is in the neighborhood of that of boiling water, and since the radiation of the moon is measured with reference to space, we may simulate the conditions of observation by measuring in the laboratory the transmission of ozone for radiation from boiling water relative to that of liquid air.

To do this, a tube 130 cm long was closed at each end with rock-salt windows of 5 cm clear aperture and 6 mm thick. Inlet and exit stopcocks were attached near the ends. Ozone was produced in a Brodie (Berthelot) ozonizer fed with commercial oxygen, which was passed through a sulphuric acid dryer and a calcium chloride tower. A 50,000-volt transformer produced the silent discharge across the space in the ozonizer. Samples taken from the exit stopcock of the ozone tube and analyzed by the usual iodine method showed an ozone content of 2 cm at N.T.P.

A blackened can of water, kept boiling by an electric heater immersed in it, was placed on a wooden slide beside a beaker of liquid air, a wood block separating the two. By moving the slide to and fro, the ozone tube could be exposed alternately to radiation from boiling water and from liquid air. The radiation passing through the ozone tube was received by a rock-salt lens of 1 inch aperture and 2 inches focal length, which formed an image of the blackened can or the beaker on a receiver of a thermocouple.

Deflections were observed first with oxygen in the tube and then with ozone, after analysis. It was found that 93 per cent of the radiation passed through. While the ozone in the atmosphere is only one-sixth that used here, it is effective on the center of the 8–14 μ transmission band of water vapor, which includes only one-fourth the radiation emitted by the moon. The absorption of lunar planetary heat due to atmospheric ozone is therefore about 4 per cent and may

vary from about 3 to 6 per cent. Probably the whole effect on a considerable number of lunar radiation measurements would not be serious.

I am indebted to Dr. Fred E. Wright for measurements of lunar radiation throughout an entire cycle of phases. I am also indebted to Mr. Earl Karr and Mr. Glenn Moore for many of the measurements included in the program, and to Miss L. Ware for the reduction of the entire series.

Carnegie Institution of Washington
Mount Wilson Observatory
July 1934

REMARKS ON LUNAR RAY CRATERS

By S. G. HACKER and J. Q. STEWART

ABSTRACT

A short bibliography and résumé of various suggestions concerning the formation of lunar rays are given. The suggestion that the rays were formed by ejection from the associated craters is examined quantitatively, and some aspects of the possible mode of formation are discussed. It is found that the minimum initial velocity required to produce the longest ray from Tycho is 1 km/sec., taking into account the moon's curvature. A "typical ray crater" has a (1) bright center floor, (2) dark annulus, (3) bright nimbus, (4) ray system. Assuming the projection to have taken place in the most efficient manner, the energy required to form the various features of Tycho is calculated (Table I). These energies are found to furnish no criterion of distinction between the volcanic and the meteoritic suggestions of formation of these craters, but are probably compatible with both.

An equal-area map of the moon shows the distribution of ray- and light-surrounded craters listed by Elger. The distribution is analyzed by octants. There is a decided tendency for these craters to appear on the maria, probably owing to their better visibility there by reason of the contrast with the dark background. There is, however, no tendency toward grouping on the maria as between one octant and another. Similarly, the distribution off the maria is also random. The randomness of distribution favors the suggestion that the ray craters are of meteoritic origin.

Any successful theory of the origin of the lunar rays must account for the following characteristics: (1) these rays are always associated with craters, and (2) emanate more or less radially from them; (3) they pass continuously over all sorts of country; (4) their visibility decreases with the angle between the line of sight from the earth and the direction of illumination from the sun (phase effect). (5) With the 100-inch telescope the rays are seen[1] as the illuminated sides of low mounds.

Many explanations of the rays have been attempted. Tomkins[2] suggested that they might be alkali tracts similar to those which he found in India: one of these was 900 miles long, 20 miles wide at the lower end, and 60 miles across at the other. He suggested that, owing to evaporation of moisture at some early time, alkali salts came to the lunar surface as white efflorescences taking the configuration of the country above the source of the material. In consequence of subsequent alternations of temperature the original alkaline crystals, in the absence of atmosphere, broke up into fine powder and remained visible.

[1] Pease, *Pub. A.S.P.*, **36**, 346, 1924.

[2] *J.B.A.A.*, **18**, 107 and 361, 1908.

Jeffreys[3] at one time suggested that the rays are magma-filled cracks. The cracks were produced by tension due to cooling in the top layers of the lunar crust immediately following solidification. They grew downward and finally, by reason of the decrease in pressure, fusion of the lower rocks—previously below their melting-point—took place, and the magma was forced up the cracks by hydrostatic pressure. This is practically the same suggestion that Nasmyth[4] also made.

One might say that these are typical explanations of the origin of rays by surface and subsurface phenomena. Then there are the suggestions that the rays were formed by material falling down upon the surface. Chacornac seems to have been the first to suggest that the rays might be due to the deposition of fine white powder thrown out from the craters by volcanic action, upon a background of lower albedo. W. H. Pickering[5] in 1892 recalled this explanation to mind. In 1919 airplane photographs of craters formed by exploding bombs dropped from planes led Ives[6] to believe that the lunar rays represent material ejected by meteoritic impact rather than by the volcanic action which Chacornac supposed.

Buell and Stewart[7] found that rays formed in the manner suggested by such an ejection theory would yield the phase effect. Their experimental study led to the conclusion that a lunar ray consists of a streak of scattered rocks of dark material matching in albedo the average surface of the moon, with the lighter-colored powder resulting from the fragmentation of the rocks spread among these. It is assumed that this material was ejected from the associated craters either by volcanic action (Chacornac) or by meteoritic impact (Ives).

It has recently been objected[8] that patches, rather than rays, would be formed by ejection of the material in this way—that the odds would be high against the formation of a ray by "one eruption

[3] *The Earth* (1924 ed), p. 147.

[4] Nasmyth and Carpenter, *The Moon* (London, 1874), p. 133.

[5] *M.N.*, **53**, 279, 1893.

[6] *Ap. J.*, **50**, 245, 1919. Attention is explicitly called to the fact that the photographs reproduced in this paper show clearly the actual formation of ray systems. One of the craters shown has a pronounced central peak.

[7] *Pop. Astr.*, **40**, 264, 1932. [8] *J.B.A.A.*, **42**, 308, 1932.

of a number of rocks, the individuals of which fall with remarkable uniformity of spacing and direction along a straight line, or a series of eruptions which no less remarkably distribute the rocks in this uniform way." But at present we know little or nothing about splashes, and the only answer that can be given now is that the photographs by Ives (*loc. cit.*) show unequivocably the formation of rays.[9]

It may be that at the time of the formation of a lunar ray crater the surface cracked radially in the immediate region around the crater and that these cracks served to guide the ejected material more or less uniformly within corresponding lateral limits. Until more becomes known about the configurations resulting from splashes, such criticisms and such answers to them as the foregoing can only be counted as personal opinion.

Meanwhile, it is of some interest to examine quantitatively the suggestion that the rays were formed by ejection from the associated craters, and to study the distribution of ray craters on the lunar hemisphere.

Taking into account the curvature of the moon's surface, we first compute the minimum initial velocity at the most favorable angle of projection to form the longest ray, namely, the one from Tycho down across the Mare Serenitatis which covers a range of 78° (order of 1300 miles). This minimum velocity turns out to be only about 1 km./sec.

This value for the velocity does not exclude either the volcanic or the meteoritic hypothesis, being compatible with both. According to the meteoritic explanation, very much greater energies are available, even exceeding the velocity of escape of 2.4 km/sec.[10] In the case of terrestrial volcanoes[11] a velocity of 1 km/sec. is not impos-

[9] Whether or not "duds" with sufficient energy could produce the same effect as the explosive bombs is not known, and no attempt is made here to discuss this or to criticize Ives's argument of the explosive action of lunar meteorites. See also F. R. Moulton, "Some Quantitative Aspects of the Fall of Meteors," *Pub. A.A.S.*, **6**, 372, 1931.

[10] This, together with the fact that there are so few very long rays on the moon, might be submitted as a possible argument against the meteoritic theory. But there are too many unknown factors for definiteness pro or con.

[11] Terrestrial volcanoes seem to be of two types: explosive, as at Lassen Peak, and lava-producing, as at Kilauea. The character of a given volcano, Day believes, depends on the gas content of the crystallizing magma.

sible. A block of rock was thrown from the Krakatoa crater[12] for a distance of 30 miles and is estimated to have risen 31 miles in its flight. Neglecting air resistance and the size of the rock, $v = 1$ km/sec. and $\alpha = 76\frac{1}{2}°$. In the case of Lassen Peak, California (May, 1915),[13] blocks of rock the size of a man's hand were thrown for 10 miles, and horizontal blasts through the northeast side of the inclosing cone hurtled blocks of rock for more than 4 miles. Again v is of the same order. In general the maximum macroscopic velocity that a gas at a certain pressure and temperature can impart to a body ejected by it is of the order of the velocity of sound in the gas. If the gas is subject to the adiabatic law,[14] then

$$q^2 - q_0^2 = \frac{2}{\gamma - 1}(c_0^2 - c^2),$$

where c is the velocity of sound and q the fluid velocity at pressure p, and where c_0 and q_0 are the corresponding velocities at p_0. If p_0, which may be taken as the pressure in the discharging vessel, is very large, it may be legitimate to put $q_0 = 0$; and as p diminishes, q increases, but only up to a certain maximum attained when $p = 0$. If $\gamma = 1.408$, this limiting velocity is $2.214c_0$.

If Tycho, Olbers, and Anaxagoras may be said to represent the most general type, the "typical ray crater" may be defined as one having the following characteristics: (1) a bright crater floor; (2) a dark annulus outside and around the crater wall; (3) a bright nimbus beyond and around the annulus; (4) a ray system beginning at, and emanating from, this nimbus. Not all of the ray craters have all these features: Kepler, which is a notable example, has a bright floor but no dark annulus; the bright nimbus begins immediately outside the crater wall and stretches for 28 miles on the north and elsewhere from 50 to 70 miles, thereby covering about 9,000 square miles. The great ray system originates in this nimbus. Some craters have nimbi but no rays; these are called below "light-surrounded," and are in-

[12] Krakatoa Committee Report, Royal Society, 1888; Iddings, *Problems of Volcanism*, p. 4.

[13] Day, *J. Franklin Inst.*, **200**, 161, 1925.

[14] *Bull. Nat'l. Res. Council*, "Report on Hydrodynamics," No. 84, 529, 1931.

cluded in the class of ray craters. Still other craters have rays but no nimbi.

On the present explanation the bright nimbi may be explained as being material thrown out in the same manner and of the same stuff as the rays but under a set of initial conditions more or less uniform. In some cases the prevailing initial conditions might have been such that there was a definite minimum range of projection of the same order as the width of the dark annulus. The bright crater floor can be explained as being due to material thrown back inside the crater;

TABLE I

TYCHO

Feature	Radius (Mi.)	Area (Cm^2)	Volume (Cc)$\times 10^{18}$	Assumed Mean Initial $v\times 10^4$ Cm/Sec.	Energy Ergs$\times 10^{27}$
Pit	27	6×10^{13}	10.9	.....	0.3
Wall	.....	.....	0.5	.....	0.01
Annulus	52	.....	.....	.....	.....
Nimbus	90	3×10^{15}	2.4	5	6.0
Rays	.....	3×10^{15}	2.4	8	15.4
Sum	.....	.....	5.3	.....	21.4

this is a bit easier to visualize on the meteoritic explanation, the material being thrown inside from the edges of the impinging meteorite.

Assuming the projection to have taken place in the most efficient manner, the energy required to form the various features of Tycho is given illustratively in Table I. The various radii are in miles; the other values are in c.g.s. units. Since the rays are seen with the 100-inch telescope at Mount Wilson as the illuminated sides of low mounds, their height is taken crudely as 25 feet. The density used is 2, and the nimbus and the rays are taken to cover the same area and to be of the same volume. This may be too liberal an estimate for the rays, giving too large a value for the energy required to form them. The energy assigned to form the crater wall is no doubt much lower than was actually required: the value given represents merely the

potential energy of a wall of density 2, of height 6000 feet,[15] and with both sides at a pitch of 60°. The great amount of energy expended in the rumpling of the wall and the surrounding region is neglected.

Since no distinction is furnished between the meteoritic and volcanic hypotheses by these energy relations, it is of interest to study the distribution of the ray craters. The distribution of lunar craters of all kinds is known not to be a random one. On the meteoritic ex-

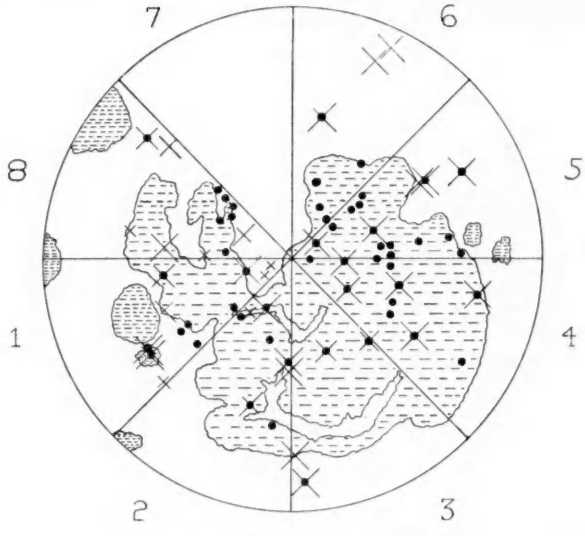

FIG. 1.—Distribution of ray craters

planation we certainly expect a random distribution. Figure 1 is an equal-area projection of the moon's surface. The data are taken from Elger's *The Moon* (1895) and are presented as an indicative, and not as an exhaustive, study of the distribution.

The black dots represent light-surrounded craters; crosses alone are craters with rays but without nimbi; crossed dots are craters with nimbi and with rays.

In Tables II–IV the ray- and light-surrounded craters are not distinguished from each other. Table II gives the distribution of these "ray craters" by octants with respect to the percentage of area of

[15] Schmidt, *Charte der Gebirge des Mondes* (Berlin, 1878), p. 290. The crater pit is also 6000 feet deep.

each octant covered by maria, as observed and as computed for a random distribution.

The distribution in each octant with reference to the maria and non-maria is, therefore, not random: only one third of the lunar

TABLE II

DISTRIBUTION OF RAY CRATERS WITH REFERENCE TO MARIA

Octant	Percentage of Area Covered by Maria	Obs. No. Off	Obs. No. On	Comp. No. On	O−C On
1	24	5	7	2.9	4.1
2	47	1	7	3.8	3.2
3	57	1	3	2.3	0.7
4	71	0	10	7.1	2.9
5	38	3	13	6.1	6.9
6	15	3	4	1.1	2.9
7	0	0	0	0.0	0.0
8	21	4	8	2.5	5.5
Sum	34	17	52	25.8	26.2

TABLE III

RANDOMNESS ON MARIA

Octant	Percentage of Total Maria	Obs.	Comp.	O−C
1	9	7	4.6	2.4
2	17	7	8.9	−1.9
3	21	3	10.9	−7.9
4	26	10	13.5	−3.5
5	14	13	7.2	5.8
6	5	4	2.8	1.2
7	0	0	0.0	0.0
8	8	8	4.1	3.9
Sum	100	52	52.0	0; |3.3|

hemisphere is covered by maria, but 52 of the 69 ray craters are on the maria. This apparent non-randomness of the distribution may be explained: the bright rays and nimbi are more readily seen on the dark background of the maria than on the bright background of the non-maria. The seventh octant is noteworthy in this respect. Except for

a very small corner near the center, it is free of maria; and Elger lists no ray craters on it. The ray craters simply may be hard to distinguish off the maria. Those that are seen there are either among the grandest systems on the moon or appear very faint.

The question then arises whether the distribution of the ray craters is random on the maria alone and random on the non-maria

TABLE IV

RANDOMNESS OFF MARIA

Octant	Percentage of Total Non-Maria	Obs.	Comp.	O−C
1	14	5	2.4	2.6
2	10	1	1.7	−0.7
3	8	1	1.4	−0.4
4	6	0	0.9	−0.9
5	12	3	2.0	1.0
6	16	3	2.7	0.3
7	19	0	3.2	−3.2
8	15	4	2.6	1.4
Sum	100	17	16.9	0.1; 1.3

alone. Tables III and IV give the answer as definitely affirmative. In so far as the number of ray craters listed in Elger may be taken as indicative of all ray craters that actually exist, the suggestion thus is favored that the ray craters are of meteoritic origin.

PRINCETON UNIVERSITY OBSERVATORY
PRINCETON, NEW JERSEY
August 31, 1934

THE SIGNIFICANCE OF RIGHT-ASCENSION ERRORS IN TRIGONOMETRIC PARALLAXES

By T. E. STERNE

ABSTRACT

The significance of the data by van Maanen (*Ap. J.*, **78**, 189, 1933), relating to systematic errors, depending upon right ascension, in the trigonometric parallaxes of eight observatories, is examined by improved statistical methods. There is good evidence, from the harmonic analysis, for the existence of systematic differences, of period 24^h in right ascension, between trigonometric parallaxes determined at the Allegheny and the McCormick observatories. The variation with right ascension cannot reasonably be attributed, entirely, to fluctuations of sampling. There is no evidence, from either the harmonic analysis or the tests for homogeneity, of any systematic variation with right ascension, of the hourly mean differences between spectroscopic parallaxes and trigonometric parallaxes determined at any of the following observatories: Mt. Wilson (60-in.), McCormick, Yerkes, Greenwich. A systematic error depending upon right ascension is suggested in the trigonometric parallaxes determined at the Allegheny Observatory. The errors, if present, are probably of period 24^h in right ascension. Systematic errors of period 24^h in right ascension are strongly suggested in the differences between the spectroscopic and the trigonometric parallaxes determined at the Sproul and the Yale (photographic) observatories, both by tests for homogeneity and by harmonic analysis. There is some evidence for the existence of a systematic variation, of period 6^h or less in the right ascension (but not necessarily exactly periodic), in the differences between the Cape photographic and spectroscopic parallaxes (the variations of longer period can be attributed to fluctuations of sampling). The point is not stressed, despite a strong indication of inhomogeneity, because of the inherent implausibility of such short-period variations. There is no evidence for the existence of systematic error depending upon right ascension, in the spectroscopic parallaxes used in the comparisons. Hence the right-ascension errors, in the few cases mentioned above where they are probably present, are most probably in the trigonometric parallaxes.

Following an earlier paper,[1] van Maanen has published a more complete compilation[2] of data relating to what he claims are systematic errors, depending upon right ascension, in the trigonometric parallaxes of stars studied at eight different observatories. In Table I of the latter paper he classifies the stars that have been measured for parallax both at the Allegheny and at the McCormick observatories into twenty-four classes, according to the hours of their right ascensions, and lists the number of stars, as well as the mean difference π Allegheny $-\pi$ McCormick, for each class. In his Figure 1 he plots, against each hour of right ascension, the average of the hourly mean differences for the hour in question, the hour preced-

[1] *Mt. W. Contr.*, No. 357, 1928.

[2] *Ap. J.*, **78**, 189, 1933; *Mt. W. Contr.*, No. 474, 1933.

ing, and the hour following. The figure suggests at first sight a systematic dependence of the three-hour means upon right ascension, and van Maanen finds that the plot can be fitted fairly closely by a trigonometric series, in right ascension, involving seven constants which he obtained by the method of least squares. He concludes that there can be no doubt that these differences are a function of right ascension. He likewise treats, for eight observatories separately, the overlapping three-hour means representing the differences between the trigonometric parallaxes and a common system of spectroscopic parallaxes selected from the list of W. S. Adams. The plots are shown in van Maanen's Figure 2, and the hourly means and numbers of stars in each hour group are given in his Table V. The plots all suggest, at first sight, a systematic dependence of the overlapping three-hour means upon right ascension, and each plot can be fitted fairly well by a trigonometric series involving seven constants, peculiar to the plot, obtained by least squares. Reasoning that the common system of spectroscopic parallaxes is not likely to contain errors depending upon right ascension, he concludes that there are systematic errors in all the trigonometric parallaxes, depending upon right ascension, and advocates their removal through the use of the corrections obtained from his least-squares solutions.

Between successive, overlapping, three-hour means of the sort plotted and analyzed by van Maanen, there must be a correlation of $+\frac{2}{3}$, even when the successive hourly means are not correlated. It is the correlation between successive points which suggests to the eye their systematic dependence upon right ascension; and after the high correlation of $+\frac{2}{3}$ is artificially introduced, even a set of quite random residuals will show the sort of irregularities apparent in van Maanen's Figures 1 and 2. To this extent the use in his figures of three-hour overlapping means was unfortunate. I show in Figure 1 the plots of the separate hourly means, drawn from van Maanen's Tables I and V; they show no very striking correlation with right ascension. The irregular dispersions are caused largely by the unequal weights of the points, since in some hour classes there are more stars than in others. The method of least squares automatically selects the values of the seven constants that give the very best fit possible between the trigonometric series and the set of three-hour

overlapping means. With seven disposable constants, it is entirely possible that the smoothed data[3] shown in van Maanen's Figures 1 and 2 could be fitted as well as they have been fitted or better, even if the original hourly means were not correlated at all with right ascension, but merely fluctuated about a mean value in an entirely random fashion.

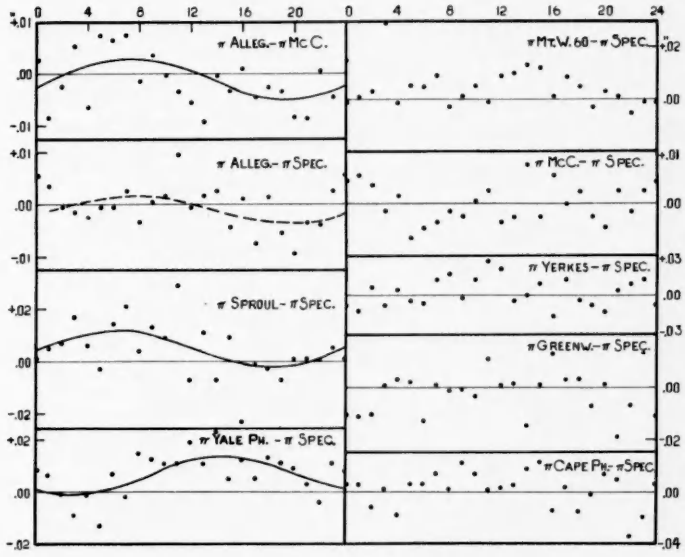

FIG. 1.—Mean differences $\pi_t - \pi_s$ grouped according to hours of right ascension

Since it is important to answer the question as to whether or not there are systematic errors in the trigonometric parallaxes, depending upon right ascension (particularly in view of van Maanen's suggestion that corrections, depending upon right ascension, should be applied[4] to the parallaxes determined at the various observatories), we

[3] Only eight of the points in each of his figures are independent.

[4] In Table IX he shows that the use of his system of corrections does on the whole reduce the discrepancy between the trigonometric parallaxes determined at different observatories; but the same reduction would have been effected whether the errors, for which he applied corrections, had been systematic or random. To correct for random errors by systematic corrections depending upon right ascension would of course not be legitimate. It is only after errors are known with certainty to be systematic that systematic corrections should be introduced.

present what is intended and believed to be a rigorous statistical discussion of the material in van Maanen's Tables I and V. We use two different methods of investigation, to which the material in the above-mentioned tables is excellently adapted.[5]

HARMONIC ANALYSIS

Van Maanen solved each of his sets of overlapping three-hour means by least squares, using twenty-four equations of condition, for a constant term and for sine and cosine terms having periods of twenty-four, twelve, and six hours in right ascension. He did not publish the mean errors of the resulting constants necessary for tests of significance. We have therefore repeated his analysis, with the difference that we have (1) used hourly means instead of overlapping three-hour means in the equations of condition, and that we have (2) sought to determine only three constants instead of seven, by confining our attention to the constant term and to terms having a period of twenty-four hours in right ascension—terms inherently more likely, perhaps, than those of shorter period. With each hourly mean used as the second member, M, of an equation of the form

$$a+b \sin \varphi+c \cos \varphi=M ,$$

the constants a, b, and c were determined by a least-squares solution. The weight of each equation was taken equal to the number of stars involved in its determination. The values of the resulting constants, with their mean errors, all in thousandths of a second of arc, are as shown in Table I.

We test the significance of the results for b and c, leaving the discussion of the significance of the a's to those who are familiar with the possible sources of constant systematic error. It would be legitimate to test the significance of the b's and c's separately, since the correlation between b and c found from the least-squares solution is in all cases small, ranging between +0.07 and −0.07 in the nine

[5] See also C. Davidson, "Systematic Errors in Trigonometric Stellar Parallaxes," *Observatory*, **57**, 236, 1934, for further comments on van Maanen's paper. *Note added October 24:* For a rediscussion of the material following the methods of van Maanen, the reader is referred to a recent paper by S. A. Mitchell in *Ap. J.*, **80**, 200, 1934. I acknowledge gratefully the opportunity of reading Professor's Mitchell's paper in proof.

cases above.[6] From tables of the normal error function, the probabilities could be found of obtaining, through fluctuations of sampling, values of b and c numerically greater than those actually found. But we are more interested in the significance of b and c jointly. Neither the amplitude $(b^2+c^2)^{\frac{1}{2}}$, nor the amplitude squared is, even roughly, a normal deviate, although b and c are normal deviates. We ignore

TABLE I

Series	a	b	c
π Alleg.$-\pi$ McC.	-1.02 ± 0.88	3.59 ± 1.13	-1.29 ± 1.33
π Mt. W. 60$-\pi$ Spec.	3.78 ± 1.42	0.83 ± 1.95	-2.64 ± 2.04
π Alleg.$-\pi$ Spec.	-0.91 ± 0.78	2.21 ± 1.03	-1.03 ± 1.27
π McC.$-\pi$ Spec.	-0.20 ± 0.75	-0.90 ± 1.00	0.43 ± 1.11
π Yerkes$-\pi$ Spec.	2.11 ± 2.13	2.24 ± 2.71	-2.44 ± 3.14
π Sproul$-\pi$ Spec.	4.88 ± 1.56	7.18 ± 2.13	-0.25 ± 2.23
π Greenw.$-\pi$ Spec.	-0.71 ± 1.53	-1.88 ± 2.14	-3.66 ± 2.17
π Yale Phot.$-\pi$ Spec.	6.38 ± 1.43	-4.45 ± 1.92	-5.37 ± 2.05
π Cape Phot.$-\pi$ Spec.	3.46 ± 2.22	0.56 ± 3.17	-6.25 ± 3.12

the trivial correlation between b and c. It can easily be shown that if t_b is the ratio of b to its mean error, and t_c that of c to its mean error (t_b and t_c being in fact almost normally distributed, with unit standard deviation), the probability that a value of $t_b^2+t_c^2$ will be obtained, through fluctuations of sampling, larger than or equal to the value observed, is $e^{-(t_b^2+t_c^2)/2}$. This probability, called P_{bc}, is listed below; it tests the significance of b and c jointly.

Series	P_{bc}	Series	P_{bc}
π Alleg.$-\pi$ McC.	0.004	π Sproul$-\pi$ Spec.	0.003
π Mt.W. 60$-\pi$ Spec.	.39	π Greenw.$-\pi$ Spec.	.16
π Alleg.$-\pi$ Spec.	.07	π Yale Phot.$-\pi$ Spec.	.002
π McC.$-\pi$ Spec.	.62	π Cape Phot.$-\pi$ Spec.	0.13
π Yerkes$-\pi$ Spec.	0.53		

The ordinary rule in astronomical work has been to regard a normal deviate as significant when it exceeds three mean errors, for which the probability of obtaining that deviate or a numerically larger one of the same sign is but 0.13 per cent; 1 per cent, corre-

[6] The coefficient of correlation is in each case the quotient of the co-factor of $[bc]$ in the determinant of the coefficients in the normal equations, divided by the geometrical mean of the co-factors of $[bb]$ and $[cc]$, and would vanish completely but for the unequal weights of the M's.

sponding to 2.33 mean errors, is more lenient and probably strict enough in practice; while 5 per cent, corresponding to 1.65 mean errors, is decidedly lax. The value of P for π Alleg. $-\pi$McC. falls short of the 1 per cent point and must be considered significant; a real error depending upon right ascension is very probably present in one or both sets of trigonometric parallaxes. The sine-curve in the π Mt.W. 60 $-\pi$ Spec. comparison cannot be said, with any assurance, to be more than a mere statistical fluctuation; nor can the sine-curves for McCormick, Yerkes, Greenwich, and Cape Photographic. Since the π McC. $-\pi$ Spec. results are not significant, while the π Alleg. $-\pi$ McC. are significant, the cause is perhaps to be found in a right-ascension error in the Allegheny parallaxes, a suggestion that is considerably strengthened by the value 0.07, in itself not particularly significant, for the π Alleg. $-\pi$ Spec. comparison. The sine-curves for Sproul and Yale Photographic (in Johannesburg) are very probably significant. The significant sine-curves are drawn solidly in Figure 1, the curve for Allegheny, of more doubtful significance, being broken; none of the others have been drawn. The values of P listed above, in the absence of systematic errors having a period of twenty-four hours, should be uniformly distributed, at random, between 0 and 1. After the values of P for π Alleg. $-\pi$ Mc.C., π Alleg. $-\pi$ Spec., π Sproul $-\pi$ Spec., and π Yale Phot. $-\pi$ Spec. are removed from the list, the remaining values cannot be said, collectively, to be significant. Two of the values are larger than 0.50, and three are smaller. The observed mean is 0.37, with an expected mean error of 0.13 equal exactly to the amount by which the observed mean falls short of the expected mean.

TESTS FOR HOMOGENEITY

In the preceding section we computed by least squares particular parameters, namely, the coefficients of the sine and cosine terms, and tested them for significance. There would have been no particular reason for testing these parameters rather than any others of the enormous set of possible parameters, had it not been for the strong presumption that if any systematic errors were present depending upon right ascension, they would be seasonal, and with a period of twenty-four hours in right ascension. To test for the reality

of a sine-curve of a particular period is artificial; and testing for the reality of any sine-curve is somewhat artificial, for even if the suspected periodicity is actually present, it is likely that more than a single term in a Fourier expansion will be needed to represent it. There is fortunately a simple and elegant general method, devised by Professor R. A. Fisher,[7] for dealing with such problems; he calls it the "analysis of variance." It does not depend upon any arbitrary

TABLE II

Hours	0^h+	4^h+	8^h+	12^h+	16^h+	20^h+
0	2.4 13	−6.3 12	−1.6 14	−5.5 6	1.0 25	−8.3 33
1	−8.3 18	7.3 16	3.4 14	9.0 9	−4.7 28	−8.8 22
2	−2.3 18	6.2 18	−0.1 11	0.3 15	−2.6 25	0.5 25
3	5.1 13	7.4 18	−3.1 8	−3.1 21	−3.3 45	−4.1 15
Means	−1.50	4.47	−0.01	−3.60	−2.60	−5.44
Weights	62	64	47	51	123	95

assumptions as to the exact nature of the inhomogeneity of the material tested. An application of it to van Maanen's data will supplement the investigations of the previous section, and will also provide an illustration of its usefulness in problems arising in astronomy.

We cast the data found in van Maanen's Table I into the form shown in our Table II. The hourly means have been grouped into six classes of four hours each. Each entry consists of two parts. First there is given the mean difference of trigonometric parallax, π Alleg. $-\pi$ McC., for the stars in that particular hour group that have been measured at both observatories. Next is given the number of stars in the group, hereafter called the "weight." Below each four-hour class is given the weighted mean difference for the class (hereafter called the "mean of the class") and the total weight for the class. The sum of all the weights is 442, and the weighted mean of all the classes is -1.87. The units used are thousandths of a second of arc. We square each hourly difference, multiply it by its weight, and sum over all the 24 hours. The result is 11,674. We square the mean of each class, multiply it by its weight, and sum over all the six classes. The result is 5721. Finally, we square the

[7] *Statistical Methods for Research Workers* (Oliver & Boyd, 1932), chap. vii.

weighted mean of all the classes and multiply by its weight, obtaining the result 1549. In Table II*a*, column 3, the top entry is the remainder 11,674–5721; the middle entry is 5721–1549; the bottom entry is 11,674–1549. The reader will recognize these numbers as merely the weighted sum of the squares of the individual entries in Table II about the weighted means of classes, the weighted sum of squares of means of classes about the weighted mean of all the classes, and the weighted sum of the squares of the individual entries

TABLE II*a*

π ALLEG.$-\pi$ McC.

Variance	Degrees of Freedom	Weighted Sum of Squares	Mean Square	S.D.
Within classes	18	5953	331	18.2
Between classes	5	4172	834	28.9
Total	23	10125		(z=0.464)

4^h classes. Inhomogeneity not suggested.

about the weighted mean of all the classes, respectively. The total number of "degrees of freedom" within classes is 18, since if the mean of a class is fixed, only three entries can vary independently in the class. Since the mean of all the classes is fixed, there are but 5 degrees of freedom between means of classes. The total, 23, is the number of degrees of freedom for all the hour groups if the mean of all the classes is fixed. Dividing the sums of the squares (in the third column) by the degrees of freedom, we obtain the entries in the fourth column; their square roots are given in the last column. It will be recognized that these are estimates of the standard deviation of an hourly mean of unit weight, the value 18.2 being an estimate obtained from within classes, and the value 28.9 being an estimate obtained from between classes. In the absence of systematic differences between the six classes, these estimates should be equal, except for possible differences due to mere fluctuations of sampling in the data. A significant excess of the "external" estimate over the "internal" estimate would prove that the classes differed significantly from each other and hence that there were systematic errors depend-

ing upon right ascension in the trigonometric parallaxes obtained at one, or both, observatories.

It can be shown that if the classes are homogeneous, the two estimates of the standard deviation behave exactly as though they had been obtained from two samples, one of nineteen individuals and the other of six individuals, drawn independently and at random from the same universe, of unknown standard deviation σ. The statistical distribution of v, the ratio of the "external" estimate of the standard deviation to the "internal," is for a normal universe exactly

$$p(v)dv = \text{const.} \times v^{n_1-1}\left(v^2+\frac{n_2}{n_1}\right)^{-\frac{n_1+n_2}{2}} dv\ ,$$

where n_1 and n_2 are the external and internal degrees of freedom, respectively. When n_1 and n_2 are nearly equal, then the function $p(v)$ is nearly symmetrical about the value 1, and $z=\log_e v$ is distributed about the mean value 0 in a nearly Gaussian fashion, with a standard deviation given roughly by $[(n_1+n_2)/2n_1n_2]^{\frac{1}{2}}$. Fisher (*loc. cit.*) has given two tables of the exact values of z (corresponding to various values of n_1 and n_2) such that the chances of exceeding them are 5 and 1 per cent, respectively. Of course, the 5 and 1 per cent points for negative values of z (i.e., values such that the chances that z will fall short of them algebraically are 5 and 1 per cent, respectively) are obtained by interchanging n_1 and n_2 as the arguments of the tables. In our case, a large negative value of z would indicate the opposite of a dependence upon right ascension. From Table II*a*, we find that $z=0.464$. For $n_1=5$, $n_2=18$, the positive 5 and 1 per cent points are 0.5099 and 0.7232, respectively, while the negative 5 and 1 per cent points are -0.7605 and -1.1312, respectively. The value of z that we have obtained from the data of van Maanen's Table I does not even reach the 5 per cent point, and cannot be regarded as significant. There is thus no evidence of any systematic dependence upon right ascension, of the differences between the Allegheny and the McCormick trigonometric parallaxes. Such slight inhomogeneity as there is could easily have arisen as a mere fluctuation of sampling.

There are three considerations governing the size of the classes into which we should divide the hourly mean differences. First, un-

less the classes are small, there is a chance that such errors as may be present, of short period in right ascension, might be smoothed out and overlooked. Second, by dividing the hourly differences into twelve classes of two hours each, instead of into six classes of four hours each, the degrees of freedom would become 12 and 11 instead of 18 and 5; resulting in comparable accuracies for the internal and external estimates of the standard deviation, in a very nearly normal distribution of z, and in the possibility of easily assigning actual probabilities to the values of z found. These two considerations both point to the advantage of using two-hour, instead of larger, classes. On the other hand, there is a third consideration, which assigns an advantage to larger classes. The weights of the hourly differences are comparable; let us suppose for simplicity that they are all equal. If there is present a real error depending upon right ascension, consisting of periodic terms the sum of whose amplitudes squared is A^2, and if we use classes of N hours each, then unless the classes are so large that some of the terms are smoothed out, the (standard deviation)^2 of the means of classes will be nearly $\frac{1}{2}A^2+a^2/N$, where a is the standard deviation of the random errors that are superposed on the systematic ones. We shall thus be led to an external estimate of the (standard deviation)^2 nearly equal to $\frac{1}{2}A^2N+a^2$. The internal estimate of the (standard deviation)^2 will be very nearly a^2. The ratio v^2 will thus be nearly equal to $1+\frac{1}{2}A^2N/a^2$, on which of course will be superposed the errors of sampling. If systematic errors are present, we shall therefore increase the chance of discovering them by using larger classes, provided always that we do not smooth out the periodic terms by so doing. It may be shown that for discovering periodic errors of a period of twenty-four hours, of an amplitude which is small in comparison with the random error a, classes of eight hours each should yield the largest ratio of the external to the internal estimate, smoothing being taken into account. For a period of twelve hours, four-hour classes should be used; and for a period of six hours, two-hour classes. The results obtained by dividing the data of van Maanen's Table I into twelve classes of two hours each are as in Table II *b*. The value of z is 0.358; the positive 5 and 1 per cent points are 0.4994 and 0.7194, respectively; the negative, -0.5126 and -0.7405. The inhomogeneity is therefore not signifi-

cant. Finally, we repeat the analysis, using three classes of eight hours each. The results are as in Table II *c*. The value of z is thus 0.565. The positive 5 and 1 per cent points are 0.6216 and 0.8772; the negative, −1.4839 and −2.2999, respectively. Thus there is no good evidence for inhomogeneity in the data of van Maanen's Table I, no matter how we treat it. Good evidence was obtained, however,

TABLE II *b*

π ALLEG. − π McC.

Variance	Degrees of Freedom	Weighted Sum of Squares	Mean Square	S.D.
Within classes	12	3524	294	17.1
Between classes	11	6601	600	24.5
Total	23	10125	.....	(z=0.358)

2^h classes. Inhomogeneity not suggested.

TABLE II *c*

π ALLEG. − π McC.

Variance	Degrees of Freedom	Weighted Sum of Squares	Mean Square	S.D.
Within classes	21	7820	372	19.3
Between classes	2	2305	1152	33.9
Total	23	10125	.....	(z=0.565)

8^h classes. Inhomogeneity not suggested.

for the existence of a right-ascension error, from the harmonic analysis of the preceding section; and we must still consider right-ascension error to be present, despite the negative results of the search for statistical inhomogeneity.

The same procedure as that by which we analyzed van Maanen's Table I has been applied to his Table V, containing the mean hourly differences, for each of eight observatories, between the trigonometric and spectroscopic parallaxes. The tables of results, analogous to our Table II*a*, follow (Table III). The values of z are tabulated in Table IV.

TABLE III

π MT. W.$-\pi$ SPEC.

Variance	Degrees of Freedom	Weighted Sum of Squares	Mean Square	S.D.
Within classes	12	3658	305	17.5
Between classes	11	4767	433	20.8
Total	23	8425	.....	(z=0.176)

2^h classes. Inhomogeneity not suggested.

π ALLEG.$-\pi$ SPEC.

Variance	Degrees of Freedom	Weighted Sum of Squares	Mean Square	S.D.
Within classes	12	6169	514	22.7
Between classes	11	6247	568	23.8
Total	23	12416	.....	(z=0.047)

2^h classes. Inhomogeneity not suggested.

π MCC.$-\pi$ SPEC.

Variance	Degrees of Freedom	Weighted Sum of Squares	Mean Square	S.D.
Within classes	12	4478	373	19.3
Between classes	11	4194	381	19.5
Total	23	8672	.....	(z=0.010)

2^h classes. Inhomogeneity not suggested.

π YERKES$-\pi$ SPEC.

Variance	Degrees of Freedom	Weighted Sum of Squares	Mean Square	S.D.
Within classes	12	11436	953	30.9
Between classes	11	7927	721	26.9
Total	23	19363	.....	(z=$-$0.139)

2^h classes. Inhomogeneity not suggested.

TABLE III—*Continued*

π SPROUL $-\pi$ SPEC.

Variance	Degrees of Freedom	Weighted Sum of Squares	Mean Square	S.D.
Within classes	12	5910	492	22.2
Between classes	11	11432	1039	32.2
Total	23	17342	.....	(z=0.372)

2^h classes. Inhomogeneity not suggested.

π GREENW. $-\pi$ SPEC.

Variance	Degrees of Freedom	Weighted Sum of Squares	Mean Square	S.D.
Within classes	12	5106	426	20.6
Between classes	11	4172	379	19.5
Total	23	9278	.....	(z=−0.055)

2^h classes. Inhomogeneity not suggested.

π YALE PHOT. $-\pi$ SPEC.

Variance	Degrees of Freedom	Weighted Sum of Squares	Mean Square	S.D.
Within classes	12	5535	461	21.5
Between classes	11	10392	945	30.7
Total	23	15927	.....	(z=0.357)

2^h classes. Inhomogeneity not suggested.

π CAPE PHOT. $-\pi$ SPEC.

Variance	Degrees of Freedom	Weighted Sum of Squares	Mean Square	S.D.
Within classes	12	2043	170	13.0
Between classes	11	8212	747	27.4
Total	23	10255	.....	(z=0.747)

2^h classes. Inhomogeneity strongly suggested.

TABLE III—*Continued*

π MT.W.$-\pi$ SPEC.

Variance	Degrees of Freedom	Weighted Sum of Squares	Mean Square	S.D.
Within classes	18	5578	310	17.6
Between classes	5	2847	569	23.8
Total	23	8425	.....	(z=0.300)

4[h] classes. Inhomogeneity not suggested.

π ALLEG.$-\pi$ SPEC.

Variance	Degrees of Freedom	Weighted Sum of Squares	Mean Square	S.D.
Within classes	18	9173	510	22.6
Between classes	5	3243	649	25.4
Total	23	12416	.....	(z=0.113)

4[h] classes. Inhomogeneity not suggested.

π MCC.$-\pi$ SPEC.

Variance	Degrees of Freedom	Weighted Sum of Squares	Mean Square	S.D.
Within classes	18	6245	347	18.7
Between classes	5	2427	485	22.0
Total	23	8672	.....	(z=0.165)

4[h] classes. Inhomogeneity not suggested.

π YERKES$-\pi$ SPEC.

Variance	Degrees of Freedom	Weighted Sum of Squares	Mean Square	S.D.
Within classes	18	15522	862	29.4
Between classes	5	3841	768	27.7
Total	23	19363	.....	(z=−0.058)

4[h] classes. Inhomogeneity not suggested.

TABLE III—*Continued*

π SPROUL $-\pi$ SPEC.

Variance	Degrees of Freedom	Weighted Sum of Squares	Mean Square	S.D.
Within classes	18	9364	520	22.8
Between classes	5	7977	1595	39.9
Total	23	17342	.....	(z=0.560)

4^h classes. Inhomogeneity suggested.

π GREENW. $-\pi$ SPEC.

Variance	Degrees of Freedom	Weighted Sum of Squares	Mean Square	S.D.
Within classes	18	7025	390	19.8
Between classes	5	2253	451	21.3
Total	23	9278	.....	(z=0.073)

4^h classes. Inhomogeneity not suggested.

π YALE PHOT. $-\pi$ SPEC.

Variance	Degrees of Freedom	Weighted Sum of Squares	Mean Square	S.D.
Within classes	18	7809	434	20.8
Between classes	5	8118	1624	40.3
Total	23	15927	.....	(z=0.663)

4^h classes. Inhomogeneity suggested.

π CAPE PHOT. $-\pi$ SPEC.

Variance	Degrees of Freedom	Weighted Sum of Squares	Mean Square	S.D.
Within classes	18	8076	449	21.2
Between classes	5	2179	436	20.9
Total	23	10255	.....	(z=−0.014)

4^h classes. Inhomogeneity not suggested.

TABLE III—*Continued*

π MT.W.$-\pi$ SPEC.

Variance	Degrees of Freedom	Weighted Sum of Squares	Mean Square	S.D.
Within classes	21	7513	358	18.9
Between classes	2	912	456	21.4
Total	23	8425	.....	(z=0.122)

8[h] classes. Inhomogeneity not suggested.

π ALLEG.$-\pi$ SPEC.

Variance	Degrees of Freedom	Weighted Sum of Squares	Mean Square	S.D.
Within classes	21	9528	454	21.3
Between classes	2	2888	1444	38.0
Total	23	12416	.....	(z=0.577)

8[h] classes. Inhomogeneity not suggested.

π MCC.$-\pi$ SPEC.

Variance	Degrees of Freedom	Weighted Sum of Squares	Mean Square	S.D.
Within classes	21	8665	413	20.3
Between classes	2	7	3.5	1.87
Total	23	8672	.....	(z=−2.385)

8[h] classes. Inhomogeneity not suggested.

π YERKES$-\pi$ SPEC.

Variance	Degrees of Freedom	Weighted Sum of Squares	Mean Square	S.D.
Within classes	21	16946	807	28.4
Between classes	2	2417	1208	34.8
Total	23	19363	.....	(z=0.199)

8[h] classes. Inhomogeneity not suggested.

TABLE III—*Continued*

π SPROUL $-\pi$ SPEC.

Variance	Degrees of Freedom	Weighted Sum of Squares	Mean Square	S.D.
Within classes	21	12584	599	24.5
Between classes	2	4758	2379	48.8
Total	23	17342	.....	(z=0.688)

8^h classes. Inhomogeneity suggested.

π GREENW. $-\pi$ SPEC.

Variance	Degrees of Freedom	Weighted Sum of Squares	Mean Square	S.D.
Within classes	21	7886	376	19.4
Between classes	2	1392	696	26.4
Total	23	9278	.....	(z=0.308)

8^h classes. Inhomogeneity not suggested.

π YALE PHOT. $-\pi$ SPEC.

Variance	Degrees of Freedom	Weighted Sum of Squares	Mean Square	S.D.
Within classes	21	9106	434	20.8
Between classes	2	6821	3410	58.4
Total	23	15927	.....	(z=1.033)

8^h classes. Inhomogeneity strongly suggested.

π CAPE PHOT. $-\pi$ SPEC.

Variance	Degrees of Freedom	Weighted Sum of Squares	Mean Square	S.D.
Within classes	21	8433	402	20.0
Between classes	2	1822	911	30.2
Total	23	10255	.....	(z=0.412)

8^h classes. Inhomogeneity not suggested.

The results of the tests for homogeneity, applied to the trigonometric minus spectroscopic parallaxes for individual observatories, may therefore be summarized as follows: The hourly mean differences, π Mt.W. 60 $-\pi$ Spec., show no significant dependence upon right ascension. The hourly mean differences, π Alleg. $-\pi$ Spec., show no significant dependence upon right ascension. The hourly mean differences, π McC. $-\pi$ Spec., show no significant dependence

TABLE IV

Data	Method of Classification			Probability of Exceeding z from 2^h Classes
	2^h Classes	4^h Classes	8^h Classes	
	z	z	z	
π Alleg. $-\pi$ McC.	0.358	0.464	0.565	0.13
π Mt.W. 60 $-\pi$ Spec.	.176	.300	0.122	.29
π Alleg. $-\pi$ Spec.	.047	.113	0.577	.44
π McC. $-\pi$ Spec.	.010	.165	−2.385	.49
π Yerkes $-\pi$ Spec.	− .139	− .058	0.199	.67
π Sproul $-\pi$ Spec.	.372	.560	0.688	.12
π Greenw. $-\pi$ Spec.	− .055	.073	0.308	.57
π Yale Phot. $-\pi$ Spec.	.357	.663	1.033	.13
π Cape Ph. $-\pi$ Spec.	0.747	−0.014	0.412	0.01
Pos. 1 per cent point	0.719	0.723	0.877	0.01
Pos. 5 per cent point	.500	0.510	0.622	.05
Neg. 5 per cent point	− .513	−0.761	−1.484	.95
Neg. 1 per cent point	−0.740	−1.131	−2.300	0.99

upon right ascension; the value $z = -2.385$ for eight-hour classes, ascribable probably to a fluctuation of sampling, is of the wrong sign for significance. The hourly mean differences, π Yerkes $-\pi$ Spec., show no significant dependence upon right ascension. The hourly mean differences, π Sproul $-\pi$ Spec., exceed the 5 per cent points in the larger classes, and systematic errors depending upon right ascension are therefore suggested, although with no very great certainty. The errors, if present, are probably of long period (longer than six hours). The hourly mean differences, π Greenw. $-\pi$ Spec., show no significant dependence upon right ascension. The hourly mean differences, π Yale Phot. $-\pi$ Spec., exceed the 5 per cent point for the four-hour classification, and the 1 per cent point for the eight-hour classification; systematic errors of long period in the right as-

cension are very probably present. The hourly differences, π Cape Phot. $-\pi$ Spec., exceed the 1 per cent point in the two-hour classification, but yield an insignificant z in the larger classes; the value for four-hour classes is negative. Systematic errors, of short period in the right ascension, are strongly suggested. If the Sproul, Yale photographic, and Cape photographic results are removed from Table III, the averages of the remaining entries in the z columns are 0.066, 0.176, and -0.102, respectively. The standard deviation of a single entry in one of the z columns is 0.3 (roughly correct; in the last column it is an underestimate), the standard errors of the means are of the order of 0.12, and thus the remaining observatories do not show any significant collective[8] evidence of systematic errors depending upon right ascension.

The last column of Table IV contains the probability of obtaining values of z algebraically larger than the observed values, for the two-hour classes. They were computed by taking advantage of the fact that for the two-hour classes, the distribution of z is very nearly normal and of standard deviation 0.31. In the absence of errors depending upon right ascension, the probabilities should be distributed uniformly and at random between 0 and 1, and they are so distributed if the values for Sproul, Yale photographic, and Cape photographic are ignored. The general mean is 0.43 ± 0.12 (m.e.), since the expected standard deviation of each value is $1/(12)^{\frac{1}{2}}$; the observed mean is thus in good agreement with the expected mean, 0.50. It will be seen that, except for the case of π Alleg. $-\pi$ McC., the results of the present tests are in substantial agreement with those of the harmonic analysis.

THE POSSIBILITY OF RIGHT-ASCENSION ERRORS IN THE SPECTROSCOPIC PARALLAXES

It is desirable to make certain, if possible, that the cause of the systematic errors in the few comparisons between trigonometric and spectroscopic parallaxes for which such errors are suggested by the preceding investigations is not in the adopted system of spectro-

[8] Sometimes statistical results, individually insignificant, may be significant collectively.

scopic parallaxes. Such systematic errors, depending upon right ascension, would if real be present in all the spectroscopic parallaxes together that were used in the comparisons, and can therefore be looked for in the material of van Maanen's Table V, as follows: We prepare a table of the mean differences between the trigonometric and the spectroscopic parallaxes. In this table each row is assigned to one of the eight observatories included in van Maanen's Table V, while the columns correspond to the right ascensions. If the hourly

TABLE V

Variance	Degrees of Freedom	Weighted Sum of Squares	Mean Square	S.D.
Within classes	42	43900	1045	32.3
Between classes	5	6227	1245	35.3
Total	47	50127	.....	(z=0.089)

TABLE V*a*

Variance	Degrees of Freedom	Weighted Sum of Squares	Mean Square	S.D.
Within classes	21	44751	2131	46.2
Between classes	2	5376	2688	51.8
Total	23	50127	.....	(z=0.114)

differences are combined into four-hour classes, there will be six columns; if into eight-hour classes, three columns. Means of the columns are taken, and inhomogeneity is looked for as usual between the columns. Weights are used proportional (as usual) to the number of stars for each entry. It did not appear worth while to take into account the differing accuracies of the various observatories, because the standard deviation of the difference between a trigonometric and a spectroscopic parallax does not really differ much for different observatories (the ratio of the largest to the smallest estimate of such a standard deviation being but 1.5 for the eight observatories considered); because, moreover, the results of tests of homogeneity are never sensitive to small changes in the weights, and

because there is no rigorous procedure by which such different variances can be allowed for (this difficulty would not, by itself, be very serious).

No significant results are obtained. If we take four-hour classes, the results are as in Table V, while the positive 5 per cent point is 0.45. With eight-hour classes the results are likewise insignificant (see Table V *a*) since the 5 per cent point for this manner of classification is 0.62. We conclude that there is no evidence for the existence of systematic errors, depending upon right ascension, in the common system of spectroscopic parallaxes used in the comparisons.

HARVARD COLLEGE OBSERVATORY
August 30, 1934

THE SPECTRUM OF P CYGNI

By OTTO STRUVE

ABSTRACT

Measurements are given of 158 absorption lines, of which 24 are unidentified, and of 63 emission lines, of which 15 are unidentified.

The *H* lines are found to be relatively sharp and strong, their contours suggesting the absence of Stark broadening and the presence of turbulence broadening. The pressure in the *H* atmosphere must be very low.

The intensities of the absorption lines suggest a spectral class similar to B1, but the lines of *C* II and *Mg* II are much too faint and those of *S* III are too strong. The absorption spectrum has certain points of resemblance to 17 Leporis and to the B5 component of β Lyrae.

The intensity gradient of the *He* I lines is steep, suggesting active turbulence. The high-level transitions in *N* II and *O* II are weakened relative to the low-level transitions. This may be a result of departures from thermal excitation, although a similar but smaller effect is observed in ordinary B stars as a result of the Boltzmann law.

Recombination is probably responsible for the lines of *H* and *He* I, and possibly for *N* II. For atoms of high ionization potential such as *Si* IV, *N* III, etc., recombination is negligible.

The weakness of *Mg* II in P Cygni and in other Be stars is attributed to the depletion of the star's continuous spectrum at the Lyman limit of *H*. Similarly, the weakness of *C* II is caused by depletion at the ultra-violet limit of *He* I.

The prevalence of low-level transitions in *O* II, and especially in *N* II, is regarded as an argument against recombination in these ions, and in favor of fluorescence.

The absorption lines are characteristic of a higher level of excitation than the emission lines. Thus, *Si* IV (45.0 volts), *C* III (47.7 volts), and *N* III (47.4 volts) occur only in absorption. The limit is probably at *He* II (54.2 volts). The absorption spectrum is roughly B0–B1, while the emission spectrum is more nearly B2–B3.

The elements of high ionization potential are found to originate at greater depths in the shell than the elements of low ionization potential. This suggests that the density of the shell decreases outward slower than $1/R^2$, or that the dilution constant increases more rapidly than R^2.

A strong line at λ 4396 agrees in position with an *O* II line. The possibility is discussed that this line is excited by Bowen's mechanism of abnormal fluorescence. In this case a line of *He* I at λ 515.60 agrees closely with *O* II 515.50. No other cases of abnormal fluorescence have been found.

The radial velocities indicate that $|V|$ increases with the intensity of the line and decreases as we pass from elements of low ionization potential to those of high ionization potential. This suggests an accelerated outward motion of the shell.

I. INTRODUCTION

There have been a number of investigations of the spectrum of P Cygni. After the discovery of bright lines by E. C. Pickering,[1] J. E. Keeler,[2] Miss Maury,[3] and Vogel and Wilsing[4] published de-

[1] *Nature*, **34**, 439, 1886. [2] *Astronomy and Astrophysics*, **12**, 361, 1893.

[3] *Harvard Ann.*, **28**, 101, 1897; **76**, 31, 1916.

[4] *Pub. Potsdam Ap. Obs.*, **12**, 13, 1899.

scriptions and identifications of its stronger lines. A Belopolsky[5] identified nitrogen and obtained the displacements of a few lines. E. B. Frost[6] and P. W. Merrill[7] made accurate measurements of the radial velocities of the stronger lines. R. H. Curtiss[8] also obtained accurate radial velocities of numerous lines. C. S. Yü,[9] B. P. Gerasimovič[10] and J. Dufay[11] investigated its continuous spectrum and derived a very low color temperature for P Cygni. C. S. Beals[12] recently applied the method of Zanstra to the emission lines of *H* and of *He* I and derived a temperature of about 20,000° K for the exciting star. C. T. Elvey[13] published a set of accurate measurements of the total absorptions and emissions of the more prominent lines, together with their radial velocities. Still more recently W. J. Williams[14] gave a brief summary of his measurements of radial velocities.

In spite of this abundance of information collected in the course of nearly half a century, the problem of P Cygni is far from its solution, and a new contribution toward its elucidation is particularly desirable at this time. Within the last few years considerable advances have been made in the interpretation of the spectra of novae and Wolf-Rayet stars on one side, and of ordinary Be stars on the other. A new point of view, not available to earlier investigators, can therefore be taken. The present work is an attempt to test the theory of an expanding nebular shell in the case of P Cygni.

The fact that P Cygni is itself an old nova (discovered in 1600) renders it especially interesting. Furthermore, its absorption lines are not only numerous, but fairly sharp, and should therefore yield reliable radial velocities. Similarly, its emission lines, though not nearly as narrow as its absorption lines, are narrower than the emission lines of most recent novae, and are therefore suitable for measurement and identification. Finally, the character of its spectrum

[5] *Ap. J.*, **10**, 319, 1899.

[6] *Ibid.*, **35**, 286, 1912.

[7] *Lick Obs. Bull.*, **6**, 156, 1911; **8**, 24, 1913.

[8] *Pop. Astr.*, **22**, 133, 1914.

[9] *Pub. A.S.P.*, **39**, 118, 1927.

[10] *Harvard Bull.*, Nos. 852, 857, 867, 1927–28.

[11] *C.R.*, **194**, 1454, 1932; *J. des obs.*, **15**, 45, 1932.

[12] *Pub. Dom. Ap. Obs. Victoria*, **6**, 95, 1934.

[13] *Ap. J.*, **68**, 416, 1928.

[14] *Pub. A.A.S.* (44th meeting), p. 377, 1930. For a complete bibliography containing forty-three references see Merrill and Burwell, *Ap. J.*, **78**, 87, 1933, star No. 338.

suggests a stage of excitation which is not usually found in the spectra of nebulae, novae, or ordinary Be stars.

The immediate incentive in beginning this study was furnished by the similarity of P Cygni, in many respects, to two other stars recently investigated at the Yerkes Observatory. It had been noticed many years ago by Frost[6] that certain spectroscopic features of P Cygni resembled those of β Lyrae, and I have recently found convincing confirmation of this.[15] No less interesting is its similarity to 17 Leporis,[16] a star containing only one emission line of the P Cygni type ($H\beta$), but possessing a set of absorption lines the behavior of which in many respects duplicates that of P Cygni.

II. OBSERVATIONAL MATERIAL

Two excellent spectrograms taken on September 12.25, 1931 (by Struve and Morgan), and on October 30.10, 1934 (by Henyey), with the single-prism Bruce spectrograph attached to the 40-inch refractor were measured for the purpose of identifying the spectral lines. Both spectrograms are on the high-contrast Eastman Process emulsion, and they record the photographic spectrum from about λ 3925 to λ 4800. Only two strong lines were measured outside this range. The results of the measurements are in Table I. The estimated intensities are on an arbitrary scale, which is not identical with that used for τ Scorpii[17] in column 6.

Table II contains all elements for which a search was made, with their ionization potentials and with the numbers of lines actually observed. The total number of absorption lines measured in P Cygni is 110, of which 10 are unidentified. The number of emission lines is 43, of which 9 are unidentified and of which all but 3 have corresponding absorption lines on their violet sides.

Special attention should be called to the unidentified lines, some of which are quite strong. They are not listed among the permitted or forbidden lines of atoms and ions which may normally be expected in P Cygni.

Plate II shows enlargements of spectrograms of P Cygni (October 30, 1934) and of τ Scorpii (July 7, 1931).

[15] *Observatory*, **57**, 265, 1934.

[16] *Ap. J.*, **76**, 85, 1932.

[17] Struve and Dunham, *ibid.*, **77**, 321, 1933.

PLATE II

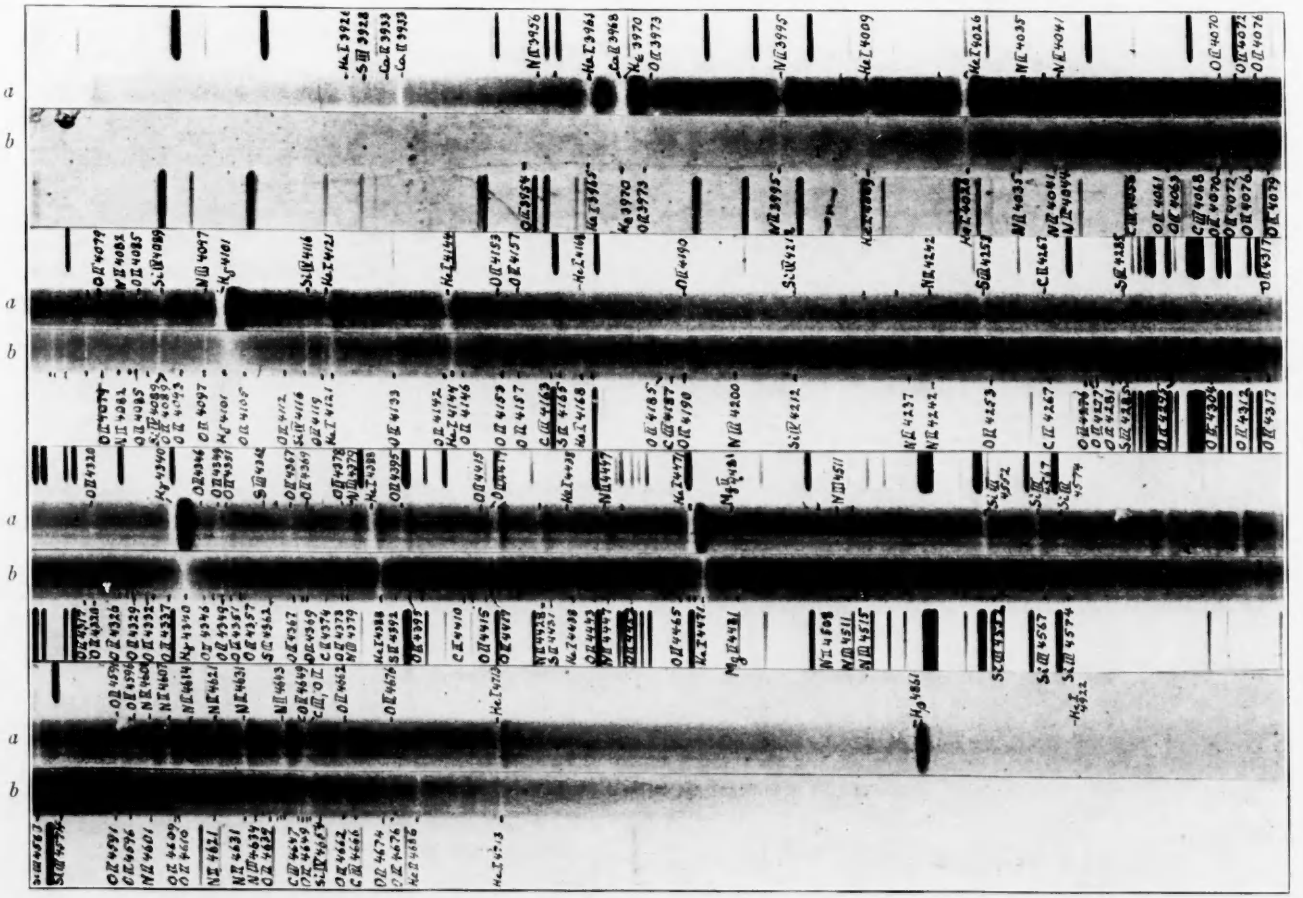

a) Spectrum of P Cygni; *b*) Spectrum of τ Scorpii

TABLE I

SPECTRAL LINES IN P CYGNI

λ	Absorption		Emission		Intensity		Remarks
	Int.	Vel.	Int.	Vel.	τ Sco	Lab.	
			H I.P. 13.5				
3970.08	20	−146	30	− 4	8?	.....	
4101.75	25	184	40	30	30	.....	
4340.48	20	195	40	6	40	.....	
4861.34	20	−200	30	− 2	.....	.....	
			He I I.P. 24.5				
3926.53	2	−122	1	− 15	.....	1	
3964.73	10	167	20	− 33	8	4	
4009.27	8	120	2	− 6	4	1	
4026.19	15	153	20	− 4	30	5	
4120.85	6	114	5	− 3	8	3	
4143.77	9	115	2	− 8	10	2	
4168.97	1	83	0	.....	6	1	
4387.93	10	123	6	− 12	20	3	
4437.55	2	104	1	+ 16	5	1	
4471.48	15	158	20	− 8	20	6	
4713.20	7	136	10	− 7	8	3	
4921.93	10	−154	10	+ 6	.....	4	
			He II I.P. 54.2				
4685.81	0–1	−118	0	.....	8	.....	Uncertain
			C II I.P. 24.3				
4267.20	1	−138	2	− 38	9	10+8	
			C III I.P. 47.7				
4187.05	1	.....	0	.....	5	10	
4647.40	1	.....	0	.....	9	10	
4650.16	1	.....	0	.....	5	9	Bl. *O* II
4651.35	1	.....	0	.....	5	8	Bl. *O* II

TABLE I—*Continued*

λ	Absorption		Emission		Intensity		Remarks
	Int.	Vel.	Int.	Vel.	τ Sco	Lab.	
			N II I.P. 29.5				
3955.85	4	−113	1	+ 3	1	6	
3995.00	9	110	9	− 13	10	10	
4035.09	1	91	1	+ 20	3	4	
4041.32	1	79	0	.....	1	5	
4043.54	1	.....	0	.....	3	3	
4082.28	1	71	0	.....	1	2	
4227.83	1	95	0	.....	2	3	
4236.98	0–1	.....	0	.....	4	6	
4241.80	1	142	0	.....	4	8	
4426.05?	1	82	0	.....	0	0	
4441.99	1	38	0	.....	1	3	
4447.04	2	122	2	− 14	3	10	
4530.37	0–1	.....	0	.....	1	5	
4601.49	4	98	4	+ 4	2	8	
4607.17	5	92	3	+ 18	2	7	
4613.88	3	86	2	+ 31	2	6	
4621.40	5	106	4	+ 12	2	7	
4630.55	7	100	9	+ 15	5	10	
4643.11	8	− 87	7	+ 8	(1)	8	Bl. *N* III
			N III I.P. 47.4				
4097.31	2	− 75	1	+ 34	6	10	Bl. *O* II
4379.09	1	.....	0	.....	3	10	
4510.92	2	54	0	.....	3	6	
4514.89	1	50	0	.....	3	7	
4634.16	1	− 46	0	.....	3	8	
4640.64	9	.....	3	.....	3	10	Bl. *N* II
			O II I.P. 34.9				
3973.27	4	− 67	0	.....	3	10	
4069.90	2	83	0	.....	7	6+4	
4072.11	2	39	0	.....	6	8	
4075.87	3	63	0	.....	8	10	
4078.86	1	51	0	.....	3	4	
4085.12	1	72	0	.....	3	3	
4119.22	2	.....	0	.....	7	8	Bl. *He* I
4132.82	1	.....	0	.....	5	6	
4153.31	1	− 60	0	.....	5	7	
4185.45	0–1	.....	0	.....	4	8	
4189.79	1	.....	0	.....	6	10	

TABLE I—*Continued*

λ	Absorption		Emission		Intensity		Remarks
	Int.	Vel.	Int.	Vel.	τ Sco	Lab.	
	O II I.P. 34.9—*Continued*						
4303.82	0–1	.....	0	.....	7	5	
4317.60	2	−105	0	.....	6	8	
4319.65	3	90	0	.....	7	8	
4345.57	1	107	1	+ 20	10	7	
4349.44	5	86	0	.....	12	8	
4351.28	1	49	0	.....	8	6	
4366.91	3	76	0–1	+ 46	8	7	
4369.28?	2	(4)	1	(+109)	1	4	
4378.40	1	74	0	.....	3	3	
4395.95	5	(144)	4	− 35	3	7	
4414.89	2	71	1	+ 11	10	10	
4416.97	2	103	0	.....	10	8	
4443.05	1	.....	0	.....	2	5	
4452.38	1	90	0	.....	2	6	
4506.50?	1	142	0	.....	1	2	
4590.98	2	64	0	.....	5	9	
4596.19	1	60	0	.....	5	8	
4638.86	2	63	0	.....	3	6	
4649.15	5	82	0	.....	6	10	Bl. *C* III
4661.65	3	69	0	.....	4	9	
4676.25	2	104	0	.....	3	8	
4705.36	1	.....	0	.....	3	8	
4710.04?	1	− 74	0	.....	1	5	
	Mg II I.P. 15.0						
4481.23	2	−118	1	− 3	8	100	
	Si III I.P. 33.3						
4552.61	8	− 95	1	− 7	7	9	
4567.83	7	103	0	.....	7	7	
4574.75	5	− 92	0	.....	6	4	
	Si IV I.P. 45.0						
4088.86	4	− 60	0	.....	10	10	
4116.10	4	− 46	0	.....	10	8	
4212.38	1	.....	0	.....	4	3	
4654.14	1	.....	0	.....	4	4	

TABLE I—*Continued*

λ	Absorption		Emission		Intensity		Remarks
	Int.	Vel.	Int.	Vel.	τ Sco.	Lab.	
	S II I.P. 23.3						
4162.64.....	1	− 32	0	.....	3	10	Bl. *C* III
	S III I.P. 34.9						
3928.59.....	1	− 98	0	.....	.....	9	
3983.76.....	1	42	0	.....	1	7	
4253.51.....	4	85	0	.....	12	10	Bl. *O* II
4285.00.....	2	118	0	.....	3	8	
4361.57.....	1	92	0	.....	3	7	
4364.77.....	1	−108	0	.....	2	5	
	Ca II I.P. 11.8						
3933.68.....	1	−133	0	.....	.....	200	Stellar
3933.68.....	9	+ 14	0	.....	.....	200	Interstellar
3968.49.....	3	− 86	0	.....	.....	150	Doubtful stellar
	Fe II I.P. 16.5						
4233.17?.....	1	− 65	0	.....	0	10	

III. COMPARISON OF P CYGNI WITH NORMAL B STARS

The spectrum of P Cygni is listed in the *Henry Draper Catalogue* as B1p. Its absorption lines may therefore be compared with those of three normal stars, τ Scorpii (B0), β Canis Majoris (B1), and γ Pegasi (B2). P Cygni exhibits a number of interesting features:

1. The *H* lines are extremely sharp; in fact, they are much sharper than in any normal B-type giant. Curtiss and Gerasimovič have reported diffuse absorption borders on the red sides of the emission lines. In the case of $H\gamma$ this must be due to the group of strong *O* II lines λλ 4345–4350; at $H\epsilon$ a similar effect is caused by *O* II 3973; at

Hδ a faint indication of absorption may be caused by *O* II 4105, although I have not measured this line. The appearance of the *H* lines suggests complete absence of Stark broadening.

2. The *He* I lines are exceptionally strong, surpassing in this respect ordinary B1 stars.

3. *He* II 4686 is almost completely absent. This is in agreement with the assignment of P Cygni to class B1.

TABLE Ia

UNIDENTIFIED LINES

λ(Star)	Int.	λ(P Cyg) Abs.	Int.	λ(P Cyg) Em.	Int.
.....	.....	3957.20	2	.....	0
.....	.....	4003.42	3	4004.62	2
.....	.....	4020.44	2	4022.12	3
4039.24	1	4037.13	2	4038.74	1
.....	.....	.....	.....	4164.07	3
4352.47	1	.....	.....	4352.07	2
.....	.....	4372.66	1	.....	.....
.....	.....	4382	1	4383.07	3
4419.62	3	4417.42	7	4419.24	5
4431.03	2	4429.04	4	4430.91	3
.....	.....	4501.14	1	.....	.....
.....	.....	.....	.....	4512.30*	0–1
.....	.....	4616.45	1	.....	.....

* Uncertain.

4. *Si* IV is fairly strong, which would place P Cygni between O9 and B2.

5. *O* II and *N* II are both strong, but exhibit peculiar intensities which are discussed separately in section v.

6. The great strength of the *S* III lines is unusual.

7. Equally unusual is the weakness of *C* II, which is very strong in all three normal stars, and of *Mg* II, which is fairly strong in τ Scorpii and in β Canis Majoris, and very strong in γ Pegasi.

It is fairly obvious that the absorption spectrum of P Cygni does not correspond to that of a normal B star. On the other hand, there is a definite resemblance to the absorption spectrum of the B5 component of β Lyrae.[18] The latter corresponds to a lower stage of excitation, and the absorption lines of *O* II, *N* II, *S* III, *N* III, etc., are

[18] H. Pillans, *ibid.*, **80**, 51, 1934; Struve, *Observatory*, **57**, 265, 1934

TABLE II

LIST OF ELEMENTS

ELEMENT	I.P.	NO. OF LINES		REMARKS
		Abs.	Em.	
H	13.5	4	4	Very strong
He I	24.5	12	11	Very strong; all lines present except λλ 3935 (1), 4023 (1), and forbidden transitions
He II	54.2	1?	0	λ 4686 is extremely faint or absent
C II	24.3	1	1	λ 4267 is surprisingly weak
C III	47.7	4	0	Strongest lines are very weak
N II	29.5	19	10	Strong
N III	47.4	6	2	All strong lines are present
O II	34.9	34	4	Many lines in absorption
O III	54.9	0	0	λ 3961.59 is absent
Ne II	40.8	0	0	Absent
Mg II	15.0	1	1	λ 4481 is surprisingly weak
Al III	28.3	0	0	Absent
Si II	16.3	0	0	Absent
Si III	33.3	3	1	Strong in absorption; extremely weak or absent in emission
Si IV	45.0	4	0	Fairly strong in absorption
P II	19.8	0	0	A weak line suspected at λ 4091 is probably not *P* II; λ 4475 is absent
P III	30.3	0	0	λλ 4080, 4222, 4247 are absent
S II	23.3	1	0	λ 4162 is extremely weak in absorption
S III	34.9	6	0	Surprisingly strong
Cl II	23.1	0	0	Probably absent; a weak line was suspected at λ 4572 but this may not be real, or may be due to *Ca* III
K II	31.7	0	0	Absent
Ca II	11.8	3	0	Stellar K and H (the latter doubtful); interstellar K
Ca III	51.0	0	0	Absent
Sc II	12.8	0	0	Absent
Ti II	13.6	0	0	Absent
V II	14.7	0	0	Strongest two lines in this range are 4005.71 (60) and 4023.39 (50). These were suspected to be identical with the stellar lines 4003.42 (abs.); 4004.62 (em.); 4020.44 (abs.); 4022.12 (em.). However, the normal velocities of −100 km/sec. for absorption lines and 0 km/sec. for emission lines leave a discrepancy of 1 A. Weaker laboratory lines of *V* II, λλ 3952 (4); 4036 (4); 4183 (35); and 4202 (35) are missing in P Cygni
Cr II	16.6	0	0	λ 4559 is absent
Mn II	15.7	0	0	Absent
Fe II	16.5	1	0	λ 4233 is probably present
Ni II	18.2	0	0	Absent
Sr II	11.0	0	0	Absent
Zr II	14.0	0	0	Absent
Unidentified		10	9	

missing. However, the character of the *H* lines, the exceptional strength of the *He* I lines, and the weakness of *Mg* II and *C* II are similar features.

Some of the strongest unidentified emission lines in P Cygni have been observed by Merrill[19] in BD+11°4673. These are λλ 4383, 4419, and 4431.

The gradient effect[20] in P Cygni is very pronounced, thus resembling such peculiar stars as 17 Leporis and the B5 component of β Lyrae. This is strikingly illustrated by the intensities of the *He* I lines in τ Scorpii, γ Pegasi,[21] and P Cygni. The estimates for τ Scorpii and γ Pegasi were made on Mount Wilson coudé spectrograms, and their scale is approximately twice as extended as that used for P Cygni. The intensities plotted in Figure 1 have been reduced to the same scale. It is clear, both from Figure 1 and from Plate II, that the strong *He* I lines predominate in P Cygni, while the weaker lines are much more conspicuous in τ Scorpii and γ Pegasi.

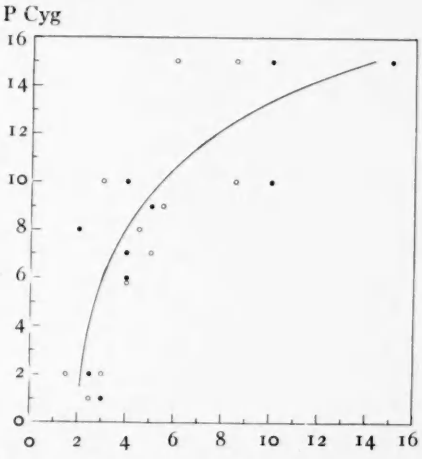

FIG. 1.—*He* I in P Cygni (ordinate), τ Scorpii (abscissa, ●) and γ Pegasi (abscissa, o).

While the gradient has not yet been measured, I estimate it to be approximately similar to that of β Lyrae (B5) and of 17 Leporis. Consequently, the total absorption is proportional to the number of atoms, for weak and moderately strong lines, while for very strong lines the total absorption is almost independent of the number of atoms.

In a recent paper on the gradient effect[20] it was pointed out that turbulence could explain the observed phenomena. It is probable that the same explanation holds for the case of P Cygni. The absorption lines, as well as the emission lines, are believed to originate

[19] *Ap. J.*, **69**, 330, 1929.

[20] Struve and Elvey, *ibid.*, **79**, 409, 1934.

[21] *Ibid.*, **74**, 225, 1931.

in an expanding nebula. The emission lines are appreciably broadened. For *He* I 4472 I find $\Delta\lambda = 2.8$ A. The contour of the bright line is fairly flat at the top, but the edges are not perfectly sharp, as would be the case if there were no dispersion in the velocities of expansion (or turbulence). In fact, Beals[12] has shown that the amount of dispersion can be determined from the contours.

The shape of the stronger absorption lines in P Cygni confirms this view. They are appreciably widened and resemble contours produced by turbulence broadening.[22]

IV. THE INTENSITIES OF THE ABSORPTION LINES

The absorption lines of *O* II and *N* II are sufficiently numerous for a detailed discussion. Table III gives the more important lines of these elements, arranged according to multiplet. The corresponding atomic transitions are shown in Figures 2 and 3, which are taken partly from Becker and Grotrian[23] and partly from Bacher and Goudsmit.[24] The multiplets of both spectra may be roughly subdivided into two groups: in *O* II the group of lower excitation starts from configurations $2s^2 2p^2 3s$ (limit $^3P_{012}$) and $2s^2 2p^2 3s$ (limit $^1D_2$) and ends in configurations $2s^2 2p^2 3p$ (limit $^3P_{012}$) and $2s^2 2p^2 3p$ (limit $^1D_2$). The lower states of these transitions connect directly with the low metastable states $2s^2 2p^2 2p[^2P$ and $^2D]$, and, in a few cases, with

[22] In this connection reference may be made to Menzel's recent criticism of our hypothesis of turbulence (*Pub. A.S.P.*, **46**, 216, 1934). The formulae used were originally derived for the case of thermal Doppler effect. Their extension naturally presupposes that the turbulence varies along the radius. This is entirely reasonable, not only in expanding nebular shells, like those of P Cygni, β Lyrae, and 17 Leporis, but also in giant atmospheres like those of ϵ Aurigae and ζ Aurigae, which have a thickness of the order of one astronomical unit. The effect of convection currents (or of turbulent velocities which are essentially constant along the radius) has been investigated in connection with our work on stellar rotation and found to be inappreciable, at least in those spectroscopic binaries in which a direct test of axial rotation is possible. The broadened lines in stars having large intensity gradients are not, however, produced by rotation. The contours of lines in 17 Leporis, ϵ Aurigae, etc., cannot be reconciled with rotational or convectional broadening. They are in good agreement with the theory of turbulence, in the limited sense specified above.

[23] *Ergebnisse der exakten Wissenschaften*, **7**, 8, 1928.

[24] *Atomic Energy States*, New York, 1932. For *O* II see Russell, *Phys. Rev.*, **31**, 27, 1928. The multiplet designations in Table III are from C. E. Moore, *A Multiplet Table of Astrophysical Interest*, Princeton, 1933.

the ground level of the *O* II ion, $2s^2 2p^2 2p^4 S$. The upper levels of these transitions do not directly connect with the low 2p-levels. In the second group the transitions, corresponding generally to higher-excitation energies, start from those levels which were upper levels in the preceding group and end in transitions $2s^2 2p^2 3d$ (limits $^3P_{012}$ and

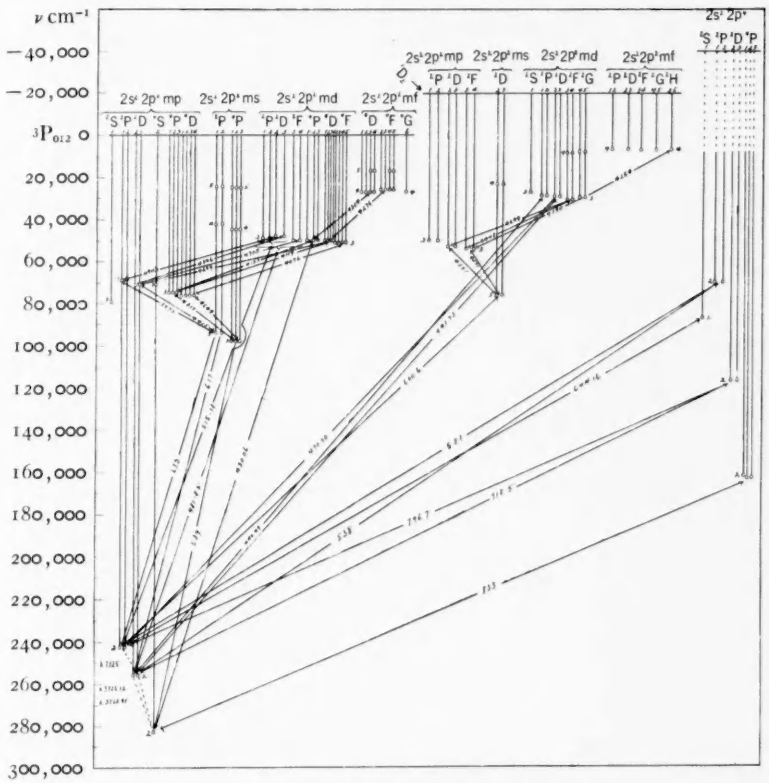

FIG. 2.—Grotrian diagram for *O* II

$^1D_2$). Finally there are a few lines, also included in the second group, which start from configurations $2s^2 2p^2 3d$ and end in configurations $2s^2 2p^2 4f$. The average excitation potentials of the two groups are 23 volts for the lower and 26 volts for the upper state, in the first group; and 26 volts for the lower and 29 volts for the upper state, in the second group.

A similar division has also been made in the case of *N* II. Here the

excitation potentials of the first group are approximately 18 and 21 volts, while those of the second group are 21 and 23 volts.

In Figure 4 I have plotted the estimated absorption intensities in the spectrum of P Cygni against those of τ Scorpii, β Canis Majoris, and γ Pegasi. The first group of lines is represented by filled circles,

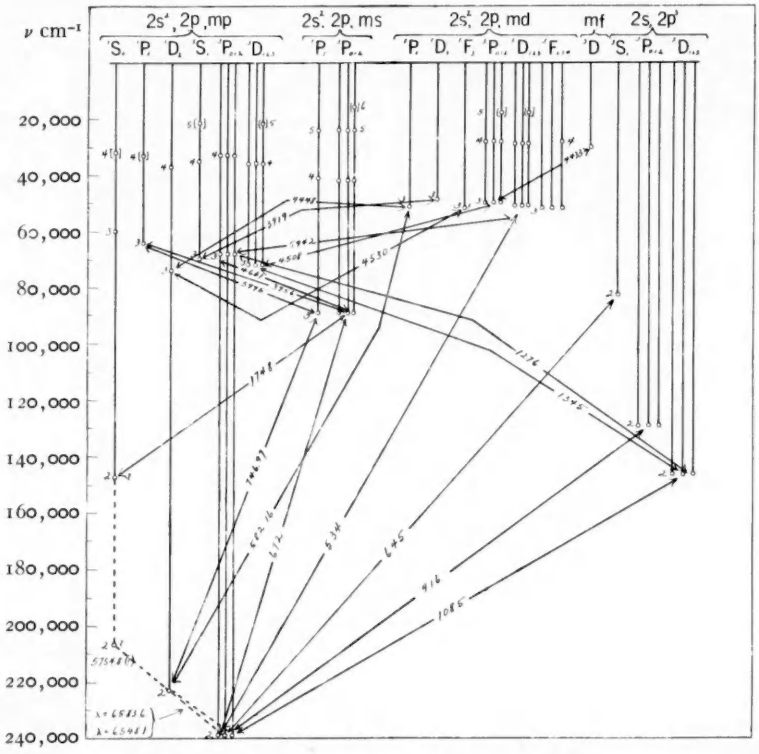

FIG. 3.—Grotrian diagram for *N* II

while the second group is represented by open circles. A few unclassified lines of *N* II have arbitrarily been added to the second group. The two *O* II lines, λ 4469 and λ 4396, have been omitted for reasons which are explained in section vii. Several other lines which are complicated by blends have been omitted. These are shown in parentheses in Table III.

In all four sections of Figure 4 the filled circles are systematically above the open circles, indicating that for both *O* II and *N* II the

upper transitions are weakened relative to normal B stars. This may also be confirmed by an inspection of Plate II.

The suggestion might be made that this is a normal effect of excitation. Indeed, I have found some time ago[25] that the *O* II lines do not all come to a maximum at the same place in the spectral se-

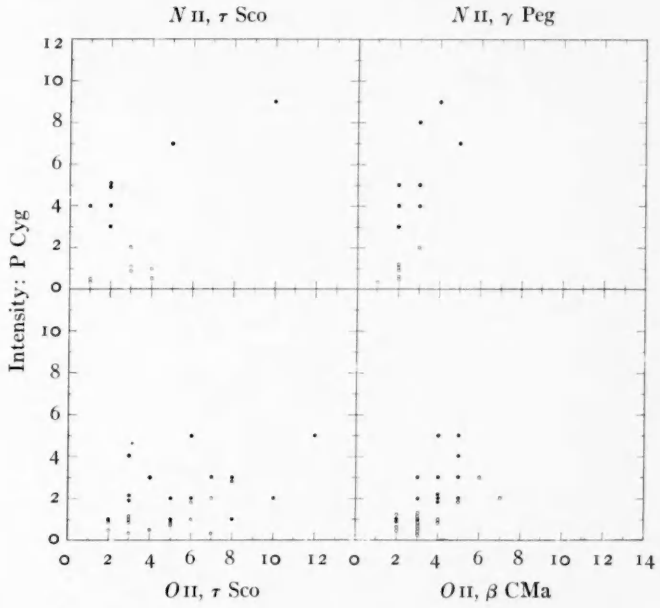

FIG. 4.—Intensities of high-level transitions (o) and of low-level transitions (●)

quence, but that those of higher excitation are, in accordance with theory, slightly stronger in the earlier spectral subdivisions.

In order to test this effect, I have compared [26] in Table IV several of the most conspicuous lines of both groups in P Cygni, 10 Lacertae (O9), and ι Herculis (B_3). Of the two comparison stars, the first corresponds to a higher general level of excitation than P Cygni and the second to a lower level. The relative strengthening of the high-level lines, in passing from class B_3 to class O9, is obvious.

[25] *Ap. J.*, **78**, 73, 1933.

[26] The intensities of lines in stars other than τ Sco are taken from *ibid.*, **74**, 225, 1931; those of τ Sco are from *ibid.*, **77**, 321, 1933.

TABLE III

Wave-Length	Multiplet	Intensity				Remarks
		P Cyg Abs.	Lab.	τ Sco	β CMa	
	Low Transitions of *O* II					
3973	$z^2P-e^2P^o$	4	10	3	5	
4415	$z^2P-e^2D^o$	2	10	10	5	
17		(2)	8	10	4	
52		1	6	2	2	
4317	$y^4P-e^4P^o$	2	8	6	4	
20		3	8	7	5	
45		(1)	7	10	3	
49		5	8	12	4	
67		3	7	8	4	
4649	$y^4P-e^4D^o$	5	10	6	5	Bl. C III in τ Sco
38		2	6	3	4	
61		3	9	4	3	
76		2	8	3	3	
4351	$y^2D-f^2D^o$	1	6	8	3	
47		(0)	5	8	2	
4591	$y^2D-e^2F^o$	2	9	5	4	
96		1	8	5	2	
	High Transitions of *O* II					
4396	$e^2D^o-x^2D$	(5)	7	3	3	
69		(2)	4	1	1	
4705	$e^2D^o-z^2F$	1	8	3	3	
4699	$e^2D^o-z^4D$	0	7	.....	2	
4153	$e^4P^o-x^4P$	1	7	5	4	
32		1	6	5	3	
4119	$e^4P^o-z^4D$	(2)	8	7	4	
4076	$e^4D^o-z^4F$	3	10	8	6	
72		2	8	6	5	
69		2	6	7	7	
78		1	4	3	3	
85		1	3	3	3	

TABLE III—*Continued*

Wave-Length	Multiplet	Intensity				Remarks
		P Cyg Abs.	Lab.	τ Sco	β CMa	
		High Transitions of *O* II—*Continued*				
4304	$x^4P-f^4D^o$	0–1	5	7	3	
4276	$z^4D-e^4F^o$	0	4	2	3	
4448	$e^2F^o-y^2F$	0	6	3	2	Bl *N* II
43		1	5	2	2	
4190	$e^2F^o-z^2G$	1	10	6	4	
85		0–1	8	4	3	
4254	$z^2G-e^2H^o$	(4)	8	12	5	Bl. *S* III
		Low Transitions of *N* II				
3995	$3s^1P^o-3p^1P$	9–9	10	10	4	
3956	$3s^3P^o-3p^1P$	4–1	6	1	2	
4631	$3s^3P^o-3p^3P$	7–9	10	5	5	
43		8–7	8	(1)	3	
21		5–4	7	2	2	
13		3–2	6	2	2	
07		5–3	7	2	3	
01		4–4	8	2	3	
		High Transitions of *N* II				
4530	$3p^1D-3d^1F^o$	0–1	5	1	2	
4508	$3p^3D-3d^3P^o$	0	3	1	1	
4448	$3p^1D-3d^1P^o$	2–2	10	3	3	
		Unclassified *N* II				
4237		0–1	6	4	2	
41		1	8	4	2	
4043		1	3	3	2	
35		1	4	3	2	
4433		0	6	1	1	

Considering the strength of some *O* II lines in P Cygni, it is somewhat difficult to assign to it a class later than B1. On the other hand, the relative intensities of the high-level and the low-level lines would place it nearer to B2, or even to B3. Such a late spectral class is not possible because of the strength of the *S* III lines and the presence of *N* III, *Si* IV, etc.

In the case of *N* II the effect is even more striking. No possible excitation can account for the enormous strengthening of low-level

TABLE IV

O II

Wave-Length	Intensity		
	P Cyg(B1p)	10 Lac (O9)	ι Herc (B3)
	Low Transitions		
4415	2	0	2
4317	2	0	3
4320	3	1	0
	High Transitions		
4076	3	4	1
4072	2	2	1
4069	2	4	2
4705	1	1	0
4699	0	1	0

lines of *N* II in P Cygni. Table V illustrates this. There is little difference between β Canis Majoris (B1) and 67 Ophiuchi (B5), and the enormous enhancement of the low-level lines in P Cygni must be due to causes other than thermal excitation.

V. COMPARISON OF EMISSION LINES WITH ABSORPTION LINES

It is generally recognized that the most effective mechanism in the production of bright lines in stellar spectra is photo-electric ionization with subsequent recombination. This mechanism has been

analyzed by Zanstra,[27] Menzel,[28] Bowen,[29] Miss Payne,[30] Beals,[31] Woolley,[32] and others. Beals has applied Zanstra's theory to the

TABLE V

N II

Wave-Length	Intensity		
	P Cyg	β CMa (B1)	67 Oph (B5p)
	Low Transitions		
3995	9	4	3
4631	7	3	4
4613	3	2	1
4621	5	1	2
	High Transitions (and Unclassified)		
4530	0–1	1	0
4448	2	2	2
4035	1	2	1
4242	1	3	2

emission lines of *H* and of *He* I in P Cygni and has found a temperature of 19,300° K in the former case and 26,000° K in the latter case.

[27] *Ibid.*, **65**, 50, 1927; *Zs. f. Ap.*, **2**, 1, 1931.

[28] *Op. cit.*, **38**, 295, 1926. [29] *Ap. J.*, **67**, 14, 1928; **81**, 1, 1935.

[30] *M.N.*, **92**, 368, 1932. Miss Payne's criticism of my rotational hypothesis of bright lines is of no consequence to this paper. There is no disagreement in so far as recombination and fluorescence is concerned. In fact, I have mentioned these mechanisms in several papers and have accumulated observational evidence in favor of recombination as the principal source of bright *H* lines in Be stars. There are five major questions to be answered in connection with stellar emission lines: (1) Where do these lines originate? (2) How do the atoms get there? (3) By what mechanism are they excited to radiation? (4) Why are some bright lines broad and flat-topped while others are narrow? (5) Why do many bright lines vary in intensity and contour? There is no discordance with regard to question 1. I have attempted to answer questions 2 and 4 by the rotational hypothesis for ordinary Be stars, and by the expanding shell hypothesis for stars of the P Cygni type. Question 3 is satisfactorily answered by the work of Rosseland, Miss Payne, and others. Question 5 has not yet been adequately answered, although McLaughlin and Gerasimovič have made interesting attempts in this direction.

[31] *Pub. Dom. Ap. Obs. Victoria*, **4**, 271, 1930. [32] *M.N.*, **94**, 631, 1934.

Since the emission lines of *He* I are very strong, it is obvious that there must be a large amount of energy in the star's spectrum toward the violet from λ 504. This agrees with the temperature derived by Beals. The energy-curve corresponding to 20,000° K and a few of the series limits are shown in Figure 5.

N II is only partly in emission, indicating that at λ 418 the energy-curve is somewhat depleted. *Si* III and *O* II appear almost exclusive-

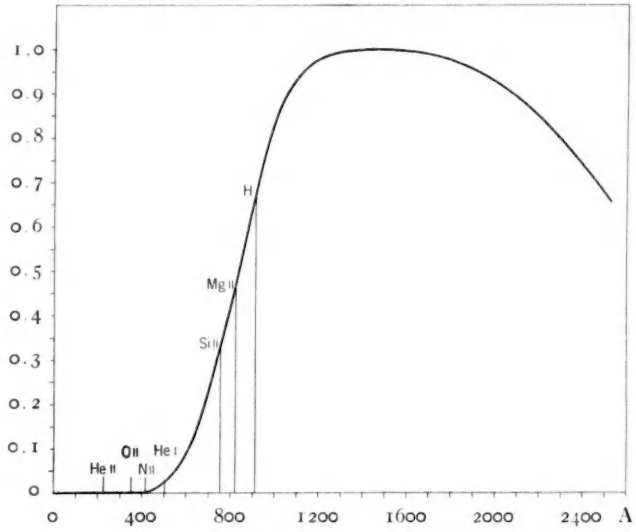

FIG. 5.—Black-body curve for $T = 20{,}000°$ K

ly in absorption, which might indicate an insufficient amount of radiation at λ 370 and λ 353. Elements of higher ionization potential, such as *S* III, *N* III, *Si* IV, and *C* III, are seen only in absorption, while *O* III is completely absent.

The emission lines agree fairly well with the recombination hypothesis, but there are a few anomalies. The absence of *Si* II and the weakness of *Mg* II are interesting. The first, though its ionization potential of 16.3 volts is slightly above that of *H*, would not normally be expected in a B2 spectrum, since in ordinary stars the relatively low ionization potentials of *Si* III and *Si* IV will lift a large number of atoms into higher stages of ionization, thus preventing a recombination spectrum of *Si* II. However, we have just pointed out that there

is probably no recombination spectrum of *Si* III, so that the majority of the *Si* atoms must be in the ground level of the *Si* III ion. Even more surprising is the weakness of *Mg* II. In normal B2 stars, λ 4481 is a fairly strong line, and it usually persists into the O's. Now, the ionization potential of *Mg* III is 80 volts, so that the majority of *Mg* atoms must be in the ground level of *Mg* III, and should thus favor recombination processes forming the line λ 4481 in emission.

The most obvious explanation of the weakness of *Mg* II, a phenomenon that seems to be prevalent in Be stars, is that the star's continuous spectrum in the neighborhood of λ 824 is still sufficiently depleted of radiation by the strong photo-electric ionization at the limit of the Lyman series of *H*, at λ 911. This would not be surprising, since the mechanism of Zanstra, which is justified by its results, demands that a large fraction of the entire energy on the violet side of λ 911 is utilized in producing the emission lines of *H*.

A similar but even more striking anomaly exists in the case of *C* II, which should normally be strong in class B2. Here the ionization potential, 24.3 volts, is almost identical with that of *He* I, 24.5 volts, and the limits, at λ 508 and λ 504, are so close to one another that the recombination spectrum of *C* II will doubtless be suppressed by continuous absorption at the ultra-violet *He* I limit.

Much less satisfactory is the behavior of *N* II. Here the ionization potential of 29.5 volts corresponds to λ 418. The amount of radiation available for ionization at this wave-length is about one-seventh of that available at the *He* I limit and about one two-hundredth of that available at the *H*-limit. At the limit of *O* II, λ 353, where no appreciable recombination occurs, the energy is one-eightieth of that at λ 504, *He* I. We are therefore uncertain whether recombination does or does not occur in *N* II.

However, the observations show clearly that the emission is limited to low-level lines, strong high-level lines being devoid of emission. This is distinctly unfavorable to the hypothesis of recombination: in the laboratory, recombination has invariably increased the intensities of high-level lines, and Mohler and Beckner[33] have even succeeded in observing new high-level lines which are not seen

[33] *J. of Research, Bureau of Standards*, **2**, 489, 1929. See also Ruark and Urey, *Atoms, Molecules and Quanta*, p. 470, 1930.

in ordinary laboratory sources. The anomaly of the *N* II emission lines is probably related to that of the absorption lines discussed in the preceding section.

The absorption lines of P Cygni are characteristic of a much higher degree of excitation than are the emission lines. The limit is probably in the vicinity of 50 volts: *Si* IV, ionization potential 45.0 volts, and *N* III, ionization potential 47.4 volts, are present; *C* III, ionization potential 47.7 volts, is very weak.

It is quite clear that while the absorption lines of P Cygni correspond to a class intermediate between Bo and B1, the emission lines are more nearly at B2 or B3. It might be thought that the appearance of emission is merely a function of the intensity of the absorption lines, but that is not true. Thus, some faint lines of *He* I and of *N* II are accompanied by emission, while some of the stronger lines of *O* II are devoid of it.

The radial velocities discussed in section viii leave no doubt that the absorption lines originate in the expanding shell, and in this respect there is no great difference between absorption lines which are accompanied by emission lines and those which are not.

There is at present no adequate theory of the origin of absorption lines in expanding nebular shells. It is obvious, however, that in a general way we are dealing with the same process of absorption and re-emission (or scattering) which gives rise to the absorption lines in a reversing layer.

Ignoring for the moment all anomalies arising through departures from thermodynamic equilibrium, such as were mentioned in the preceding paragraphs, we should expect that for a thin shell of radius R around a star of radius r, the ratio of absorption intensity to emission intensity would be roughly proportional to the ratio of the volume of gas projected upon the star's disk to that of the entire shell visible to the observer. This gives

$$\frac{A}{E}=\frac{1-\sqrt{1-\frac{r^2}{R^2}}}{1+\sqrt{1-\frac{r^2}{R^2}}}\,f(N,\sigma)\,.$$

Accordingly, if for two equal absorption lines the emission lines are not the same, we conclude that they must originate in layers of differ-

ent R. The function of (N, σ), depending upon the number of atoms and the absorption coefficient, takes care of the gradient effect, etc. The formula, of course, fails if $R=r$, for then we should use the customary treatment of a scattering reversing layer. The factor $f(N, \sigma)$ also shows that it is not permissible to compare unequal absorption lines.

Since we have shown that equal absorption lines may have widely different emission lines, we conclude that, in general, the former originate in other shells than do the latter. This agrees with the result that the level of excitation is much higher for absorption than for emission.

This effect is seriously complicated by departures from thermodynamic equilibrium. These must be made responsible for the enormous difference in the emission and absorption ratios of *He* I lines belonging to different series. Thus, Schwede[34] has found, in agreement with Elvey:[13]

He 4388: total absorption . .	0.62 A	*He* 4388: total emission	0.16 A
4472: total absorption . .	0.69	4472: total emission	1.56

It is difficult to explain this result, unless the processes of absorption and emission are far from being balanced.

Eddington[35] has shown that the state of ionization in a nebula is equal to that of a reversing layer having a density of $\rho\delta$, where ρ is the density of the nebula and δ the dilution factor $4R^2/r^2$. Since, for the absorption lines of highest excitation, A/E is smaller than for lines of low excitation, we conclude that $R(\text{high exc.}) < R(\text{low exc.})$, and that, consequently, the factor $\rho\delta$ decreases as we approach the star. Since $\delta \sim R^2$, we find that ρ must increase inward more slowly than $1/R^2$. According to Eddington,[36] in an isothermal nebula $\rho \sim 1/R^2$. An alternative explanation would be that δ increases outwardly more rapidly than R^2.

VI. NORMAL EXCITATION OF SPECTRAL LINES IN P CYGNI

If the absorption lines of P Cygni originate in an expanding shell, it may not be permissible to apply to them the ordinary theory of stellar absorption lines. Especially does it seem dangerous to apply the Boltzmann law for the derivation of the numbers of atoms in

[34] *Ap. J.*, **77**, 348, 1933.

[35] *Internal Constitution of the Stars* (German ed.), p. 478, 1928. [36] *Ibid.*, page 489.

various quantum states. The problem of radiative equilibrium in a nebula has been treated by Rosseland[37] and applied by him to the case of three levels of increasing energy, 1, 2, 3. If a_{ki} and a_{ik} are the transition probabilities, the condition of equilibrium is

$$\sum_k a_{ki}x_k = 0;\ a_{ii} = -\sum_k a_{ik}\ .$$

The solution of these equations gives the numbers of atoms in the various states,

$$x_k = \lambda_m a^{km}\ ,$$

where λ_m is a constant and a^{km} is the subdeterminant of the determinant a_{km}. For three states we have

$$a^{11} = a_{21}(a_{31}+a_{32})+a_{23}a_{31}\ ,$$
$$a^{21} = a_{12}(a_{31}+a_{32})+a_{13}a_{32}\ ,$$
$$a^{31} = a_{13}(a_{21}+a_{23})+a_{12}a_{23}\ .$$

Rosseland applies these formulae to the case where the second level is metastable, i.e., $a_{21} = a_{12} = 0$, and finds that in this case the number of atoms in the metastable level is similar to that given by Boltzmann's law.

To represent more closely the conditions prevailing in the lower levels of the two groups of transitions of *O* II and of *N* II, we shall assume that $a_{31} = a_{13} = 0$. In that case

$$a^{11} = a_{21}a_{32}\ ,\quad a^{21} = a_{12}a_{32}\ ,\quad a^{31} = a_{12}a_{23}\ ,$$

and, accordingly,

$$\frac{x_2}{x_1} = \frac{a^{21}}{a^{11}} = \frac{a_{12}}{a_{21}}\ ,$$

$$\frac{x_3}{x_1} = \frac{a^{31}}{a^{11}} = \frac{a_{12}a_{23}}{a_{21}a_{32}}\ .$$

Now, according to Einstein, for emission $a_{ki} = \alpha_{ik}(1+\bar{\rho}[\nu_{ik}])$ and for absorption $a_{ik} = \alpha_{ik}^{-}(\nu_{ik})\ \omega_k/\omega_i$.

$\bar{\rho}(\nu_{ik})$ is the energy density of the radiation divided by $8\pi h\nu^3/c^3$. Accordingly,

$$\bar{\rho}(\nu_{ik}) = \frac{1}{\delta}\,\rho(\nu_{ik})\ ,$$

[37] *Astrophysik auf atomtheoretischer Grundlage*, p. 224, 1931.

where $\rho(\nu_{ik})$ is the energy density given by Planck's law. Substituting this, we find

$$\frac{x_2}{x_1}=\frac{\omega_2}{\omega_1}\,\frac{\rho(\nu_{12})}{1+\frac{1}{\delta}\rho(\nu_{12})}\cdot\frac{1}{\delta},$$

$$\frac{x_3}{x_1}=\frac{\omega_3}{\omega_1}\,\frac{\rho(\nu_{12})\rho(\nu_{23})}{(1+\frac{1}{\delta}\rho[\nu_{12}])(1+\frac{1}{\delta}\rho[\nu_{23}])}\cdot\frac{1}{\delta^2}.$$

For small values of $\rho(\nu)$ the number of atoms in the second state is proportional to $1/\delta$ and the number in the third state is proportional to $1/\delta^2$. It is obvious that if δ is large enough, there must be a markedly smaller number of atoms in state 3 than would be given by Boltzmann's law. Furthermore, it would appear that for suitable values of δ, x_3 is smaller if $a_{13}=a_{23}=0$ than if $a_{13}=a_{23}\neq 0$.

In a nebula with large δ we should therefore expect that aside from recombination lines and resonance lines (which, for most atoms, are not in the observable range), only those lines would be strong which have lower levels connecting directly with the ground level or with one of the low metastable levels.[38] This condition is fulfilled for *N* II and probably also for *O* II. It may hold in the case of *Si* III, whose lower levels are reached directly from the metastable ^{3}P-state, but it is violated in the case of *Si* IV, whose lines λ 4089 and λ 4116 originate in the $2s^2$S-state, which does not directly connect with the ground level, $1s^2$S, but can only be reached from it by two or more jumps. It is therefore probable that, at least for *Si* IV, δ is not very large. A numerical evaluation of the quantities involved is not, at present, possible. We can only conclude that slight departures from thermal excitation are present, but that for *Si* IV conditions resemble those prevalent in ordinary stars.

VII. ABNORMAL FLUORESCENCE

The spectrum of P Cygni contains a peculiarly strong line, present both in absorption and in emission, at λ 4396. This line has been

[38] We ignore transition probabilities from the ground level to the upper states of the high-level lines. Although this is not rigorously correct, it seems probable that these transitions will have little effect in lifting atoms into a state from which emission of the high-level lines is possible. In the first place, the continuous spectrum in the required wave-lengths (λ 430±) is relatively weak; in the second place, their coefficients a are probably small.

tentatively identified as *O* II 4395.95, and all available measurements prove that the agreement in wave-length is excellent. However, the violet absorption line is distinctly too strong for its laboratory intensity and the emission line, if really due to *O* II, is by far the strongest line of this atom.

Two possibilities suggest themselves: either (1) the agreement in wave-length is a mere coincidence, the line being really unidentified, or (2) the *O* II atom has an abnormal tendency to enhance this particular transition.

It is difficult either to support or to disprove the first possibility. There are four other unidentified lines in the region λλ 4300–4500, and λ 4396 may belong to this group. On the other hand, a chance coincidence of an unidentified line with *O* II 4395.95 is improbable.

The second possibility merits a careful scrutiny. Bowen[39] has recently found a powerful secondary mechanism of excitation which depends upon the close agreement in wave-length of a strong ultraviolet emission line (itself produced by the primary mechanism of recombination) with an absorption line of another atom. The question in our case is: Is there such an anomalous mechanism at work in *O* II which would lift an abnormal number of atoms into either the upper or the lower level of the line λ 4396?

The line *O* II 4396 is a member of the multiplet $2s^2 2p^2 3d^2D - 2s^2 2p^2 3p^2D$. The upper terms are $\nu = 48{,}618.4$ and $\nu = 48{,}566.4$. The lower terms are $\nu = 71{,}498.9$ and $\nu = 71{,}308.2$. The first upper level leads to the lines λ 4369.28 (4) and λ 4406.02 (1), while the second gives λ 4395.95 (7) and λ 4359.38 (1). The two upper levels do not connect with the ground level, which is a ^4S, but they connect with the very low metastable level $2s^2 2p^2 2p^2P$, viz., $\nu = 242{,}555.5$ and $\nu = 242{,}560.0$. These lead to the two following close pairs: λ 515.62 and λ 515.49. Bowen[39] has actually measured λ 515.62 (2) and λ 515.47 (2). The first of these feeds λ 4367 and the second feeds λ 4396.

Bowen has pointed out that only *H* and *He* could reasonably be expected to produce abnormal fluorescence. *H* and *He* II have no lines near λ 515. But there is a conspicuous *He* I line, $1^1S - 5^1P$ (see Grotrian diagram, Fig. 6), which gives, from the term values, λ 515.07 and which has been measured by Lyman[40] at λ 515.65 and

[39] *Phys. Rev.*, **29**, 243, 1927. [40] *Ap. J.*, **60**, 11, 1924.

by Hopfield[41] at λ 515.596. The agreement of this value with the two *O* II lines is rather striking, being 0.02 A in the first case and 0.11 A in the second.[42] The second, larger, residual applies to the case of *O* II 4395.

The visible *He* I lines, especially of the series $2^1S - m^1P$, are very strong in emission. The width of λ 4472 is approximately 2.8 A, and

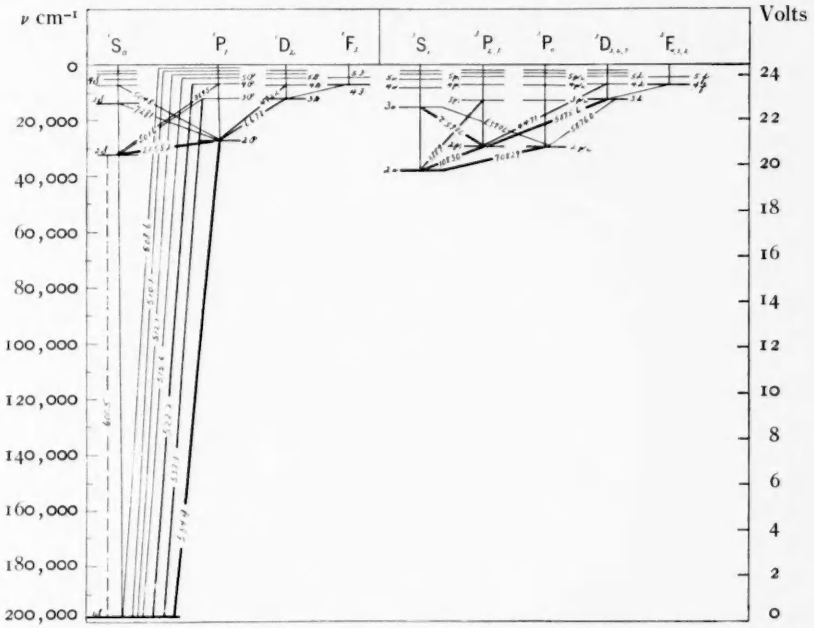

FIG. 6.—Grotrian diagram for *He* I

the contour is fairly flat at the top. Since the broadening is due to Doppler effect of expansion,[43] we have

$$\Delta\lambda \sim \lambda ,$$

[41] *Ibid.*, **72**, 136, 1930.

[42] Since writing the foregoing, Professor Bowen has called my attention to the measurements of the *O* II lines by B. Edlén (*Nova Acta Regiae Societatis Scientiarum Upsaliensis* [4th ser.], **9**, No. 6, 1933): λ 515.640 and λ 515.498. These values are estimated to be accurate to 0.01 A or 0.02 A. The residuals are therefore reduced to 0.098 A in the case of λ 4396 and 0.044 A in the case of λ 4369. There is still a decided preference for λ 4369. Professor Bowen also mentions that K. T. Compton and J. C. Boyce (*J. of Franklin Inst.*, **205**, 497, 1928) found for the *He* I line a value which is 0.004 A higher than Hopfield's more recent result.

[43] Beals has found that in the visible region the line widths are proportional to their wave-lengths (*op. cit.*, p. 297).

and the width of *He* I 515.60 should be 0.32 A. Allowing a similar width for *O* II 515.5, we find that both *O* II lines should profit from the excessive radiation available for absorption from the bright *He* I line. It is obvious, however, that unless our computation is in error, λ 4369 should profit a great deal more than λ 4395. Normally λ 4369, of laboratory intensity 4, would not be expected to show in P Cygni. There is a faint, but definite, absorption line at approximately the correct wave-length, and there is also an emission line, but its position is rather markedly displaced toward the red. (A slight displacement of the absorption line in the same direction is not serious, because it blends with a weak bright line at *O* II 4367.) I am therefore in doubt whether λ 4369 is really the *O* II line. Should it not be *O* II, I should be inclined to abandon also the hypothesis of abnormal fluorescence in λ 4396 (laboratory intensity 7) and should prefer to regard this line as unidentified.

Unfortunately, no other multiplets which are easily observable arise from the *O* II level $\nu = 48{,}566.4$. The multiplet λλ 4941, 4943, 4956 cannot be photographed with the Eastman Process emulsion.

I have made a search for other coincidences in ultra-violet wave-lengths (see Fig. 7). The nearest are:

H	937.81	*He* I	601.4	*He* I	537.1
S II	937.69	*O* II	600.6	*O* II	537.8
S II	937.41			*O* II	538.3

The first coincidence may be sufficiently close to produce observable effects, but unfortunately the ordinary lines of *S* II are all faint. Not one of the unidentified emission lines agrees with classified lines of *S* II listed by S. B. Ingram.[44] The second coincidence is not close enough; furthermore, the *He* line corresponds to a forbidden transition and is probably weak in P Cygni. The third case is too remote.

VIII. THE RADIAL VELOCITIES

It has been known for a long time that radial velocities obtained from different lines of P Cygni are not consistent among themselves. Thus, the absolute values of the negative velocities from the *H* lines become larger as we pass from the violet to the red, and for this reason the hypothesis has been advanced that $V = f(\lambda)$. For *He* I

[44] *Phys. Rev.*, **32**, 172, 1928.

this functional relationship was found to hold when only a few of the stronger lines were measured.

I have made no attempt to obtain accurate velocities from the stronger lines, but have measured velocities for as many lines as possible. The results are given in Table I and are summarized in Table VI, in which there are given for each element the mean veloc-

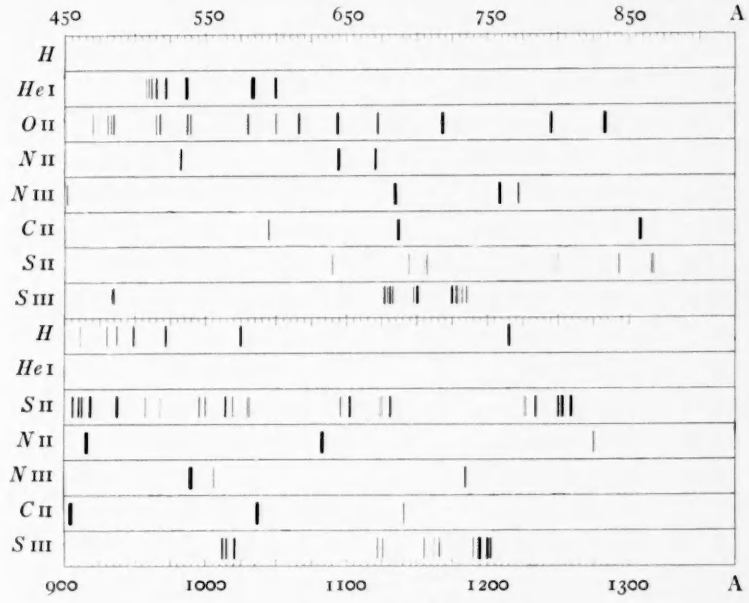

FIG. 7.—Ultra-violet spectra

ities corresponding to lines of approximately equal absorption intensity. The elements are arranged in order of their ionization potentials.

In spite of the large scatter, there is a fair degree of correlation between intensity and velocity; for any given element the strong lines show a larger velocity of approach than the faint ones. There can be no doubt that this is the true correlation, and that the physically absurd correlation with wave-length was merely a result of the general tendency in *H* and *He* I for the stronger lines to have the longer wave-lengths. Exactly the same phenomenon has been observed in the B5 component of β Lyrae.

The most interesting result, however, is the obvious correlation between velocity and ionization potential: for two lines of a given intensity, the one of lower ionization potential has the larger velocity of approach. This effect is not caused by the presence of emission lines; thus for *C* II and *Mg* II, which are very little affected by emission, $|V|$ is much larger than for *N* II, which has strong emission. Furthermore, the transition from emission to absorption is gradual, not sudden.

TABLE VI

RADIAL VELOCITIES IN P CYGNI

Element	Average Intensity (Absorption)	Average Velocity	No. of Lines
		km/sec.	
H (13.5)	22	−181	4
Mg II (15.0)	2	118	1
C II (24.3)	1	138	1
He I (24.5)	1	83	1
He I	2	113	2
He I	7	123	3
He I	10	140	4
He I	15	156	2
N II (29.5)	1	85	7
N II	3	105	4
N II	5	99	2
N II	8	99	3
Si III (33.3)	5	92	1
Si III	7.5	99	2
S III (34.9)	1	85	4
S III	3	102	2
O II (34.9)	1	78	10
O II	2	79	8
O II	3	75	4
O II	4.5	78	3
Si IV (45.0)	4	53	2
N III (47.4)	1	48	2
N III	2	− 64	2

We have consistently been led to the result that lines of high excitation originate deeper inside the shell. Consider a single element, e.g., *He* I. The strong lines originate in smaller optical depths within the nebula than the fainter lines. The velocities of the strong lines are greater than those of the faint lines, suggesting an accelerated motion of the nebula outward. Now consider two lines of the same intensity but of different elements. The one of lower potential, as

found in section vi, originates at a greater distance from the star than the one of higher potential. Consequently, the former should show a larger velocity of approach than the latter. This is in agreement with observation.

There is good evidence in favor of this acceleration, from the emission lines. These are by no means all of equal width, but a closer study of their behavior must be postponed until actual contours are available. In passing, however, attention may be called to the sharpness of the unidentified emission line λ 4164.

IX. THE ULTRA-VIOLET AND GREEN REGIONS

For completeness I have measured several spectrograms on coarse-grained, isochromatic plates taken by Mr. J. A. Hynek with the prism-spectrograph attached to the 69-inch Perkins reflector. The measures are uncertain, especially in the green region, where the dispersion is small and where the comparison lines are not favorably located. The list contains the designations or the laboratory wave-lengths of all identified lines and the measured wave-lengths (corrected to the sun) of the unidentified lines. Attention is called to the peculiar intensity of *Si* III 3806.56, which is a high-level line. The forbidden *O* II lines λλ 3726, 3729 are not present, thus confirming the conclusion that δ is relatively small. The *O* II multiplet 4941, 43, 56 (referred to in section vii) is not definitely seen on the coarse-grained plates, although the first member may be identical with λ 4938.01 (unidentified). The list contains 48 absorption lines (of which 14 are unidentified) and 20 emission lines (of which 6 are unidentified).

ABSORPTION LINES

H_{25} (1) −136; H_{23} (1) −122; H_{22} (2) −143; H_{21} (2) −143; H_{20} (2) −138; H_{19} (2) −105; H_{18} (3) −134; H_{17} (4) −152; H_{16} (7) −164; H_{15} (4) −122; H_{14} (4) −146; H_{13} (4) −105; H_{12} (5) −133; H_{11} (4) −142; H_{10} (7) −138; H_9 (8) −143; $H_\zeta = H_8$ (20 bl. *He* I) *He* I: 3587.30 (2) −198; 3613.64 (3) −183; 3634.30 (6) −113; 3705.10 (bl. *H*); 3819.63 (8) −132; 3867.50 (3) −111; 3871.80 (3) −91; 5015.68 (7) −180; 5047.74 (1) −176; *O* II 3727.33 (2) −95; *S* III: 3632.03 (1) −216?; 3709.37 (2) −72; 3717.77 (1) −130; 3778.91 (1) −96; 3860.64 (1) −47; *Si* III? 3791.41 (1) −152; *Si* IV? 3773.13 (1) −68.

Unidentified: 3599.56 (3); 3602.51; 3648.34 (1); 3723.89 (1); 3782.19 (2); 4938.01 (*O* II 4941.12?); 5052 (1); 5071 (1); 5082 (2); 5097 (1); 5125 (2); 5131 (1); 5139 (2); 5154 (3).

EMISSION LINES

H_{18} (1) −17; H_{17} (2) +1; H_{16} (3) +21; H_{15} (2) +26; H_{14} (2) −14; H_{13} (3) −26; H_{12} (3) −17; H_{11} (3) −14; H_{10} (4) −14; H_9 (6) +0; *He* I 3819.63 (6) −10; 3888.90 (bl. *H*); 5015.68 (10) −6; *Si* III 3806.56 (4) −32.

Unidentified: 3600.88 (3); 3603.49 (2); 3757.57 (1); 5055 (3); 5127 (2); 5156 (3).

X. CONCLUSIONS

As a result of the preceding discussion the following tentative picture of P Cygni suggests itself:

The nucleus is a star of effective temperature 20,000° K, situated at a distance of approximately 1000 parsecs from the sun. Owing to its great distance, the interstellar line K is exceptionally strong. Selective interstellar absorption reduces the color temperature to approximately 6000° K. There is no line spectrum belonging to a stationary reversing layer similar to that found in 17 Leporis. The absorption lines and the emission lines originate in an expanding nebular shell. The velocity of this shell is accelerated outward, being approximately 200 km/sec. in the region of formation of the *H* lines and approximately 50 km/sec. in the region where *Si* IV and *N* III are formed.

For a given element the stronger absorption lines originate at lesser depths than the weaker lines. For two equal lines of different elements the one of higher ionization potential originates at the greater depth.[45]

The mechanism of line excitation deviates from thermal excitation, and peculiar cases of fluorescence may be present. It is probable, however, that the dilution constant in P Cygni is much smaller than that found for novae or planetary nebulae.

YERKES OBSERVATORY
November 1934

[45] Since this paper was written, I have received the November, 1934, issue of the *Observatory*, containing an article by C. S. Beals on P Cygni (p. 319). It is gratifying to find that his conclusions in regard to stratification in the shell agree with mine. In this connection attention may be called to the star 17 Leporis in which the ratio emission/absorption is very small and for which I concluded that the ratio: radius of shell/radius of star, must be relatively close to 1; this is, of course, the same result as that given by *O* II and by other atoms of high ionization potential, in P Cygni (*Ap. J.*, **76**, 103, 1932). Beals now favors a temperature of 30,000° K.